*Quarterly Reviews of Biophysics* **30**, 4 (1997), pp. 365–429. Printed in the United Kingdom 


# Infrared spectroscopy of proteins and peptides in lipid bilayers

LUKAS K. TAMM AND SUREN A. TATULIAN

*Department of Molecular Physiology and Biological Physics, University of Virginia Health Sciences Center, Post Office Box 10011, Charlottesville, Virginia 22906-0011*

SUMMARY

Infrared spectroscopy is a useful technique for the determination of conformation and orientation of membrane-associated proteins and lipids. The technique is especially powerful for detecting conformational changes by recording spectral differences before and after perturbations in physiological solution. Polarized infrared measurements on oriented membrane samples have revealed valuable information on the orientation of chemical groupings and substructures within membrane molecules which is difficult to obtain by other methods. The application of infrared spectroscopy to the static and dynamic structure of proteins and peptides in lipid bilayers is reviewed with some emphasis on the importance of sample preparation. Limitations of the technique with regard to the absolute determination of secondary structure and orientation and new strategies for structural assignments are also discussed.

## 1. INTRODUCTION

Many functions that are crucial to cellular life are carried out by membrane proteins that are bound to or embedded in lipid bilayers. It is still difficult to determine the structure of membrane proteins by X-ray crystallography, electron crystallography, or NMR spectroscopy. To date the structures of only about eight different membrane proteins (photosynthetic reaction centres, porins, bacteriorhodopsin, cytochrome *c* oxidase, light-harvesting complexes from bacteria and plants, $\alpha$-hemolysin, and prostaglandin synthase) have been solved to atomic resolution. In view of these difficulties for obtaining high-resolution structures of membrane proteins, lower-resolution techniques can often yield valuable, global structural information on these proteins. In many cases a detailed atomic structure may not be needed to understand certain aspects of the function of a membrane protein. On the contrary, the ability to monitor structural changes in response to a physiological stimulus may be more useful in some instances. Infrared spectroscopy of membrane proteins in physiological environments is a powerful technique that operates in this low-resolution physiological regime. Unlike in other spectroscopic techniques, the presence of the lipid bilayer does not limit spectroscopic resolution or sensitivity, and membrane proteins can be studied in their native lipid environment. Since vibrational modes of lipids and proteins are present in the IR spectrum, the influence of different lipid structures on the protein, and vice versa, can also be investigated by infrared membrane spectroscopy.

A technique that has become increasingly popular for membrane spectroscopy in recent years is attenuated total reflection (ATR) Fourier transform infrared (FITR) spectroscopy. ATR–FTIR spectroscopy has several advantages: (1) information can be obtained not only on the secondary structure, but also on the

orientation of membrane molecules from measurements with polarized light; (2) the technique is very sensitive, requiring only sub-milligram quantities for sample preparation and detection; (3) conformational states can be measured in aqueous environments; and (4) the physiological conditions of a sample can be varied *in situ*.

This review focuses on structural studies on membrane proteins and peptides with a special emphasis on current methods of sample preparation. The basic methods of IR spectroscopy, data processing, and assignment of group vibrations are presented only very summarily. For more detailed descriptions of these methods, the reader is referred to a number of comprehensive recent reviews (Krimm & Bandekar, 1986; Braiman & Rothschild, 1988; Arrondo *et al.* 1993; Goormaghtigh *et al.* 1994; Haris & Chapman, 1995; Jackson & Mantsch, 1995). ATR–IR spectroscopy is treated here in more detail, although several excellent previous reviews which each emphasize different aspects of ATR spectroscopy are available (Fringeli & Günthard, 1981; Goormaghtigh & Ruysschaert, 1990; Fringeli, 1993; Dluhy *et al.* 1995; Axelsen & Citra, 1996).

## 2. TRANSMISSION VERSUS ATTENUATED TOTAL REFLECTION SPECTROSCOPY

Infrared spectroscopy is based on the absorption of electromagnetic radiation by matter due to different vibrational modes of the chemical bonds. The most common experimental configuration is a transmission experiment. Infrared light is passed through the sample and the absorbance, defined as

$$A = -\log (I/I_0), \tag{1}$$

is calculated from the intensities of transmitted and incident light, $I$ and $I_0$, respectively. The ratio $T = I/I_0$ is called the transmittance. The absorbance is directly proportional to the concentration, $c$, of the absorbing molecules and the path length, $l$, of the measuring cell (Beer–Lambert's law)

$$A = \epsilon cl \tag{2}$$

where $\epsilon$ is the molar extinction coefficient. Two important factors have to be considered in transmission IR spectroscopy of aqueous solutions of proteins. First, the vibrational extinction coefficients are generally relatively low (e.g. a few hundred $\text{M}^{-1}\ \text{cm}^{-1}$ for the amide I mode). Second, absorption bands of liquid water overlap with several bands that are of interest in protein and membrane spectroscopy. To minimize these problems, relatively high protein concentrations ($\geqslant$ 1 mg $\text{ml}^{-1}$) and short path lengths are used in transmission FTIR spectroscopy. The excellent performance of FTIR spectrometers allows for accurate background subtraction and the reliable recording of protein spectra in aqueous solutions, which was not possible with the older, dispersive instruments.

In internal reflection spectroscopy, the IR beam is reflected within an IR-transparent internal reflection element. An evanescent wave of the same frequency as the incoming IR light is set up in the optically rarer medium, such as an

aqueous solution that is adjacent to the interface. The amplitude of the electric field, $E$, falls off exponentially with distance, $z$, from the interface.

$$E = E_0 \, e^{-z/d_p} \tag{3}$$

with a characteristic decay length (depth of penetration),

$$d_p = \frac{\lambda/n_1}{2\pi\sqrt{[\sin^2\gamma - (n_3/n_1)^2]}}, \tag{4}$$

where $\lambda$ denotes the wavelength of the IR light, $n_1$ and $n_3$ are the refractive indices of the internal reflection element and water, respectively, and $\gamma$ is the angle of incidence. Because $d_p$ is of the order of only a few hundred nm in many typical applications, internal reflection spectroscopy is a surface-sensitive technique. Samples, such as membranes, that are deposited at the solid–liquid (or solid–gas) interface absorb electromagnetic radiation of the evanescent wave, and thereby reduce the intensity of the reflected light. Hence, the technique is referred to as 'attenuated total reflection spectroscopy'. A major advantage of ATR spectroscopy is that absorption due to water and other molecules in the bulk solution is greatly reduced. Another advantage is that molecular orientations can be determined in oriented samples with polarized light. However, sample preparation and, in some instances, data interpretation, are more complex in ATR than in transmission spectroscopy. These issues, as applied to membrane spectroscopy, will be discussed in detail in Sections 5 and 6.

## 3. GROUP VIBRATIONS FREQUENTLY ENCOUNTERED IN MEMBRANE SPECTROSCOPY

A non-linear molecule of N atoms has 3N-6 normal vibrational modes. As a result of this large number of vibrations and the intrinsic width of vibrational absorption bands, IR spectra of large molecules are generally very complex and not well resolved in many regions of the spectrum. However, despite this complexity absorption bands at distinct group frequencies can be assigned to various functional groups in protein, lipid and water molecules. The infrared absorption frequencies of $H_2O$, HOD, and $D_2O$ are listed in Table 1. The $H_2O$ bending mode at $\sim 1645$ cm$^{-1}$ overlaps with the amide I mode of proteins and the HOD bending mode (present in mixed $D_2O/H_2O$ samples) at $\sim 1455$ cm$^{-1}$ overlaps with the amide II′ mode of proteins and the $CH_2$ scissoring mode of lipid fatty acyl chains (see below). The $D_2O$ association band at $\sim 1555$ cm$^{-1}$ interferes with the amide II vibrations of proteins and $D_2O$ bending at $\sim 1215$ cm$^{-1}$ overlaps with the antisymmetric phosphate stretching mode of phospholipids. Therefore, the choice of the solvent depends on the spectral region of interest in each sample and its proper selection is important.

Lipids absorb in many different regions of the IR spectrum. Approximate frequencies of some important vibrational modes are listed in Table 2. For more comprehensive lists of lipid absorptions, the reader is referred to the literature (Fringeli & Günthard, 1981; Mendelsohn & Mantsch, 1986; Arrondo *et al.* 1993; Jackson & Mantsch, 1993; Lewis & McElhaney, 1996). The exact frequencies of

Table 1. *Infrared absorption frequencies of liquid $H_2O$, HOD and $D_2O$ (in $cm^{-1}$)*[a]

| Assignment | | $H_2O$ | HOD | $D_2O$ |
|---|---|---|---|---|
| O-X stretching | ($\nu_{as}$) | 3490 (s) | 3380[b] (s) | 2540 (s) |
| | ($\nu_s$) | 3280 (s) | 2500[c] (s) | 2450 (s) |
| Association | ($\nu_A$) | 2125 (w) | — | 1555 (w) |
| Bending | ($\delta$) | 1645 (s) | 1450 (s) | 1210 (s) |

[a] s, strong; w, weak.
[b] O-H.
[c] O-D.

Table 2. *Important infrared absorption bands of membrane lipids*

| Assignment | | Approximate frequency ($cm^{-1}$)[a] | Estimated direction of dipole moment |
|---|---|---|---|
| $CH_3$ antisymm. stretch (choline) | ($\nu_{as}$) | 3038 (w) | |
| $CH_3$ antisymmetric stretch | ($\nu_{as}$) | 2956 (s) | |
| $CH_2$ antisymmetric stretch | ($\nu_{as}$) | 2920 (s) | $\perp$ to bisector of HCH angle |
| $CH_3$ symmetric stretch | ($\nu_s$) | 2870 (s) | |
| $CH_2$ symmetric stretch | ($\nu_s$) | 2850 (s) | $\parallel$ to bisector of HCH angle |
| C═O stretch | ($\nu$) | 1730 (s) | $\sim \parallel$ to C═O bond |
| $NH_3^+$ antisymmetric bend | ($\delta_{as}$) | 1630 (m) | |
| $COO^-$ antisymmetric stretch | ($\nu_{as}$) | 1623 (s) | |
| $NH_3^+$ symmetric bend | ($\delta_s$) | 1571 (m) | |
| $N^+(CH_3)_3$ antisymmetric bend | ($\delta_{as}$) | 1485 (m) | |
| $CH_2$ scissoring (triclinic) | ($\delta$) | 1473 (m) | |
| $CH_2$ scissoring (hexagonal) | ($\delta$) | 1468 (m) | $\parallel$ to bisector of HCH angle |
| $CH_2$ scissoring (orthorhombic) | ($\delta$) | 1472 (m) | |
| | ($\delta$) | 1463 (m) | |
| $CH_3$ antisymmetric bend | ($\delta_{as}$) | 1460 (m) | |
| $N^+(CH_3)_3$ symmetric bend | ($\delta_s$) | 1405 (m) | |
| $CH_3$ symmetric bend | ($\delta_s$) | 1378 (m) | |
| $CH_2$ wagging band progression | (w) | 1200–1400 (w) | $\parallel$ to hydrocarbon chain (all-trans) |
| $PO_2^-$ antisymmetric stretch | ($\nu_{as}$) | 1228 (s) | $\perp$ to bisector of O–P–O angle |
| CO—O—C antisymmetric stretch | ($\nu_{as}$) | 1170 (m) | |
| $PO_2^-$ symmetric stretch | ($\nu_s$) | 1085 (m) | $\parallel$ to bisector of O–P–O angle |
| CO—O—C symmetric stretch | ($\nu_s$) | 1070 (m) | |
| C—O—P—O—C stretch | ($\nu$) | 1060 (m) | |
| $N^+(CH_3)_3$ antisymmetric stretch | ($\nu_{as}$) | 972 (m) | |
| $N^+(CH_3)_3$ symmetric stretch | ($\nu_s$) | 920 (m) | |
| P—O antisymmetric stretch | ($\nu_{as}$) | 820 (m) | |
| $CH_2$ rocking | ($\gamma$) | 720–730 (m) | $\perp$ to bisector of HCH angle |

[a] s, strong; m, medium; w, weak.

Table 3. *Amide bands of proteins*[a]

| Designation | Frequency range ($cm^{-1}$)[b] | Description[c,d] |
|---|---|---|
| Amide A | ~ 3300 (s) | $NH_s$ |
| Amide B | ~ 3100 (s) | $NH_s$ |
| Amide I | 1600–1700 (s) | $CO_s$ (76%), $CN_s$, (14%), $CCN_d$ (10%) |
| Amide II | 1510–1580 (m) | $NH_{ib}$ (43%), $CN_s$ (29%), $CO_{ib}$ (11%), $CC_s$ (9%), $NC_s$ (8%) |
| Amide III | 1200–1400 (w) | $NH_{ib}$ (55%), $CC_s$ (19%), $CN_s$ (15%), $CO_{ib}$ (11%) |
| Amide V | 610–710 (w) | $CN_t$ (66%), $NH_{ob}$ (34%) |

[a] Adapted from Krimm and Bandekar, 1986.
[b] s, strong; m, medium; w, weak.
[c] The percentages are approximate and refer to the potential-energy distribution calculated for *N*-methylacetamide (Bandekar, 1992).
[d] s, stretch; d, deformation; t, torsion; ib, in-plane bend; ob, out-of plane bend.

the absorption bands that are associated with methylene vibrations of the fatty acyl chains depend on the physical state of these chains. Therefore, precise measurements of $CH_2$ stretching, scissoring, and rocking band progressions can be used to probe the physical state of lipids under various conditions. The ester carbonyl stretching band is very sensitive to hydrogen bonding and, therefore, has been used to monitor hydration at the membrane-water interface (see Section 7 for further details on lipid absorptions). It should be noted that the antisymmetric amine-$NH_3^+$ stretch of phosphatidylethanolamines and phosphatidylserines and the antisymmetric carboxylate stretch of phosphatidylserines overlap with the amide I region and the $CH_2$ scissoring bands overlap with the amide II′ region of proteins. The amide III mode of proteins overlaps with the $CH_2$ wagging band progression modes of lipids.

Proteins give rise to backbone and side-chain vibrations. The approximate frequencies for the backbone amide vibrations are listed in Table 3. All amide frequencies are conformation-sensitive, but amide I is by far the most widely used vibrational mode to determine conformations of proteins. Several workers have proposed empirical correlations between amide I frequencies and the secondary structures of proteins whose structures had been solved by X-ray crystallography (see Byler & Susi, 1986; Arrondo *et al*. 1993; Goormaghtigh *et al*. 1994; Jackson & Mantsch, 1995, for reviews). Taking a different approach, Krimm and coworkers calculated amide I frequencies of different secondary structures based on their known molecular geometries and specific force fields. The force fields that were used in these calculations were determined experimentally using *N*-methylacetamide and other model compounds (reviewed in Krimm & Bandekar, 1986). Although the correlations obtained by both methods are satisfactory in many cases, they are unfortunately not absolute and many exceptions to the general rules exist that warrant caution when quantitating secondary structures of proteins with

Table 4. *Correlations between common protein secondary structures and amide I frequency*[a]

| Secondary structure | Amide I frequency ($cm^{-1}$) |
|---|---|
| Antiparallel $\beta$-sheet/ aggregated strands | 1675–1695 |
| Turns | 1660–1685 |
| $3_{10}$-helix[b] | 1660–1670 |
| $\alpha$-helix[c] | 1648–1660 |
| Unordered | 1652–1660 (deuterated: 1640–1648) |
| $\beta$-sheet | 1625–1640 |
| Aggregated strands | 1610–1628 |

[a] Adapted from Jackson & Mantsch, 1995, and Arrondo *et al*. 1993. These correlations are guidelines only. The ranges are given for mostly protonated amide I bands as found in secondary structures that are relatively resistant to H/D exchange. About 10 $cm^{-1}$ lower frequencies may be expected for fully H/D exchanged secondary structures, shown here only for unordered structures (see text, for more detail).

[b] Some alanine-rich peptides which may form $3_{10}$-helices (or mixtures of $3_{10}$- and $\alpha$-helices) exhibit amide I′ frequencies in the 1634–1640 $cm^{-1}$ range (Miick *et al*. 1992; Martinez & Millhauser, 1995).

[c] Helical coiled coils appear to have lower amide I frequencies in the 1630–1640 $cm^{-1}$ range (Heimburg *et al*. 1996; Reisdorf & Krimm, 1996).

unknown structure (Surewicz *et al*. 1993). A list of correlations between standard secondary structures of proteins and amide I frequency ranges is given in Table 4. These correlations are guidelines only. There are proteins and peptides that absorb outside the frequency range given in the table. Some examples of membrane proteins and peptides with unusual amide I frequencies will be given in Sections 8 and 9. It should also be noted that amide I frequencies decrease by $\sim$ 10 $cm^{-1}$ upon complete H/D exchange of the amide protons. Since unordered structures undergo H/D exchange at much higher rates than regular secondary structures, this effect is often used to distinguish between $\alpha$-helical and random structures which overlap in $H_2O$, but are well separated after a relatively short time of exposure to $D_2O$ (Table 4). The frequency of the amide II band decreases by about 100 $cm^{-1}$ upon H/D exchange of amide protons. Therefore, this band has been frequently used to measure the extent of amide-proton exchange in proteins and peptides. The amide modes are referred to as amide I′, II′, III′ etc., when measured in $D_2O$. Many amino acid side chains absorb in or near the amide I and amide II regions of the IR spectrum. A list of side chain absorptions in $H_2O$ and $D_2O$ (with exchangeable side chain protons fully H/D exchanged) is given in Table 5. Depending on residue composition and the solvent used, side chain contributions may have to be subtracted to obtain pure amide I or II bands (Venyaminov & Kalnin, 1990*a*, *b*). Even if amide I and II spectra can be faithfully decomposed (see Section 4) and the components assigned to particular secondary structures, the resulting band areas may have to be weighted by the somewhat

Table 5. *Approximate frequencies of amino acid side chain absorptions in the 1400–1800 cm$^{-1}$ region*[a]

| Vibration | | | In $H_2O$ $\nu_0$ (cm$^{-1}$)[b] | In $D_2O$ $\nu_0$ (cm$^{-1}$)[b] |
|---|---|---|---|---|
| Terminal | —COOH | ($\nu$) | 1740 (m) | 1720 (m) |
| Asp | —COOH | ($\nu$) | 1716 (m) | 1713 (m) |
| Glu | —COOH | ($\nu$) | 1712 (m) | 1706 (m) |
| Asn | —C═O | ($\nu$) | 1678 (s) | 1648 (s) |
| Arg | $-CN_3H_5^+$ | ($\nu_{as}$) | 1673 (s) | 1608 (s) |
| Gln | —C═O | ($\nu$) | 1670 (s) | 1635 (s) |
| Arg | $-CN_3H_5^+$ | ($\nu_s$) | 1633 (m) | 1586 (s) |
| Terminal | $-NH_3^+$ | ($\delta_{as}$) | 1631 (m) | |
| Lys | $-NH_3^+$ | ($\delta_{as}$) | 1629 (m) | |
| Asn | $-NH_2$ | ($\delta$) | 1622 (m) | |
| Gln | $-NH_2$ | ($\delta$) | 1610 (m) | |
| Tyr | Ring—$O^-$ | | 1602 (m) | 1603 (s) |
| Terminal | $-COO^-$ | ($\nu_{as}$) | 1598 (m) | 1592 (s) |
| His | Ring | | 1596 (w) | |
| Asp | $-COO^-$ | ($\nu_{as}$) | 1574 (s) | 1584 (s) |
| Glu | $-COO^-$ | ($\nu_{as}$) | 1560 (s) | 1567 (s) |
| Terminal | $-NH_2$ | ($\delta$) | 1560 (s) | |
| Lys | $-NH_3^+$ | ($\delta_s$) | 1526 (m) | |
| Tyr | Ring—OH | | 1518 (m) | 1615 (m), 1515 (s) |
| Terminal | $-NH_3^+$ | ($\delta_s$) | 1515 (m) | |
| Tyr | Ring—$O^-$ | | 1498 (s) | 1500 (s) |
| Phe | Ring | | 1494 (w) | |

[a] Adapted from Chirgadze *et al.* 1975 and Venyaminov & Kalnin, 1990*a*, *b*.
[b] s, strong; m, medium; w, weak.

different integrated molar extinction coefficients of the different secondary structures. Chirgazde *et al.* (1973), Chirgazde & Brazhnikov (1974), and Venyaminov & Kalnin (1990*b*) reported weighting ratios of 46:57:35 and 76:69:46 for the major amide I components of $\alpha$-helix: $\beta$-sheet: random coil in $D_2O$ and $H_2O$, respectively.

## 4. DATA PROCESSING

Infrared bands of complex biological molecules in solution are intrinsically broad and often overlap with neighbouring bands to produce a complex absorption profile. The investigator is often interested in identifying the component bands that give rise to the observed composite spectrum. As elaborated in more detail in later sections, component band identification is of particular interest for determining secondary structures of proteins from their amide I bands. Two resolution-enhancement techniques, differentiation and Fourier self-deconvolution, are commonly used to identify the component bands. Both methods do not increase instrumental resolution, but are mathematical procedures

that yield narrower component bands. Although in many cases deconvolved amide I bands have been used to determine secondary structure by curve fitting, it should be recognized that resolution-enhanced spectra, especially derivative spectra do not reproduce true band intensities and relative component fractions cannot be obtained directly from them. Finally, noise is enhanced in these spectra which, depending on initial data quality, puts a limit on the extent to which resolution can be enhanced reliably. Despite these caveats, both methods are extremely useful for identifying component frequencies in complex spectra and these band positions can then be used as fixed input parameters in component band-fitting routines applied to the original, unprocessed spectra. Before any of these routines are applied, peaks due to residual water vapour must be carefully subtracted from the raw spectra, because spurious spectral contaminants like those from water vapour will also be enhanced by these techniques. The sharp peaks of water vapour can be reliably subtracted by inspecting the amide I region ($\sim 1650$ cm$^{-1}$) of the spectrum. When $H_2O$ buffers are used and an analysis of the amide I band is attempted, the spectral region around 2125 cm$^{-1}$ is well suited to check for the correct subtraction of liquid water because this region is usually free from protein and lipid absorbance. In some cases a complete subtraction of the water bands is not possible because water bound to proteins can exhibit altered band shapes.

Differentiation is normally accompanied by smoothing to avoid the amplification of noise. Second order (or higher even-order) derivative spectra (which for ease of visual inspection are often inverted around the frequency axis) are well suited to identify component bands in a complex spectral region. Since excessive smoothing and differentiation can build up side lobes and periodic noise which may be confused with true spectral features, the number of differentiations and the amount of smoothing should be kept to a minimum.

In Fourier self-deconvolution the interferograms are multiplied first with an exponentially increasing function to compensate for the natural decay of the interferogram and then with a more slowly decaying apodization function which becomes zero at an arbitrarily selected cutoff value. This procedure results in a spectrum with narrowed bands after Fourier transformation. The amount of resolution enhancement is usually described by the resolution enhancement factor, $K$, which is the ratio of the bandwidths before and after resolution enhancement and is typically of the order of 2 to 3. Unfortunately, the choice of the deconvolution parameters is quite subjective and each band may have its own optimum parameters. For this reason, we prefer the differentiation method to identify component bands. As in differentiation, excessive Fourier self-deconvolution increases noise, which in extreme cases becomes periodic.

After component analysis, the original, except for water vapour removal and baseline correction, unprocessed spectra may be curve-fitted with component bands using Lorentzian or Gaussian (or mixtures of the two) lineshapes and the identified component band positions as input parameters. Since many local minima exist in many of these fits, we strongly urge to restrict the number of free parameters and components used for curve-fitting to an absolute minimum. Even

though molecular dynamics calculations predict Lorentzian lineshapes for simple infrared absorptions, we find that Gaussian lineshapes better fit most experimental spectra of complex molecular assemblies, especially in ATR spectroscopy.

## 5. POLARIZED SPECTROSCOPY AND ORIENTATIONAL DISTRIBUTIONS

Molecular orientations can be obtained from polarized IR spectra of oriented samples. This is due to the fact that the IR absorbance is proportional to the square of the product of the transition dipole moment, $M$, and the projection of the electric field, $E$, of the polarized IR beam on $M$, i.e. $|ME|^2 \cos^2 \zeta$, where $\zeta$ is the angle between the directions of $M$ and $E$. Therefore, the relevant parameter for optical orientation measurements, the dichroic ratio,

$$R = \frac{A_\parallel}{A_\perp} = \frac{\int A_\parallel(\nu)\,\mathrm{d}\nu}{\int A_\perp(\nu)\,\mathrm{d}\nu} = \frac{\cos^2 \zeta_\parallel}{\cos^2 \zeta_\perp} \tag{5}$$

is largest for $M$ parallel to $E_\parallel$ and smallest for $M$ parallel to $E_\perp$. $A_{\parallel,\perp}$, $\int A_{\parallel,\perp}(\nu)\,\mathrm{d}\nu$, and $\zeta_{\parallel,\perp}$ in eqn (5) denote the peak absorbances, the absorbances integrated through an entire absorbance band, and the respective angles for parallel and perpendicular polarized incident light, respectively. In practice, because of orientational fluctuations of the molecules in lipid bilayers, an ensemble of molecular orientations contribute to the measured dichroic ratio. Therefore, it is convenient and customary in membrane spectroscopy to analyse polarized IR data in terms of order parameters defined as

$$S_\theta = (3 \langle \cos^2 \theta \rangle - 1)/2, \tag{6}$$

where $\theta$ is the angle between the main axis of symmetry of the structural element of interest (i.e. the molecular director) and the membrane normal and the angular brackets denote a time- and ensemble-average. Eqn (6) is only appropriate for describing axially symmetric distributions, i.e. for distributions that are completely isotropic around a defined axis. A single angle ($\theta$) is usually sufficient to describe orientations in membranes, because of the complete rotational disorder of the constituent molecules around the membrane normal in fluid lipid bilayers. The order parameter is a function of the distribution of molecular orientations in the sample and occasionally is interpreted in terms of models with specific distribution functions. $S$ ranges from $-0{\cdot}5$ for $\theta = 90°$ to $+1{\cdot}0$ for $\theta = 0°$. For other values of $S$, the molecular orientation should be described by a distribution function rather than by a single angle $\theta$. For example for the special case of $S = 0$, the orientation could be interpreted by a unique angle $\theta = 54{\cdot}7°$ (if the distribution function is a $\delta$ function) or as an isotropic distribution if all angles are equally probable. Two techniques, using either transmission or ATR spectroscopy, can yield information on the orientation of membrane proteins. Both will be briefly described below.

### 5.1 *Orientation from transmission spectroscopy*

Due to the isotropic distribution of membrane molecules around the membrane normal, no dichroism ($R = 1$) is expected for polarized IR spectra of oriented

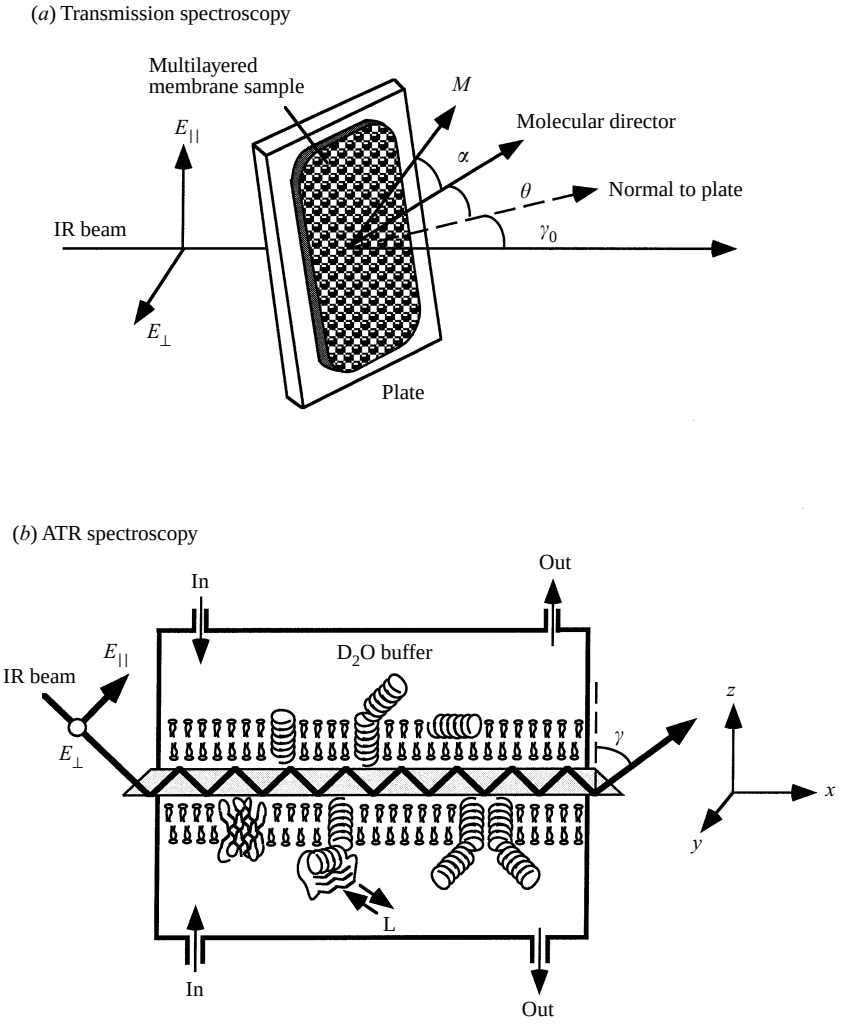


Fig. 1. Experimental setups for determining molecular orientation from (*a*) transmission and (*b*) ATR–FTIR spectroscopy. Two single supported bilayers with reconstituted membrane proteins, attached to both surfaces of a trapezoidal internal reflection element, and held in a perfusable liquid sample cell are shown in (*b*). *M*, transition dipole moment; $E_{\parallel,\perp}$, electric field vectors parallel and perpendicular to the plane of incidence defined by the IR beam and the normal to the surface; L, ligand.

membrane samples measured with the membranes positioned with their normal parallel to the IR beam. However, when the samples are tilted by an angle $\gamma_0$ relative to the IR beam, as shown in Figure 1*a*, a dichroic ratio different from 1 is expected, unless $S = 0$. An equation has been derived which relates $R$, $S$ and $\gamma$ (Rothschild & Clark, 1979a; Goormaghtigh & Ruysschaert, 1990):

$$R = 1 + 3\sin^2\gamma S/(1 - S). \tag{7}$$

Here $S$ is the order parameter with regard to the angle of the transition dipole moment to the normal of the substrate that supports a stack of coplanar membranes. Angle $\gamma$ is the angle of incidence of the IR beam in the sample and

is related to $\gamma_0$ by Snell's law, i.e. $\gamma = \sin^{-1}(\sin\gamma_0/n)$, where $n$ is the refractive index of the sample. It can also be shown that an axially symmetric distribution of transition dipole moments around the molecular main axis contributes to $S$ by a factor of

$$S_\alpha = (3\cos^2\alpha - 1)/2, \tag{8}$$

where $\alpha$ is the angle between the transition dipole moment and the molecular director. An equivalent relation holds for the contribution, $S_{ms}$, of the 'mosaic spread', i.e. angular deviations from a perfect coplanar alignment of the membranes, to the overall order parameter. Therefore,

$$S = S_{ms} S_\theta S_\alpha \tag{9}$$

for a set of nested axially symmetric distributions. A molecular interpretation of eqn (9) is shown in Fig. 2. To determine molecular orientation by transmission IR spectroscopy, a series of experiments with the sample oriented at different tilt angles is performed. The measured $R$ values are plotted vs. $\sin^2\gamma$ which yields a straight line with a slope of $3S/(1-S)$ (see eqn (7)) from which S is determined. The quantity of interest, $S_\theta$, is then calculated from eqn (9). The angle $\alpha$ is known for many groups from the literature (Table 2, Fig. 2, and see below) and $S_{ms}$ is often assumed to be unity or close to unity.

### 5.2 *Orientation from ATR spectroscopy*

Figure 1*b* depicts a typical experimental set-up for ATR–FTIR spectroscopy on supported membrane systems and defines the coordinates and polarization vectors in a commonly used notation (Fringeli & Günthard, 1981; Frey & Tamm, 1991). The dichroic ratio of an ATR experiment can be written as

$$R^{ATR} = \frac{A_\parallel}{A_\perp} = \frac{\int A_\parallel(\nu)\,d\nu}{\int A_\perp(\nu)\,d\nu} = \frac{E_x^2 k_x + E_z^2 k_z}{E_y^2 k_y}, \tag{10}$$

where $E_{x,y,z}$ are the electric field amplitudes of the evanescent wave at the surface of the internal reflection element and $k_{x,y,z}$ are the components of the integrated absorption coefficient in the fixed laboratory coordinate system (Fig. 1*b*). Expressions have been derived for the electric field amplitudes (Harrick, 1967)

$$\left.\begin{aligned} E_x &= \frac{2\cos\gamma\,\sqrt{(\sin^2\gamma - n_{31}^2)}}{\sqrt{(1-n_{31}^2)}\,\sqrt{[(1+n_{31}^2)\sin^2\gamma - n_{31}^2]}} \\ E_y &= \frac{2\cos\gamma}{\sqrt{(1-n_{31}^2)}} \\ E_z &= \frac{2\cos\gamma\, n_{32}^2 \sin\gamma}{\sqrt{(1-n_{31}^2)}\sqrt{[(1+n_{31}^2)\sin^2\gamma - n_{31}^2]}} \end{aligned}\right\} \tag{11}$$

They depend on $\gamma$, the angle of incidence of the IR beam at the solid–liquid interface and on the refractive indices $n_{1,2,3}$ ($n_{31} = n_3/n_1$, $n_{32} = n_3/n_2$), where the subscripts 1, 2 and 3 denote the internal reflection element, the thin film (membrane), and the bulk medium. Eqn (11) refers to the so-called 'thin film

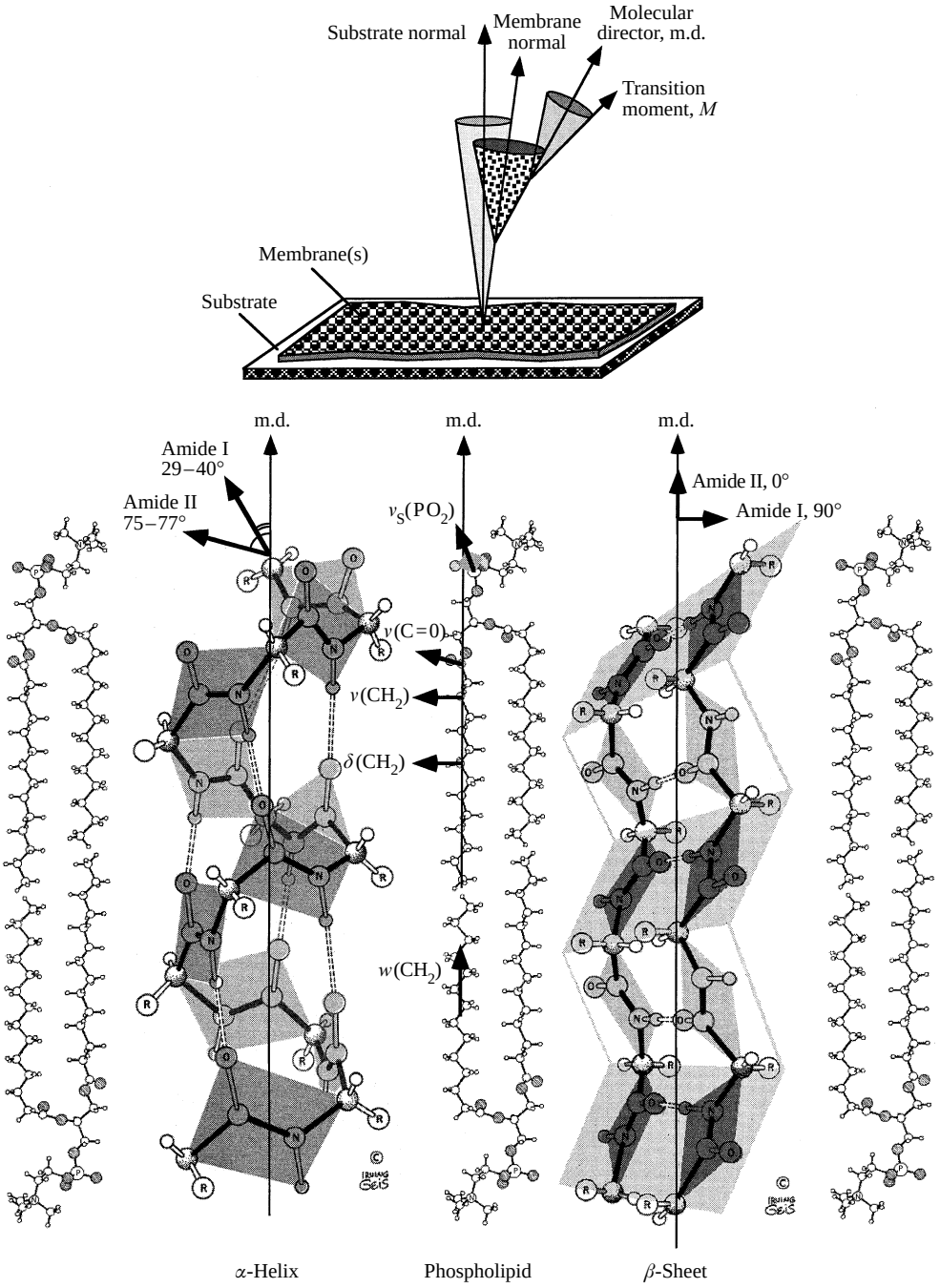


Fig. 2. Order parameters in a set of nested axially symmetric distributions (see text) and directions of some important transition dipole moments in common lipid and protein structures in membranes. The values for the directions of the amide transition dipole moments in $\alpha$-helices are taken from Miyazawa & Blout (1961), Bradbury *et al.* (1962), and Tsuboi (1962), and those of the strongest absorptions of $\beta$-sheets are from the theoretical work of Miyazawa (1960; see also Suzuki, 1967, Fraser & Suzuki, 1970, and Marsh, 1997 on the orientation of transition dipole moments in $\beta$-sheets).

approximation' (Harrick, 1967), which is thought to apply when the film is much thinner than the penetration depth $d_p$ of the evanescent wave (see eqn (4)). For thick samples, e.g. stacks of multilayers thicker than $d_p$, only the phases 1 and 2 are considered, the bulk medium is substituted by the sample ($n_2 = n_3$), and $n_{32}$ in eqn (11) is set to 1. The values of $k_{x,y,z}$ depend on the order parameter $S_\theta$ and the previously defined angle $\alpha$ (Fraser & MacRae, 1973)

$$\left.\begin{aligned} k_x = k_y &= K[(S_\theta \sin^2\alpha)/2 + (1 - S_\theta)/3] \\ k_z &= K[S_\theta \cos^2\alpha + (1 - S_\theta)/3] \end{aligned}\right\} \tag{12}$$

where $K$ is a constant. When eqn (12) is inserted into eqn (10) and solved for $S_\theta$, one obtains

$$S_\theta = \frac{2(E_x^2 - R^{ATR}E_y^2 + E_z^2)}{(3\cos^2\alpha - 1)(E_x^2 - R^{ATR}E_y^2 - 2E_z^2)}. \tag{13}$$

It follows from eqn (13) that for an isotropic sample ($S = 0$), $R_{ISO}^{ATR} = (E_x^2 + E_z^2)/E_y^2$. It should be noted that due to the particular magnitudes of $E_{x,y,z}$, $R_{ISO}^{ATR}$ is not unity. For example if $\gamma = 45°$, $n_1 = 4$ (germanium), $n_2 = 1{\cdot}43$ (lipid), and $n_3 = 1{\cdot}33$ (water), $R_{ISO}^{ATR} \approx 1{\cdot}72$.

Several aspects of determining $S_\theta$ from eqn (13) warrant special attention. First, it is necessary to know the angle $\alpha$ between the transition dipole moment and the molecular axis of symmetry. The directions of the transition moments of some important group vibrations of lipids are listed in Table 2. The order of lipid acyl chains is often determined from the symmetric methylene stretch or scissoring vibrations. The angles $\alpha$ of these vibrations are 90° which reduces eqn (13) to a simpler form to calculate lipid order parameters from the corresponding dichroic ratios

$$S_L = -2\frac{E_x^2 - R^{ATR}E_y^2 + E_z^2}{E_x^2 - R^{ATR}E_y^2 - 2E_z^2}. \tag{14}$$

In aperiodic structures or small model compounds such as N-methyl-acetamide, the transition moment of the amide I band is oriented about 20° from the amide C═O bond towards the N→$C_\alpha$ bond (Fraser & MacRae, 1973; Krimm & Bandekar, 1986). Miyazawa (1960) showed by normal mode calculations that coupled amide transitions in periodic secondary structures consist of components that are either parallel or perpendicular to the chain axis. The $\alpha$-helix has two amide I components which occur at almost the same frequency (1650–1655 $cm^{-1}$). They can hardly be distinguished experimentally, and therefore, both contribute to the effective orientation of the transition dipole moment (Miyazawa & Blout, 1961; Krimm & Bandekar, 1986; Reisdorf & Krimm, 1995). The angle between this transition moment and the $\alpha$-helix long axis has been determined experimentally by several groups. In these experiments, homopolymeric model peptides were oriented on IR windows, their orientation was measured by X-ray fibre diffraction, and the angles $\alpha$ were determined by correlating the polarized IR and diffraction data. Following these procedures, several values ranging from 29 to 40°, most of them between 35 and 40° were reported in the literature (Miyazawa

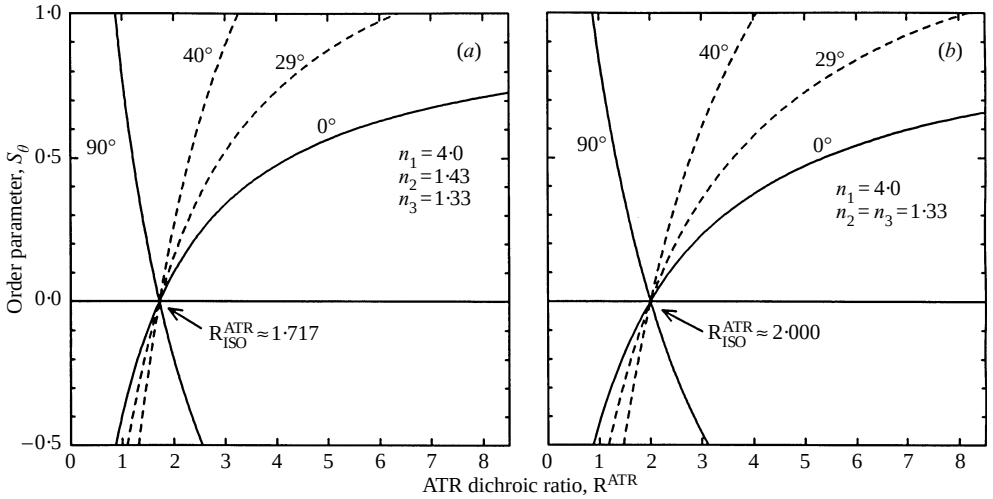


Fig. 3. Dependence of the molecular order parameter, $S_\theta$, on the ATR dichroic ratio, $R^{ATR}$, calculated by eqn (13) for the thin film approximation (*a*) and the two-phase model (*b*). The refractive indices that were used for calculating the electric field components by eqn (11) are indicated in each panel. The angle of incidence of the IR beam, $\gamma$, is 45° in all cases. Plots for different orientations of the transition dipole moment relative to the molecular director (angle $\alpha$) are shown in each panel.

& Blout, 1961; Bradbury *et al.* 1962; Tsuboi, 1962). In our work, we have typically used $\alpha = 39°$, i.e. the value reported by Tsuboi (1962). Theoretical calculations of Reisdorf & Krimm (1995) show that $\Delta\nu$ between axial and radial components and the orientation angle of the resultant transition dipole moment should depend on the length of the $\alpha$-helix. While shifts in $\Delta\nu$ of up to 7 $cm^{-1}$ can be expected (shorter helices have larger $\Delta\nu$), the length dependence of $\alpha$ amounts to less than 5°. The order parameter for an $\alpha$-helix then becomes

$$S_H = 2{\cdot}46\frac{E_x^2 - R^{ATR}E_y^2 + E_z^2}{E_x^2 - R^{ATR}E_y^2 - 2E_z^2}. \quad (15)$$

For $\alpha < 54{\cdot}7°$, smaller angles $\alpha$ yield smaller absolute values of the order parameter; the opposite is true for $\alpha > 54{\cdot}7°$. This is illustrated in Fig. 3.

Antiparallel $\beta$-sheets exhibit two well resolved amide I components with pure polarizations, namely the strong $\nu_\perp(\pi, 0)$ band at $\sim 1635\ cm^{-1}$, and the weak $\nu_\parallel(0, \pi)$ and band at 1680–1695 $cm^{-1}$. The third predicted IR-active band, $\nu_\perp(\pi, \pi)$ is weak, has been rarely observed experimentally, and its exact position (between 1680–1720 $cm^{-1}$) is not well established (Miyazawa & Blout, 1961; Fraser & Suzuki, 1970; Moore & Krimm, 1976). In this notation, the polarizations refer to the directions of the transition dipole moments relative to the strand axis. Practically, only the $\nu_\perp(\pi, 0)$ band at $\sim 1635\ cm^{-1}$ can be used in dichroic measurements of complex systems, because the other bands have very low extinction coefficients and may overlap with mutually perpendicular polarizations. Despite the clear separation of the polarized amide I component bands in $\beta$-sheets, an expression equivalent to eqn (15) cannot be derived, because $\beta$-sheets

are not axially symmetric structures in the most general case. The situation is different if the sheet folds into a closed $\beta$-barrel, in which case axial symmetry is restored (Rodionova *et al.* 1995). The following expression can be derived for the order parameter of a $\beta$-barrel

$$S_B = \frac{2(E_x^2 - R^{ATR}E_y^2 + E_z^2)}{(3\cos^2\beta - 1)(E_x^2 - R^{ATR}E_y^2 - 2E_z^2)}. \quad (16)$$

Here, $\beta = 90° - \delta$, where $\delta$ is the angle of the $\beta$-strands relative to the barrel axis. Therefore, $S_B$ can be determined only if $\delta$ is known, or alternatively if $S_B$ is known (e.g. $\sim$ 1), $\delta$ may be determined. Eqn (16) is slightly different from eqn (7) in Rodionova *et al.* (1995), because the prediction that the $\nu(\pi, 0)$ amide I band should be strictly perpendicular polarized was overlooked in that study (Marsh, 1997; but see also Suzuki, 1967 and Fraser & Suzuki, 1970, for experimental values of the direction of the amide I transition dipole moment that support the original treatment of Rodionova *et al.* 1995). Based on the same symmetry arguments outlined above for the amide I band, Marsh (1997) also suggested that the $\nu_{\parallel}(0, \pi)$ amide II band at 1530–1540 $cm^{-1}$ could be used to determine the orientation of $\beta$-sheets. The weaker $\nu_{\perp}(\pi, 0)$ mode has been predicted and observed at $\sim$ 1560 $cm^{-1}$ and, therefore, is spectrally not as well separated from the parallel amide II mode as in the case for the amide I modes (Moore & Krimm, 1976; Venyaminov & Kalnin, 1990*b*). As for the amide I mode, direct measurements of the orientation of this transition dipole moment in well characterized model systems are needed to confirm the theoretical predictions. Another practical problem with the amide II′ band is its spectral overlap with a residual HOD band in systems that are hydrated with $D_2O$ (see above). Despite these caveats, the order parameter that describes the orientation of the strands of $\beta$-sheets relative to the bilayer normal may well be estimated from the dichroic ratio of the amide II band at 1530–1540 $cm^{-1}$

$$S_S = \frac{E_x^2 - R^{ATR}_{amide\,II}E_y^2 + E_z^2}{E_x^2 - R^{ATR}_{amide\,II}E_y^2 - 2E_z^2}. \quad (17)$$

This single order parameter does not fully specify the average orientation of the $\beta$-sheet in the membrane because $\beta$-sheets lack axial symmetry. However, when the order parameter defined in eqn (17) is combined with a second orthogonal order parameter, e.g. that of the $\nu_{\perp}(\pi, 0)$ amide I band at $\sim$ 1635 $cm^{-1}$, the average strand *and* sheet orientation can be determined, using the equations given by Marsh (1997).

A second important issue concerns the correct estimation of the electric field amplitudes at the interface. As seen from eqn (11), their values depend on the refractive indices. Typical internal reflection plates are made out of germanium ($n_1$ = 4·0), zinc selenide ($n_1$ = 2·4), or KRS ($n_1$ = 2·35). The average refractive index of water ($H_2O$ or $D_2O$) is 1·32–1·33 in many (including the amide I and II) regions of the spectrum, but there is anomalous dispersion in regions of water absorption (Downing & Williams, 1975, Bertie *et al.* 1989). Anomalous dispersion leads to $n_{H2O}$ = 1·39 and $n_{D2O}$ = 1·22 at $\nu$ = 2850 $cm^{-1}$, and $n_{H2O}$ = 1·29 at $\nu$ = 1650 $cm^{-1}$.

Condensed phase hydrocarbons and presumably also proteins have a refractive index of about 1·4–1·5 in the spectral region of interest. We have obtained reasonable and self-consistent results using $n_2 = 1{\cdot}43$ for biomembranes, but lower values may be warranted for regions of membranes with substantial amounts of bound water (e.g. the interface, see below). $E_{x,y,z}$ also depend on the angle of incidence, $\gamma$. Although this angle is nominally 45° with the geometry shown in Fig. 1, there may be in practice a distribution of angles $\gamma$ because the substrates are not perfectly flat. Surface roughness and microcrystallinity may also depolarize polarized light in the ATR crystal to some extent (A. Gericke and R. Mendelsohn, personal communication). Both of these effects would tend to underestimate the absolute value of order parameters that are calculated from measurements of $R^{ATR}$. Finally and as mentioned above, $E_z$ depends very critically on whether the thin film approximation or a model with only two bulk phases with refractive indices $n_1$ and $n_2$ is used. The difference between the two models is largest for large differences between $n_2$ and $n_3$ and vanishes as $n_2$ approaches $n_3$. Even a relatively small error in the value of $n_{32}$ has profound consequences on the calculated order parameters, because this factor enters as $n_{32}^4$ into eqn (13) in the thin film approximation. Although the thin film approximation has been successfully used by most investigators (including ourselves) studying thin membrane samples by ATR–FTIR spectroscopy, it has recently been argued that the two-phase model is better suited to treat such systems (Citra & Axelsen, 1996). The arguments of these authors were based on measurements of the infrared dichroism of model polymers in hydrated thin films. Unfortunately, the orientations of these polymers were not verified by independent diffraction measurements nor has their precise location in the film (depth and coverage with lipid) been assessed. Nevertheless, this work indicates that the orientation of segments of proteins that are largely exposed to water may be better evaluated with the two-phase model, or equivalently, the effective refractive index $n_2$ of the environment surrounding these groups has to be smaller than previously thought. The orientation of segments of proteins that are deeply embedded in the membrane are probably adequately evaluated with the thin film approximation as described above. Curves of $S_\theta$ *vs.* $R^{ATR}$ calculated for the thin film approximation and the two-phase model with several practically useful parameter sets are presented in Figure 3. The discrepancy between the two models increases as the difference between $n_2$ and $n_3$ increases. For example, the choice of the proper model is much more critical when working with samples in air ($n_3 = 1$) than with fully hydrated samples ($n_3 \approx 1{\cdot}33$).

## 6. METHODS OF SAMPLE PREPARATION

### 6.1 *Vesicle dispersions*

The simplest membrane samples for unoriented transmission spectroscopy are vesicle dispersions sandwiched between IR-transparent (e.g. $CaF_2$) windows. Pathlengths of 50 $\mu$m and 10 $\mu$m are typically chosen for samples in $D_2O$ or $H_2O$, respectively. Spectroscopy in $H_2O$ requires very high protein concentrations (20

to 50 mg/ml) to achieve adequate signal-to-noise ratios. In $D_2O$ protein concentrations of 0·1 to 1 mg/ml are often sufficient.

### 6.2 *Oriented multibilayers*

Oriented multibilayers have been used most frequently in polarized transmission and ATR IR studies. They are most adequate for studying pure lipid bilayers without inserted proteins (Fringeli & Günthard, 1981). Multibilayers of phospholipids are best prepared by casting them from organic solvent. Typically, a 10 $\mu$l drop of a 5 mM solution of lipid in chloroform or chloroform/methanol (4:1) is deposited on a carefully cleaned flat surface. The methanol helps to wet hydrophilic surfaces and ensures a smoother lipid deposition. This drop is then spread by slowly moving a thin glass or teflon rod along the surface and parallel to it until the solvent has evaporated. If evenly spread, the sample will become uniformly iridescent. For ATR spectroscopy it is important to roughly estimate the number of bilayers formed (i.e. the thickness of the film relative to $d_p$), which will affect whether the thin film approximation or the two-phase model has to be used for interpreting the polarized data (see above).

A second method that works well for multilayers of fatty acids, but not so well for phospholipids is the Langmuir–Blodgett–Kuhn technique (Kuhn, 1983). In this case, the plate is repeatedly immersed into the aqueous phase and withdrawn through a lipid monolayer that is spread at the air–water interface of a Langmuir trough. A single monolayer of lipid is transferred to the substrate at each passage through the interface as the surface pressure is kept constant throughout the procedure. This leads to more regular and better defined multilayer assemblies than can be achieved by solvent casting, but unfortunately, phospholipids do not transfer well after the first monolayer. However, up to 50 phosphatidylcholine bilayers could be deposited in the presence of 10 $\mu$M uranyl acetate (Peng *et al.* 1987). Multiple layers of phosphatidylethanolamines in the solid-condensed state can also be transferred under appropriate conditions (Akutsu *et al.* 1981).

Some researchers have simply deposited phospholipid vesicles in water (or buffer) which may or may not include incorporated proteins on the surface of ATR plates and then have let the water evaporate (Goormaghtigh & Ruysschaert, 1990). It is not clear whether pure lipid films prepared by this procedure are better or less well ordered than the solvent-cast ones. An isopotential spin-dry method has also been reported for the orientation of protein-containing membrane fragments on IR-transmitting substrates (Clark *et al.* 1980). In this method, large membrane fragments are centrifuged at high $\boldsymbol{g}$ forces. The bottom of a specially designed centrifuge cell is shaped according to the surface of a cylinder that is coaxial with the spin axis. This geometry provides for a gravitationally isopotential surface at high $\boldsymbol{g}$, which allows for a gradual coplanar deposition of the membrane fragments during evaporation of the solution.

The secondary and tertiary structures and the orientation of peptides and proteins may depend on the water content in the sample. Sometimes the dry planar membranes (prepared by either method) are reported to have been

'rehydrated' by extensively purging the sample compartment with vapour of $D_2O$ or $H_2O$. This most likely leads to a partial, but not to a full hydration of the interfacial region of the membrane. In addition, transient dehydration may irreversibly alter the structure of membrane proteins, particularly if they contain water-exposed domains. Salts and buffers which are often present to keep membrane proteins in their native conformation may lead to extreme ionic strength and pH conditions during drying which can be an additional source for irreversible structural changes of membrane proteins. Therefore, we believe that fully hydrated supported lipid bilayers (see below) provide more physiological conditions for IR studies of reconstituted membrane proteins.

### 6.3 *Monolayers*

FTIR spectroscopy is sensitive enough to measure spectra from monolayers of lipid at the air–water interface or transferred to a solid substrate. Monolayers at the air–water interface are measured by external reflection IR spectroscopy using a single external reflection (reviewed in Dluhy *et al.* 1995 and Mendelsohn *et al.* 1995*a*). This method has the advantages that monolayers can be studied *in situ*, i.e. unperturbed by a solid substrate, and that parameters such as surface pressure can be easily adjusted. The disadvantage is the relatively poor signal-to-noise ratio, especially if information is to be gathered from a complex amide I bandshape. Single lipid and lipid/peptide monolayers have been transferred to hydrophilic (Briggs *et al.* 1986; Cornell *et al.* 1989) and hydrophobic (Axelsen *et al.* 1995*a*) substrates and studied by ATR spectroscopy. In these experiments, a greater signal-to-noise ratio is achieved than in external reflection experiments due to the multiple internal reflections. When transferred to a hydrophilic support, the polar headgroups of the lipids (and the polar groups of proteins, if present) interact with the substrate and the spectra are generally recorded in the dry state. These conditions may influence some lipid and protein conformational properties. To mimic the interior of a lipid bilayer, Axelsen *et al.* (1995*a*) derivatized the internal reflection element with long chain alkyl groups before transferring a monolayer. This orients the monolayer with the headgroups facing away from the substrate and allows spectra to be recorded with the monolayers completely immersed in water. However, bilayer-spanning integral membrane proteins cannot be accommodated in any of these monolayer model systems.

### 6.4 *Supported bilayers*

Supported bilayers are single planar phospholipid membranes supported on a hydrophilic substrate and fully immersed in water or buffer (Tamm & McConnell, 1985). A thin (10–20 Å) film of water separates the bilayer from the solid substrate. This space permits integral membrane proteins to be functionally reconstituted in supported bilayers, provided the hydrophilic domains on at least one (i.e. the substrate-exposed) side are not too large. Lateral diffusion experiments established that the lipids in both leaflets of the bilayer are mobile and thus provide a physiological environment for membrane proteins (Tamm &

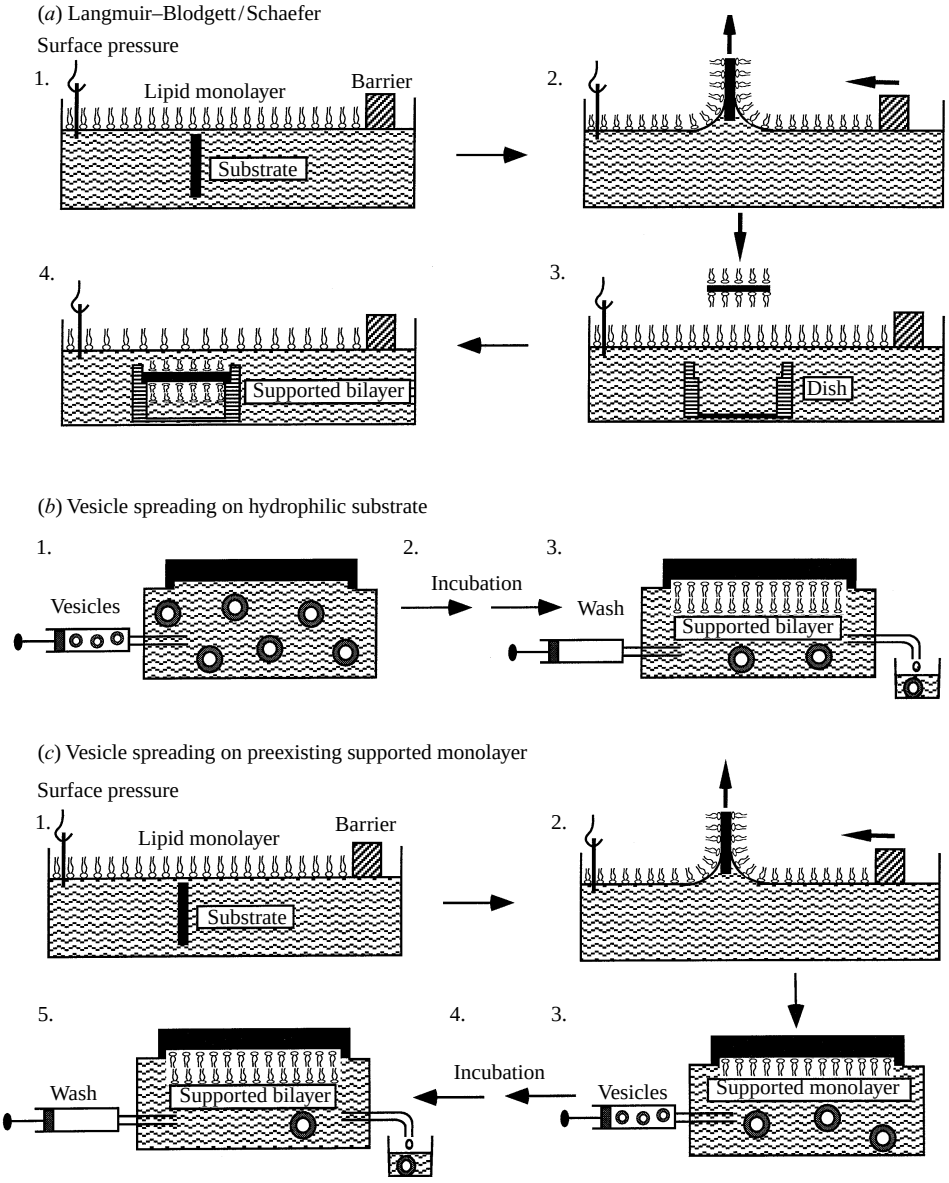


Fig. 4. Methods for preparation of fully hydrated supported lipid bilayers. (*a*) Langmuir-Blodgett/Schaefer technique. (*b*) Spreading of small unilamellar vesicles on a hydrophilic substrate. (*c*) Spreading of small unilamellar vesicles on a preexisting supported monolayer. (Adapted from Tamm & Kalb, 1993; see text for more detail.)

McConnell, 1985; Kalb *et al.* 1992; Tamm & Kalb, 1993). There are three methods to prepare supported bilayers (Fig. 4). The first is the Langmuir–Blodgett/Schaefer method (Tamm & McConnell, 1985). In this method, a monolayer is first transferred from the air–water interface of a Langmuir trough to the hydrophilic support at a constant surface pressure of

32–36 mN/m, i.e. the bilayer equivalence pressure. A second monolayer is deposited onto this surface by horizontal apposition of the substrate to a monolayer at the same pressure. The substrate with the bilayer is then collected in a dish or measuring cell under water avoiding any subsequent exposure to air. Fully hydrated high quality bilayers are obtained by this procedure which, however, is inadequate for reconstituting membrane proteins. A second method to prepare supported bilayers is by spreading vesicles on a hydrophilic substrate (Brian & McConnell, 1984). A dispersion of small unilamellar lipid vesicles which may also include reconstituted membrane proteins is brought into contact with the clean hydrophilic surface of the internal reflection element assembled in a liquid holding cell. These vesicles will spontaneously spread on the substrate and form a continuous planar bilayer in about an hour at room temperature. Again, these bilayers must not be exposed to air after formation, but excess vesicles can be easily flushed out of the cell by a large volume of buffer. At least two membrane proteins were incorporated into supported bilayers with a random transbilayer topology by this method (Contino *et al*. 1994; Erb *et al*. 1997). Most ATR work on supported bilayers has been carried out with samples prepared by a third method, i.e. the spreading of vesicles on a preexisting supported monolayer (Kalb *et al*. 1992; Wenzl *et al*. 1994). In this method, which sometimes is also referred to as monolayer fusion, a lipid monolayer is first transferred from the air–water interface of a Langmuir trough to the hydrophilic internal reflection element at the bilayer equivalence pressure. The monolayer-coated plate is then assembled in the liquid ATR holding cell and a dispersion of lipid vesicles with or without reconstituted proteins is injected. As in the direct spreading method, a bilayer forms by spontaneous self-assembly and excess vesicles are removed by flushing the cell with buffer. A $D_2O$-containing buffer may be introduced either at this or a later stage. The monolayer fusion method allows for the reconstitution of integral membrane proteins. Influenza virus hemagglutinin has been shown to become unidirectionally incorporated into supported bilayers by this method (Hinterdorfer *et al*. 1994). Generally, we find it advantageous to use a lipid monolayer in the solid-condensed phase as the coupling monolayer. For example, bilayers of DMPC undergo a chain melting phase transition at about 24 °C. Therefore, for best results the monolayer can be transferred below and the vesicles assembled above the phase transition temperature. Spectra may then be measured and compared at either temperature. When zwitterionic lipids in the liquid-expanded phase are used in the coupling monolayer, better surface coverage is obtained with a mildly acidic buffer (e.g. 10 mM Tris-acetic acid, pH 5·0) as the subphase in the Langmuir trough.

## 7. PURE LIPID SYSTEMS

FTIR spectroscopy on pure lipid systems, such as vesicles, monolayers, bilayers, or multibilayers has been successfully used to examine many structural properties of lipids in membranes such as their conformation, orientational order, phase

transitions, phase separation in multicomponent systems, state of ionization, ion binding, hydration, hydrogen bonding and others. This section is organized into separate discussions of the use of FTIR spectroscopy to probe the hydrophobic and interfacial regions of lipid membranes, followed by a brief summary of studies using FTIR spectroscopy to investigate chain melting phase transitions and lateral phase separations. For a comprehensive recent review on FTIR spectroscopy of unoriented hydrated lipid systems, the reader is referred to Lewis & McElhaney (1996).

### 7.1 *The hydrophobic region*

The frequency of the methylene stretching vibrations $\nu(CH_2)$ provides a sensitive qualitative measure of the conformational order of the lipid acyl chains. The frequencies of symmetric and antisymmetric $CH_2$ stretching vibrations of lipids increase from $\sim$ 2849 and $\sim$ 2917 $cm^{-1}$ to $\sim$ 2853 and $\sim$ 2923 $cm^{-1}$, respectively, upon a transition of the lipid from the ordered gel to the disordered liquid-crystalline phase (Cameron *et al.* 1980; Mendelsohn & Mantsch, 1986; Mantsch & McElhaney, 1991). Isotopic substitution of lipid acyl chain hydrogens with deuterium decreases the methylene stretching frequencies by 730–760 $cm^{-1}$. The symmetric and antisymmetric $CD_2$ stretching frequencies are centred at $\sim$ 2089 and $\sim$ 2194 in the gel phase and $\sim$ 2093 and $\sim$ 2196 $cm^{-1}$ in the liquid-crystalline phase, respectively (Mendelsohn *et al.* 1984*a*; Mendelsohn & Mantsch, 1986). Selective lipid acyl chain perdeuteration has been used to monitor the conformational order, phase transitions, and lateral phase separations of individual lipid components in two- or multi-component lipid bilayers in response to various external perturbations such as temperature, binding of ions, proteins, or fatty acids (Mendelsohn *et al.* 1984*b*; Dluhy *et al.* 1985; Muga *et al.* 1991*b*; Villalaín & Gómez-Fernández, 1992; Flach *et al.* 1993; López-García *et al.* 1994; Dibble *et al.* 1996). Acyl chain perdeuterated lipids were also used as probes to study lipid transfer between vesicles and supported bilayers (Reinl & Bayerl, 1994) and asymmetric lipid distribution between two leaflets of biomembranes (Moore *et al.* 1996).

Other methylene vibrational modes, such as scissoring $\delta(CH_2)$, wagging $w(CH_2)$, and rocking $\gamma(CH_2)$, have been used to study lipid systems. The methylene scissoring mode proved especially useful. In solid lipid phases, this vibrational mode is split, due to a coupling between transition dipoles in ordered hydrocarbon chains that depends on the chain packing. For example, the frequency of one component increases from $\sim$ 1463 to $\sim$ 1468 $cm^{-1}$ and that of the other decreases from $\sim$ 1473 to $\sim$ 1470 $cm^{-1}$ as a result of a solid–solid phase transition that converts orthorhombically packed into hexagonally packed chains. The corresponding shifts for perdeuterated ($CD_2$) lipids are from $\sim$ 1084 to $\sim$ 1088 $cm^{-1}$ and from $\sim$ 1093 to $\sim$ 1091 $cm^{-1}$, respectively (Casal & Mantsch, 1984; Mendelsohn *et al.* 1995*b*; Snyder *et al.* 1996). The coupling is short range and only occurs between isotopically identical methylene groups. Acyl chain

interdigitation can also be studied by monitoring the splitting of the scissoring $\delta(CH_2)$ mode at $\sim 1470\ cm^{-1}$ in bilayers. For example, chain interdigitated bilayers were induced in sulphogalactosyl-glycerolipids by $Na^+$, but not by divalent cations as detected by a pronounced splitting of the $\delta(CH_2)$ mode (Tupper *et al*. 1994). In ordered phases, the methylene wagging modes couple to produce band progressions, occurring between 1350 and $1180\ cm^{-1}$, that are sensitive to lipid acyl chain conformation and packing (Chia & Mendelsohn, 1992; Snyder *et al*. 1996). These progressions are absent in liquid-crystalline phases, but relatively localized wagging modes occur at 1368, 1353, and $1341\ cm^{-1}$. The relative intensities of these modes can be used to estimate the number of kink, double *gauche* and end *gauche* conformations, respectively (Chia & Mendelsohn, 1992; Senak *et al*. 1992; Lewis *et al*. 1994*a*). Isotopic substitution of selected segments in the hydrocarbon chain region has been developed into a powerful tool to probe the local bilayer structure in that region. For example, selective deuteration of lipid acyl chains was used to determine the propensities for trans-*gauche* isomerization at particular depths in the bilayer, based on the conformation-sensitive rocking modes of the $CD_2$ groups which occur between 610 and $680\ cm^{-1}$ (Mendelsohn *et al*. 1989; Mendelsohn & Snyder, 1996). These studies showed that the propensities of *gauche* conformers in DPPC in the liquid-crystalline phase are relatively constant in the acyl chain positions 4, 10 and 12 ($\sim 10\%$), but rise sharply to $\sim 40\%$ in position 14. Although different parameters at very different time scales are measured by the two techniques, the reason for the quite different *gauche* concentration and order parameter profiles measured by IR and $^2H$-NMR spectroscopy, respectively, are not clear. The $CD_2$ rocking modes overlap with the amide V band, and therefore, cannot be reliably analysed in the presence of proteins.

To determine the average orientational order of the hydrocarbon chain segments in lipid bilayers, the dichroic ratio of a corresponding absorbance band is measured and the order parameter is calculated by eqns (13) or (14). The methylene stretching or scissoring modes at 2800–3000 and $\sim 1470\ cm^{-1}$, respectively, have been used most often for this purpose. We stress that extreme care must be taken when interpreting and comparing dichroic ratios of oriented lipid films that were prepared by different methods. Dry lipid multibilayers, multibilayers that are hydrated by exposure to a high relative humidity atmosphere, and lipid bilayers in bulk water may exhibit different hydrocarbon chain order. The thickness of the sample and the proper refractive indices for the lipid films must be taken into account when order parameters are calculated from ATR dichroism measurements as noted in Section 5. Therefore, dichroic ratios, the precise experimental conditions, and the parameters that were used for the calculation of order parameters should be reported when IR dichroism results are described.

Okamura *et al*. (1990) studied the order of fully hydrated (85% water by weight) thick DPPC multibilayers by ATR–FTIR spectroscopy as a function of temperature. The order parameter derived from the symmetric methylene stretching vibration was 0·78 in the gel and $P_{\beta'}$ ('ripple') phase, but decreased to

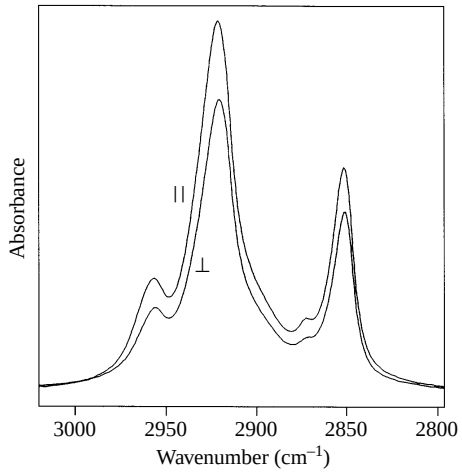


Fig. 5. ATR–FTIR spectra in the methylene stretching region of a fully hydrated single supported bilayer of DMPC, prepared by the monolayer fusion technique, at parallel and perpendicular polarizations of the IR beam. The measuring temperature was approximately 21 °C. The dichroic ratio and the derived order parameter are $1{\cdot}25 \pm 0{\cdot}02$ and $0{\cdot}45 \pm 0{\cdot}02$, respectively. (Reproduced from Tatulian *et al.* 1995*b*.)

0·40 in the liquid-crystalline phase. The chain melting phase transition was considerably broadened in partially hydrated bilayers, resulting in intermediate order parameters above the chain melting phase transition, $T_m$, of the fully hydrated membranes. Hübner & Mantsch (1991) report methylene stretching order parameters of 0·76–0·82 for DMPC and DPPC bilayers in the dry state; for hydrated bilayers the order parameter was 0·7 and 0·54 below and above $T_m$, respectively. These authors also measured the corresponding order parameters derived form the $CH_2$ scissoring and wagging band progressions. The scissoring band order parameters agreed extremely well with those derived from the methylene stretching bands, but the wagging band progression order parameters, when observable, were slightly lower. Lipids with unsaturated chains usually exhibit smaller order parameters than corresponding lipids with saturated chains. For example, the order parameter of dry DMPA multibilayers was $\sim 0{\cdot}75$ compared to that of eggPA which was $\sim 0{\cdot}4$ (Désormeaux *et al.* 1992; Nabet *et al.* 1994). Obviously, unsaturated chains do not pack as well in the dry state as those of saturated lipids. Similar differences have been reported for PCs in dry or partly hydrated films (Brauner *et al.* 1987; Frey & Tamm, 1991; Ishiguro *et al.* 1993; Arkin *et al.* 1996*a*). Polarized ATR spectra in the methylene stretching region of a fully hydrated supported DMPC bilayer that was prepared by the monolayer fusion technique are shown in Fig. 5. These spectra show the antisymmetric methyl stretching, the antisymmetric methylene stretching, the symmetric methyl stretching, and the symmetric methylene stretching bands at 2956, 2921, 2873 and 2851 cm$^{-1}$, respectively. These frequencies and the order parameter ($0{\cdot}45 \pm 0{\cdot}02$) that was derived from the dichroic ratios of both methylene stretching bands indicate that this supported lipid bilayer is within the chain melting phase

transition at ~ 21 °C, i.e. a result that is in agreement with fluorescence recovery after photobleaching experiments on the same system (Tamm, 1988). Typical order parameters in fully hydrated single supported bilayers are 0·3–0·5 for saturated PCs and 0·1–0·3 for unsaturated PCs at room temperature (Frey & Tamm, 1991; Tamm & Taulian, 1993; Tatulian *et al.* 1995*b*; Rodionova *et al.* 1995; Gray *et al.* 1996; Ishiguro *et al.* 1996). Order parameters in the range between 0·2 and 0·4 are expected from $^{2}$H-NMR experiments of selectively chain-deuterated lipids in the liquid-crystalline phase (Seelig & Seelig, 1980). Order parameters between 0·6 and 0·7 were obtained for DMPC or DPPC monolayers that were deposited on silane-coated Ge crystals and immersed in water (Axelsen *et al.* 1995*a*, *b*), which shows that very good lipid order can be achieved in this system.

### 7.2 *The interfacial region*

*Carbonyl stretching mode*. The ester carbonyl stretching vibration of *O*-acylated lipids is sensitive to the hydrogen bonding and other parameters that affect the structure of the interfacial region. For fully hydrated diacyl phosphatidylcholines, the ester C=O stretching vibration generates a broad band centred at ~ 1733 cm$^{-1}$ (Bush *et al.* 1980; Mendelsohn *et al.* 1981, 1984*b*; Levin *et al.* 1982; Wong & Mantsch, 1988; Blume *et al.* 1988; Villalaín & Gómez-Fernández, 1992; Lewis & McElhaney, 1993*a*; Lewis *et al.* 1994*b*). The corresponding peak frequency in phosphatidylethanolamines is centred at ~ 1739 cm$^{-1}$ (Blume *et al.* 1988; Wong & Mantsch, 1988; Cheng, 1994). In both lipid classes the ester C=O stretching frequency of anhydrous samples is increased by several cm$^{-1}$ as compared to that of hydrated samples (Wong & Mantsch, 1988; Lewis *et al.* 1994*b*; Salgado *et al.* 1995). The carbonyl stretching band in bilayers of hydrated mixed chain phosphatidylserines is split into two components at ~ 1742 and 1720–1728 cm$^{-1}$. The higher frequency band is more intense than the lower frequency band at low temperatures, but the intensities of the two components become comparable and the frequencies approach each other at higher temperatures (Dluhy *et al.* 1983; Mendelsohn *et al.* 1984*b*; Casal *et al.* 1987*a*). Resolution enhancement techniques revealed two carbonyl band components also in hydrated bilayers of PC, PE, PG and cardiolipin. They are centred at ~ 1742 and ~ 1728 cm$^{-1}$ (Babin *et al.* 1987; Blume *et al.* 1988; Wong & Mantsch, 1988; Muga *et al.* 1991*b*; Lewis *et al.* 1994*b*; Müller *et al.* 1996). Some of the earlier studies attributed the higher and lower frequency components to the *sn*-1 and *sn*-2 ester carbonyl groups, respectively, and the frequency shift was explained in terms of conformational differences between the two groups. However, later experiments using phospholipids with individually $^{13}$C=O labelled acyl chains showed that both chains contributed to both bands (Blume *et al.* 1988; Lewis *et al.* 1994*b*). A model study on triacetyl glycerol showed that the frequencies decreased from 1748 to 1732 (in $H_2O$) and 1728 (in $D_2O$) cm$^{-1}$ as a result of hydrogen bonding between water and the carbonyls of the glyceride (Mushayakarara *et al.* 1986). Thus, the higher and lower frequency components

of $\nu$(C═O) are due to dehydrated and hydrated carbonyl groups, respectively (Blume *et al.* 1988; Lewis *et al.* 1994*b*). In DMPC bilayers the *sn*-2 C═O group was more strongly hydrogen bonded than the *sn*-1 group, whereas the opposite was found in DMPG bilayers (Blume *et al.* 1988). Incorporation of dipalmitoylglycerol or $^{13}$C-labelled palmitic acid into hydrated DPPC bilayers resulted in an upward shift of the $\nu$(C═O) band, which was interpreted in terms of membrane dehydration by diacylglycerol and fatty acid (Villalaín & Gómez-Fernández, 1992; López-García *et al.* 1994). In hydrated sulfogalactosylglycerolipids the C═O stretching band was split into two components at ~ 1735 and ~ 1715 cm$^{-1}$, and the lower frequency component, which was likely generated by hydrogen-bonded C═O groups, decreased in intensity in response to divalent cation binding, presumably due to divalent cation-induced lipid dehydration (Tupper *et al.* 1994). $Ca^{2+}$-induced dehydration was also observed at the level of the ester carbonyl groups in mixed DMPC/deacetyl ganglioside $G_{M1}$ bilayers (Müller *et al.* 1996). Typical order parameters defined for the transition dipole moment of the ester carbonyl groups and derived from polarized ATR–FTIR spectra range from −0·18 to −0·26 (Hübner & Mantsch, 1991; Frey & Tamm, 1991; Désormeaux *et al.* 1992; Nabet *et al.* 1994; Müller *et al.* 1996).

*Phosphate $PO_2^-$ stretching modes*. Since the phosphate groups of phospholipids are strongly acidic and provide hydrogen bonding acceptors, the spectral characteristics of the antisymmetric and symmetric $PO_2^-$ stretching vibrations are very sensitive to hydrogen bonding and interactions with organic or inorganic cations including divalent cations, local anaesthetics, and basic peptides. Upon hydration, the $\nu_{as}(PO_2)$ frequency of anhydrous phosphatidylcholines decreases from ~ 1260 to 1220–1240 cm$^{-1}$ (Wong & Mantsch, 1988; Choi *et al.* 1991; Ueda *et al.* 1994). The $\nu_s(PO_2)$ mode occurring at ~ 1090 cm$^{-1}$ is less sensitive to hydration. At temperatures below the chain melting phase transition, the relatively broad $\nu_{as}(PO_2)$ band overlaps with the $CH_2$ wagging progressions of phospholipids. The frequency of $\nu_{as}(PO_2)$ increases by 2–3 cm$^{-1}$ at the pretransition (gel-to-$P_{\beta'}$) temperature of PCs, but is insensitive to the chain melting phase transition (Okamura *et al.* 1990; Lewis *et al.* 1996). In DMPS dispersions, the main phase transition is accompanied by a ~ 2 cm$^{-1}$ increase in the $\nu_{as}(PO_2)$ frequency (Casal *et al.* 1987*b*). Interestingly the $\nu_{as}(PO_2)$ frequency decreases from 1231 to 1220 cm$^{-1}$ upon substitution of acyl chains by alkyl chains in di($C_{16}$)PC, although acyl lipids are expected to be more strongly hydrated because of the presence of the carbonyl groups (Lewis *et al.* 1996). Displacement of water by alcohols further decreases the $\nu_{as}(PO_2)$ frequency (Chiou *et al.* 1992). Similarly, the frequency of $\nu_{as}(PO_2)$ in reverse micelles of DPPC decreases from 1238 to 1233 cm$^{-1}$ upon addition of the cationic local anaesthetic lidocaine (Ueda *et al.* 1994). The order parameters of the phosphate and choline groups of PCs were close to zero, which may indicate that the transition moments of these groups are oriented near the magic angle (Hübner & Mantsch, 1991; Désormeaux *et al.* 1992; Nabet *et al.* 1994).

The $\nu_{as}(PO_2)$ frequency of dry phosphatidylethanolamines is found at

1218–1224 $cm^{-1}$, i.e. at a lower frequency than the corresponding band of dry PCs. This frequency shift has been attributed to intermolecular headgroup hydrogen bonding in PE bilayers (Lewis & McElhaney, 1993*b*; Salgado *et al.* 1995). This interpretation is consistent with the absence of significant changes in $\nu_{as}(PO_2)$ of PEs upon hydration. The $\nu_{as}(PO_2)$ vibration of dry DOPS occurs at $\sim$ 1238 $cm^{-1}$ and decreases to 1221–1223 $cm^{-1}$ upon hydration (Choi *et al.* 1991). However, this frequency shift is reversed upon addition of equimolar quantities of $Ca^{2+}$ which is a good indication for dehydration of the phosphate group by $Ca^{2+}$ ions (Casal *et al.* 1987*a*, *b*; Flach & Mendelsohn, 1993). The influence of $Ca^{2+}$ is stronger on 1:1 DPPC:DPPS than on pure DPPC, consistent with a stronger binding of $Ca^{2+}$ to the negatively charged lipid bilayers (Flach *et al.* 1993).

*Other vibrational modes*. Other vibrational modes of lipids that are sensitive to their structure and interactions with the environment include the choline vibrations of PCs, the carboxyl vibrations of PSs and gangliosides, the amide modes of gangliosides, and the $SO_2$ stretches of sulphatides. The choline antisymmetric C–N–C stretch occurs at $\sim$ 971 $cm^{-1}$ (Casal & Mantsch, 1984; Wong & Mantsch, 1988). This frequency increases by $\sim$ 2 $cm^{-1}$ upon hydration. The symmetric choline stretch is conformation-sensitive; it gives rise to bands at 920–930 $cm^{-1}$ and $\sim$ 900 $cm^{-1}$ which have been attributed to *trans* and *gauche* conformers of the O–C–C–N group, respectively (Fringeli & Günthard, 1981; Grdadolnik *et al.* 1991).

The carboxyl group of PS gives rise to vibrations at $\sim$ 1740 and $\sim$ 1622 $cm^{-1}$ in the protonated (COOH) and ionized ($COO^-$) forms, respectively (López-García *et al.* 1995). The relative intensities of these two bands can be used in pH titrations to determine the apparent pK of PSs in lipid bilayers. An analogous approach has been used to determine apparent pKs of fatty acids in lipid bilayers by IR spectroscopy (Lieckfeld *et al.* 1995; Villalaín & Gómez-Fernández, 1992). The $SO_2^-$ symmetric and antisymmetric stretching modes of sulphogalactosyl-glycerolipids occur at 1040–1080 and 1200–1240 $cm^{-1}$, respectively. The latter was used to study the interactions of these lipids with divalent cations (Tupper *et al.* 1992, 1994).

Gangliosides exhibit two absorbance bands at $\sim$ 1730 and $\sim$ 1605 $cm^{-1}$ due to the antisymmetric stretching of protonated and deprotonated carboxyl groups of sialic acids. In addition, a broad amide I band centred at 1629 $cm^{-1}$ is found in spectra of these complex lipids (Müller & Blume, 1993; Müller *et al.*, 1996). Some gangliosides ($G_{M1}$ and $G_{M3}$) exhibit an additional band at $\sim$ 1650 $cm^{-1}$ which has been attributed to partially dehydrated amide groups. Binding of $Ca^{2+}$ changed the amide I region of some gangliosides in mixtures with DMPC, but did not affect the $\nu_{as}(COO^-)$ band (Müller *et al.* 1996).

### 7.3 *Lipid phase transitions*

IR spectroscopy has been utilized extensively to study phase transitions of phospholipid bilayers and their modification by a large number of different substances. Consequently, the literature on this topic is extremely large and a

detailed summary is beyond the scope of this review. More comprehensive recent summaries on IR studies of lipid phase transitions can be found in Jackson & Mantsch (1993) and Lewis & McElhaney (1996). Here, we will only highlight a few main conclusions. The most frequently used marker to study the chain melting phase transition of lipid bilayers is a shift of the $\nu_s(CH_2)$ frequency. For example, the $T_m$ of a homologous series of phospholipids was found to decrease gradually upon *N*-methylation from DPPE to DPMePE to $DPMe_2PE$ to DPPC (Casal & Mantsch, 1984). This shift of the $T_m$ correlated with a progressive decrease in intermolecular headgroup hydrogen bonding as deduced from changes in $\nu_{as}(PO_2)$. $T_m$ has also been detected by changes of the scissoring, rocking and wagging band progressions. Because these latter modes are sensitive to details of chain packing in lipid bilayers they offer the additional possibility to monitor various types of sub-gel phase transitions. The bandwidths of the lipid $CH_2$ stretching, scissoring and rocking vibrational modes increase cooperatively at the lipid gel-to-liquid-crystalline phase transitions, indicating increased conformational disorder in the liquid-crystalline phase (Casal & Mantsch, 1984; Mendelsohn & Mantsch, 1986; Brumm *et al.* 1996). The ester carbonyl stretching vibration $\nu(C{=}O)$ shows a marked response to $T_m$ and the lamellar-to-hexagonal phase transition (Mantsch *et al.* 1981). The order parameters of the hydrocarbon chains of DPPC bilayers decrease upon melting of the hydrocarbon chains, but those of the phosphate and choline groups are more affected by the pretransition, demonstrating a large effect of the latter transition on the headgroup structure of PCs (Okamura *et al.* 1990).

The induction of lipid phase transitions by ion binding has also been studied by IR spectroscopy. For example, the binding of divalent cations to acidic lipid bilayers decreased the $CH_2$ stretching frequencies, indicating a decreased conformational flexibility of the lipid acyl chains (Dluhy *et al.* 1983; Casal *et al.* 1987*a*, *b*; Flach *et al.* 1993; Hübner *et al.* 1994). Protonation of DMPG at pH 2 resulted in an increase of $T_m$ by $\sim$ 18 °C and a decrease of similar magnitude is observed upon deprotonation of $DMPA^-$ to $DMPA^{2-}$ (Tuchtenhagen *et al.* 1994). Incorporation of cholesterol in DPPC bilayers increases $\nu_s(CH_2)$ below $T_m$ and decreases $\nu_s(CH_2)$ above $T_m$, indicating that cholesterol decreases (increases) the conformational order of lipids below (above) $T_m$ (Cortijo *et al.* 1982; Reis *et al.* 1996). Similarly, addition of cholesterol to PS bilayers with bound $Ca^{2+}$ introduces acyl chain disorder as judged from an increase in $\nu_s(CH_2)$ and further accentuates the $Ca^{2+}$-induced dehydration of PS bilayers (Choi *et al.* 1991).

### 7.4 *Lateral phase separation and lipid domains*

Lateral phase separation occurs spontaneously in lipid bilayers with immiscible components or may be caused by exogenous agents. Lipid phase separation can lead to the formation of domains in membranes which may have a number of biologically important consequences (Thompson *et al.* 1995). FTIR spectroscopy has been used to monitor lipid phase separation by measuring the temperature dependence of the $\nu(CH_2)$ and $\nu(CD_2)$ frequencies of lipids with fully

hydrogenated and deuterated acyl chains, respectively. Miscibility of the two components is then measured by the extent to which the melting temperature and cooperativity of the individual components are retained in the mixture. Using this method, well-defined phase-separated domains were identified in DPPC/DMPC-$d_{54}$ (Dluhy *et al.* 1985) and DPPC-$d_{62}$/dipalmitoylglycerol (López-García *et al.* 1994) binary systems as well as in DPPC-$d_{54}$/DMPS-$d_{54}$/dioleoylglycerol and DMPC/DMPS-$d_{54}$/dioleoylglycerol ternary systems (Dibble *et al.* 1996). The result of the latter study indicated that dioleoylglycerol may interact more favourably with DMPS than with DMPC, which is likely to contribute to the activation of protein kinase C. Villalaín & Gómez-Fernández (1992) showed that DPPC-$d_{62}$ and palmitic acid were ideally miscible at pH 7·4, but were phase separated at pH 11, when the fatty acid was fully ionized. In an external reflection FTIR study, it was shown that $Ca^{2+}$ ions do not cause segregation in DPPC-$d_{62}$/DPPS monolayers at the air/water interface, although $Ca^{2+}$ phase-separates bilayers of similar composition (Flach *et al.* 1993). The phase separation in DMPC-$d_{54}$/DSPC bilayers that were supported on glass beads depended on size of the beads; separation into solid DSPC and fluid DMPC-$d_{54}$ phases increased with increasing curvature of the bilayers (Brumm *et al.* 1996). Using the effect of short-range coupling between methylene scissoring modes of isotopically identical hydrocarbon chains in close-packed systems, Snyder *et al.* (1995) and Mendelsohn *et al.* (1995*b*) detected microdomains with orthorhombically packed chains in various binary lipid systems. The FTIR method to detect phase separation is not limited to pure lipid systems, but has also been applied to study lateral and transmembrane segregation of DMPC-$d_{54}$ and DMPS-$d_{54}$ in erythrocyte membranes (Moore *et al.* 1996, 1997). Incubation of red cells with DMPC-$d_{54}$ and DMPS-$d_{54}$ resulted in echinocytic and stomatocytic morphology of the cells, respectively. Only DMPC-$d_{54}$ segregated into distinct domains in the outer leaflet, whereas DMPS-$d_{54}$ was uniformly distributed in the inner leaflet of the erythrocyte membranes.

## 8. CONFORMATION AND ORIENTATION OF MEMBRANE-BOUND PEPTIDES

FTIR spectroscopy has become an important tool to study the conformation and orientation of membrane-bound peptides. Studies of peptide structure in lipid bilayers have become particularly rewarding because interpretation of spectra of peptides with relatively short amino acid sequences is quite straightforward and the effect of small sequence changes on the spectral parameters can be easily assessed by chemically synthesizing variant peptides with altered sequences. In addition and as already mentioned, the method requires only small amounts of material, does not depend on introducing spectroscopic probes, and is not influenced by light scattering artifacts or otherwise limited by the size of the object. Therefore, FTIR spectroscopy can be applied to peptides in solution, detergent micelles, or lipid bilayers which allows one to investigate structural changes of peptides as a function of their environment, for example in the course of a binding experiment. Polarized FTIR spectroscopy on oriented samples, is

perhaps the easiest of the presently available methods to determine peptide orientation in lipid bilayers. As a general note of precaution, investigators planning to analyse amide I bands of synthetic peptides should be aware that some solvents that are commonly used in peptide synthesis and purification absorb in the amide I region and need to be removed before this band is analysed. Most importantly, trifluoroacetic acid absorbs at $\sim 1673\ cm^{-1}$.

*Peptide hormones*. Some of the earliest IR studies on peptide-lipid interactions were carried out by Fringeli, Schwyzer and coworkers. Their primary interest was to determine by ATR spectroscopy the secondary structure and orientation of membrane-bound hormones such as adrenocorticotropin, dynorphin and bombesin (Gremlich *et al*. 1983, 1984; Erne *et al*. 1985; Erne & Schwyzer, 1987). Adrenocorticotropin is a 24-residue peptide with a hydrophobic N-terminus (residues 1–10) and an amphiphilic and highly charged C-terminus (residues 11–24). The authors investigated the complete peptide as well as the hydrophobic effector or 'message' domain and the amphiphilic 'address' domain of the hormone. They concluded that the hydrophobic domain was inserted into the membrane as a perpendicularly oriented helix and that the charged domain adopted an amphipathic secondary structure at the membrane surface. The covalent linkage of the message and address domains was necessary for efficient membrane binding. Conformational changes of atriopeptin III as a result of membrane binding were investigated by Surewicz *et al*. (1987*a*). This peptide had no secondary structure in solution, but adopted a large fraction of $\beta$-structure when bound to bilayers. Similar conclusions were reached with angiotensin (Surewicz & Mantsch, 1988). These early studies on peptide hormones touched on several themes that are recurring in many of the later investigations on peptide structures in lipid bilayers: upon membrane-binding peptides often undergo a conformational change from random structures to $\alpha$-helix or $\beta$-structures; depending on their particular sequences, the peptides adopt amphipathic structures at the interface or transverse structures in the hydrophobic core of the lipid bilayer; and, studies of fragments often facilitate the interpretation of spectra of more complex peptides. The adsorption to supported lipid bilayers and concomitant changes in secondary structure of human calcitonin were investigated in a more recent ATR spectroscopic study (Bauer *et al*. 1994). It was concluded that a small fraction of $\alpha$-helix was first formed upon membrane binding and that the formation of a larger fraction of $\beta$-sheet was kinetically delayed relative to the formation of $\alpha$-helix which was already very slow.

*Alamethicin and related peptides*. Alamethicin is a 19-residue hydrophobic antibiotic peptide which under appropriate conditions forms voltage-gated ion channels in membranes and, therefore, has often served as a model for larger channel proteins. The peptide is rich (8 residues) in the unusual amino acid amino-isobutyric acid (Aib). Its structure in crystals that were grown from acetonitrile/methanol solution is known to be predominantly $\alpha$-helical (Fox & Richards, 1982). An amide I band centred at $1662\ cm^{-1}$ has been found in membrane-incorporated alamethicin (Haris & Chapman, 1988). This frequency is about 6–10 wavenumbers above the frequency that is normally found for soluble

or membrane-inserted $\alpha$-helices, although unusually high amide I frequencies occur in some $\alpha$-helices in lipid bilayers (see below). The authors conclude that this higher frequency is an indication for a partial $3_{10}$-helix structure of alamethicin in lipid bilayers. A weaker band at 1639 $cm^{-1}$ has also been assigned to this structure. This interpretation is supported by FTIR studies on a family of Aib-rich model peptides that are known to contain $3_{10}$-helices (Kennedy *et al.* 1991). These peptides have their main amide I band at 1662–1666 $cm^{-1}$ and two minor bands at 1644–1646 $cm^{-1}$ and 1678–1681 $cm^{-1}$. Fringeli & Fringeli (1979) concluded that alamethicin was incorporated into dry multibilayers with its helix axis oriented perpendicular to the plane of the bilayer.

*Gramicidins*. Gramicidins are antibiotic peptides which have also served as models for ion channels. Since their sequences comprise alternating L- and D-amino acids, they form $\beta^{6,3}$-helices in lipid bilayers. The $\phi$ and $\psi$ torsion angles and the hydrogen bonding patterns of this structure resemble those of $\beta$-sheets more closely than those of the $\alpha$- or $3_{10}$-helices. Therefore, it is not surprising that the major amide I component of gramicidins A and D in lipid bilayers is centred at 1635–1638 $cm^{-1}$ (Nabedryk *et al.* 1982*a*; Okamura *et al.* 1986; Bouchard & Auger, 1993; Axelsen *et al.* 1995*b*). These studies also concluded that the gramicidin helix is oriented approximately perpendicular to the plane of the membrane in dry multibilayers and supported monolayers, although in some of these studies the peptide order parameter was not particularly high ($S_\theta \approx 0{\cdot}3$–$0{\cdot}6$).

*Melittin*. Another frequently studied model peptide with hydrophobic and positively charged surfaces is the 26-residue bee venom peptide melittin. The crystal structure shows that melittin forms a highly amphipathic $\alpha$-helix (Terwilliger *et al.* 1982). This structure is preserved in lipid bilayers (Vogel & Jähnig, 1986; Ikura *et al.* 1991). Interest in melittin arises because it induces voltage-gated pores in lipid bilayers at low concentrations and is membranolytic at higher concentrations. Its structure is consistent with a surface location (e.g. at low peptide/lipid ratio and in the absence of a membrane potential) or with a membrane-spanning topology when assembled into an oligomer (e.g. at higher peptide/lipid ratios or in the presence of a trans-negative membrane potential). The orientation of melittin in lipid bilayers has been controversial. Early polarized IR experiments on dry membrane preparations suggested a transmembrane helix orientation (Vogel *et al.* 1983; Brauner *et al.* 1987; Weaver *et al.* 1992). However, this orientation was inconsistent with spin-label EPR results which indicated that melittin binds at the interface with its helix approximately parallel to the plane of the membrane (Altenbach *et al.* 1989; Kleinschmidt *et al.* 1997). This apparent discrepancy could be resolved when it was shown that the orientation of melittin in lipid bilayers depends on the kind of model membranes that were used (Frey & Tamm, 1991). In this study, it was found that melittin was oriented preferentially perpendicular to the plane of the membrane in dry multibilayers, but preferentially parallel to the membrane when bound to fully hydrated supported bilayers. Polarized ATR spectra in the amide I′ and II′ region of melittin bound to supported bilayers in $D_2O$ are shown in Fig. 6. Apparently, partial rehydration of dry multibilayers by water vapour is not sufficient to switch

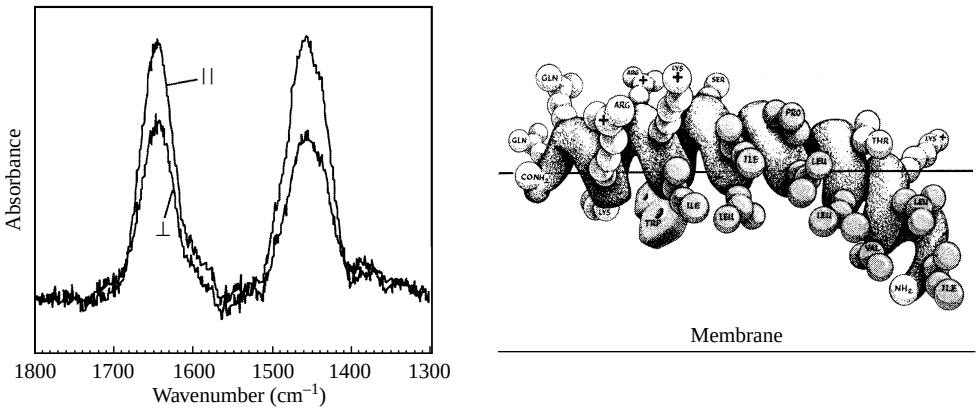


Fig. 6. ATR–FTIR spectra in the amide I′ and II′ region of melittin bound to a fully hydrated single supported bilayer of POPC:POPG (4:1) at parallel and perpendicular polarizations of the IR beam (left) and a model for the membrane-bound structure of melittin. (Adapted from Frey & Tamm, 1991 and Terwilliger *et al.* 1982.)

the orientation of melittin (Vogel, 1987). Based on these experiences with melittin, we recommend to use fully hydrated model membranes to determine secondary structure and orientation of peptides that combine polar and apolar character.

*Other hydrophobic and amphiphilic model peptides*. Beginning in the early 1990s, we have witnessed a large increase in FTIR studies (especially using polarized ATR–FTIR) of peptide-lipid complexes. Of particular interest for understanding general principles of membrane protein structure and folding are studies conducted with hydrophobic and amphiphilic model peptides. An interesting series of peptides that served as excellent models for transmembrane helices was developed by Bloom, Hodges and coworkers (Davis *et al.* 1983). These peptides consist of a hydrophobic core of leucines or alternating leucines and alanines, flanked by two lysines each at the N- and C-termini. The length of the hydrophobic core sequence has been changed; 24 residues best accommodate the peptide in relatively long chain fluid lipid bilayers. These peptides are designated $L_{24} = K_2[G]L_{24}K_2[A]$ (G and A are optional) and $LA_{12} = K_2(LA)_{12}K_2$, respectively. McElhaney and coworkers studied these peptides inserted into lipid bilayers by FTIR spectroscopy (and differential scanning calorimetry) in quite some detail. Zhang *et al.* (1992*a*, 1995*a*) found that $L_{24}$ and $LA_{12}$ were predominantly $\alpha$-helical and that there were fast and slowly exchanging populations of amide protons in organic solvents. The more slowly exchanging population was attributed to amide groups in the leucine core of the peptide and this population became virtually unexchangeable when the peptides were incorporated in phosphatidylcholine bilayers. The amide I frequency of $L_{24}$ increased from $\sim$ 1655 to $\sim$ 1658 cm$^{-1}$ when a long chain lipid bilayer went through the liquid-crystalline-to-gel phase transition (Zhang *et al.*, 1992*b*). One possible explanation of this effect is that the hydrophobic thickness of the fluid lipid bilayer matches with the hydrophobic length of this model peptide, but the

gel-phase bilayer is too thick and therefore stretches the transmembrane helix, leading to increased intra-helical hydrogen bond lengths and an increased amide I frequency (see below). This effect was much larger for $LA_{12}$ for which the amide I frequency increased from $\sim 1656\ cm^{-1}$ to $\sim 1667\ cm^{-1}$ when the bilayer thickness was increased by a transition to the gel phase (Zhang *et al.*, 1995*b*). The orientations of both peptides were measured in dry multibilayers by ATR spectroscopy (Axelsen *et al.* 1995*b*; Zhang *et al.* 1995*a*) and found to be approximately parallel to the acyl chains, i.e. in agreement with results obtained by X-ray diffraction of similarly prepared samples (Huschilt *et al.* 1989). Ishiguro *et al.* (1993, 1996) studied the orientation of an amphipathic helix-forming model peptide in dry multibilayers and hydrated supported bilayers. The peptide was oriented close to parallel to the plane of the membrane in both model systems. A similarly designed amphipathic helical model peptide inserted perpendicularly into multibilayers (Goormaghtigh *et al.* 1991*a*). The reasons for this apparent discrepancy are not known.

*Signal peptides*. Signal peptides are N-terminal extensions of proteins that are targeted to cellular membranes. They assist the insertion and translocation of such proteins in membranes. Many signal peptides form amphipathic helices in lipid environments (Gierasch, 1989; Tamm, 1991) and, therefore, share several features with melittin (see above). The signal peptide of the *E. coli* $\lambda$ phage receptor LamB was investigated in dry transferred lipid monolayers by ATR spectroscopy (Briggs *et al.* 1986; Cornell *et al.* 1989). At low lipid surface pressure this peptide was found to be inserted in the lipid bilayer as an $\alpha$-helix, but at higher surface pressures it adsorbed to the monolayer in a $\beta$-strand conformation. Although these studies were extremely valuable as early demonstrations of the power of the ATR-FTIR technique to detect conformational equilibria of membrane-bound peptides, the physiological relevance of these results obtained under rather extreme conditions may be limited. The conformations and orientations of several wild-type and mutant signal peptides of the PTS permeases of *E. coli* were studied in hydrated supported lipid bilayers (Tamm & Tatulian, 1993). The wild-type peptides formed amphipathic helices that were preferentially oriented parallel to the membrane surface, whereas the mutant peptides, although helical, were more randomly or more obliquely inserted.

*Fusion peptides*. Fusion peptides are highly conserved, relatively hydrophobic sequences of fusion proteins that are critical for membrane fusion, such as in virus infection or fertilization. There is strong evidence that the fusion peptides (and only the fusion peptides) insert into the lipid bilayer of target membranes during viral membrane fusion (see, e.g., Durrer *et al.* 1996). The conformations and orientations in lipid bilayers of several fusion peptides have been investigated by FTIR spectroscopy. The fusion peptide of gp41 of human immunodeficiency virus (HIV) was helical in negatively charged lipid bilayers at low peptide-to-lipid ratios, but adopted $\beta$-structure at higher peptide-to-lipid ratios or when bound to uncharged lipid bilayers (Rafalski *et al.* 1990). Nieva *et al.* (1994) concluded that the HIV fusion peptide adopted $\beta$-structure when bound to POPG bilayers in the presence of $Ca^{2+}$, i.e. conditions supporting peptide-mediated membrane fusion,

but was $\alpha$-helical in the absence of $Ca^{2+}$, i.e. conditions supporting leakage of the vesicle contents. A shorter version of this peptide contained $\sim 50\%$ $\beta$-structure and $\sim 25\%$ $\alpha$-helix when incorporated into multibilayers consisting of PC/PE/sphingomyelin/cholesterol or PC/sphingomyelin/cholesterol (Martin *et al*. 1993). The orientation of the helical segment depended on the presence of PE in the host bilayer in this study. Variants of this peptide with deletions at the N-terminus also changed their orientation in the membrane (Martin *et al*. 1996). The secondary structure and orientation of the fusion peptide of influenza virus hemagglutinin (HA) were studied in multibilayers (Lüneberg *et al*. 1995) and hydrated supported bilayers (Gray *et al*. 1996). Both studies found that the HA fusion peptide contained about 40% $\alpha$-helix which inserted at an oblique angle. In addition, Gray *et al*. (1996) suggested that the wild-type fusion peptide contained about 30% $\beta$-structure which was also inserted at an oblique angle. The fraction of $\beta$-structure was increased and the fraction of $\alpha$-helix decreased in several non-fusogenic mutant HA fusion peptides (Gray *et al*. 1996). The fusion peptide of the sperm fusion protein fertilin underwent a conformational change from an unordered to $\beta$-structure when it bound to charged or uncharged lipid vesicles (Muga *et al*. 1994).

*Segments of channel and other transmembrane proteins*. The secondary structure and orientation in lipid bilayers of synthetic or proteolytically produced putative trans-membrane (TM) segments of several integral membrane proteins, including ion channels, were investigated by FTIR spectroscopy. For example, the hydrophobic segment corresponding to residues 71–99 of glycophorin A (GPA) reconstituted into supported lipid bilayers was $\sim 70\%$ $\alpha$-helical in DMPC bilayers and exhibited an order parameter of 0·35–0·5, i.e. an orientation that is relatively close to, but not exactly parallel to the membrane normal (Smith *et al*. 1994). A study in which a slightly different proteolytic fragment including residues 66–95 of GPA was investigated found a similar content and orientation of the $\alpha$-helix in DMPC bilayers, but in addition identified some $\beta$-structure, which presumably is located at the N-terminus of this peptide (Challou *et al*. 1994). While GPA forms a helical dimer in the erythrocyte membrane, phospholamban (PLB) most likely exists as a pentameric coiled-coil in cardiac sarcoplasmic reticulum, where it regulates the Ca-ATPase through direct protein interaction and/or through forming a Ca-channel of its own. Two recent ATR–FTIR studies found that the C-terminal putative TM segments of PLB inserted as approximately perpendicular helices in lipid bilayers (Arkin *et al*. 1995; Tatulian *et al*. 1995*b*). The five subunits assemble by interaction of several leucines ('leucine zipper') in the membrane (Simmerman *et al*. 1996). However, slightly different structures were deduced for the N-terminal cytoplasmic segments in these two works. Although there is agreement that these segments are partially helical, Arkin *et al*. (1995) modelled PLB with a single continuous helix, whereas the model of Tatulian *et al*. (1995*b*) includes a small amphipathic $\beta$-hairpin which separates the cytoplasmic and TM helices (Fig. 7). A possible reason for this discrepancy is that fully hydrated membranes were used by Tatulian *et al*. (1995*b*), whereas Arkin *et al*. (1995) reconstituted PLB in stacks of

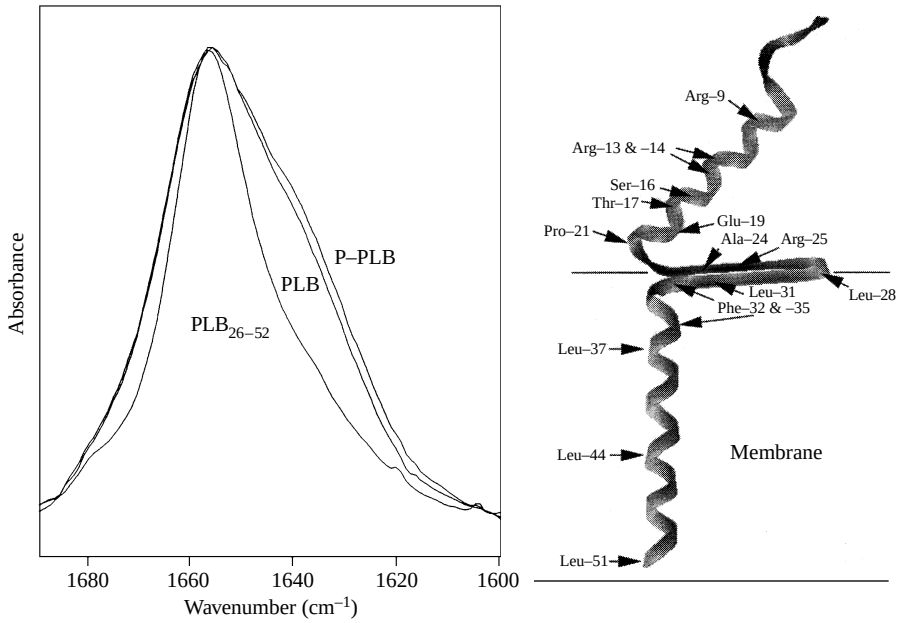


Fig. 7. Parallel polarized ATR–FTIR spectra in the amide I′ region of phospholamban (PLB), phosphorylated phospholamban (P–PLB) and the transmembrane segment of phospholamban ($PLB_{26–52}$) inserted into fully hydrated single supported bilayers of DMPC (left) and a model for the structure of phospholamban (only one subunit of the homopentamer is shown) in a lipid bilayer. (Adapted from Tatulian *et al.* 1995*b*).

dry multibilayers. The helical structure of the TM segment was subsequently confirmed with a site-directed isotopically ($^{13}C_{amide}$) labelled TM-peptide (Ludlam *et al.* 1996) and the rotational orientation of the TM helices in the membrane was probed by H/D exchange experiments of the lipid-exposed peptide sulphydryl groups (Arkin *et al.* 1996*b*). The single hydrophobic helices of the coat proteins of the bacteriophages M13 and Pf3 were found by ATR spectroscopy to be oriented preferentially parallel to the membrane normal ($S_\theta \approx 0{\cdot}81$ and $0{\cdot}58$, respectively) in air-dried samples of these proteins reconstituted in POPC/POPG bilayers (Thiaudière *et al.* 1993). When IR spectra of the Pf1 coat protein were compared in the phage and reconstituted into lipid bilayers, a shift of the amide I band from $\sim 1652$ to $\sim 1658$ $cm^{-1}$ was noted upon transfer into the membrane (Azpiazu *et al.* 1993). About 50–60% of the amide hydrogens could be exchanged with deuteriums within 24 hours. The non-exchanging fraction presumably represents the membrane-embedded helix of this protein.

The extracellular loop connecting the proposed fifth and sixth TM helices (S5–S6) of the *Shaker* potassium channel confers ion selectivity to the channel and, therefore, has been proposed to fold back into the membrane. FTIR spectra of a 19-residue peptide analog of this sequence in detergent micelles or lipid bilayers indicated mainly $\alpha$-helical secondary structure (Haris *et al.* 1994). Since, based on site-directed mutagenesis studies, $\beta$- or $\alpha$- and $\beta$-structures have been proposed for these 'pore loops', it is possible that either some of the predictions

about these structures are wrong or that the synthetic peptides do not correctly reflect their structure in the context of the whole protein. The hydrophobic segments S3 and S4 of the *Shaker* $K^+$ channel have also been synthesized. S3 was partially $\alpha$-helical ($\sim 30\%$) and only partly TM-oriented ($S \sim 0{\cdot}23$), whereas the amphipathic voltage sensor S4 was about $\sim 50\%$ $\alpha$-helical and oriented approximately parallel to the membrane surface ($S \sim -0{\cdot}32$) (Peled-Zehavi *et al.* 1996). The putative TM segment of the slow voltage-gated potassium channel IsK assumed an almost complete $\beta$-structure in lipid bilayers, possibly with the strands tilted from the membrane normal by a large angle (Aggeli *et al.* 1996). Even if these results obtained with fragments of large integral membrane proteins are perhaps insufficient to describe their structure in the complete protein, they may offer valuable insight into possible folding pathways of these proteins.

*Other antimicrobial peptides*. The antimicrobial peptides magainin, tachyplasin, trichopolin and hypelcin (and some relatives) bound to lipid bilayers were investigated by (ATR–)FTIR spectroscopy (Jackson *et al.* 1992; Matsuzaki *et al.* 1991, 1993). Some of these peptides adopt $\alpha$-helices and others $\beta$-structures in lipid bilayers. The structures of these peptides are rather amphiphilic and, therefore, they most likely bind to the interface or form transmembrane oligomers. Their binding generally induces leakage of contents from closed membrane vesicles, i.e. a reaction which likely reflects their antimicrobial activity. Cecropin P1 is a basic 31 residue peptide from mammalian small intestine that has antibacterial activity. The peptide forms an amphipathic $\alpha$-helix in various solvents as determined by NMR spectroscopy (Sipos *et al.* 1992) and binds to membrane surfaces in a preferentially parallel orientation as determined by ATR–FTIR spectroscopy (Gazit *et al.* 1996).

## 9. INTEGRAL MEMBRANE PROTEINS

A quite large number of membrane proteins have been investigated by FTIR spectroscopy. Rather than providing a complete review of these studies, only a few representatives of the major groups of integral membrane proteins that may be instructive for future studies of integral membrane proteins by FTIR spectroscopy are discussed in this section. In accordance with the general focus of this review, we mainly describe polypeptide backbone conformations and lipid–protein interactions. Excellent reviews pertaining to changes of side chain structures in the catalytic cycle of several membrane-bound enzymes, particularly in photobiological systems, can be found elsewhere (Braiman & Rothschild, 1988; Mäntele, 1993; Nabedryk, 1996).

*Seven-helix receptors*. Although not G-protein coupled, bacteriorhodopsin (BR) has become the structural prototype for this class of membrane proteins. Since its structure has been solved by electron crystallography and X-ray diffraction to high resolution (Grigorieff *et al.* 1996; Pebay-Peyroula *et al.* 1997), BR has served as the major integral membrane protein for the calibration of many spectroscopic techniques. Especially helpful for secondary structure determination by FTIR spectroscopy is the fact that BR is almost exclusively $\alpha$-helical with 3 helices

spanning the membrane perpendicularly and 4 helices being inclined at angles of about 20° from the membrane normal. In addition almost the entire protein is embedded in the lipid bilayer with only relatively few loop residues being exposed to the aqueous solvent. Early FTIR studies revealed that the amide I frequency of $\sim$ 1665 $cm^{-1}$ recorded for BR in $H_2O$ or $D_2O$ was outside the normal range (1650–1656 $cm^{-1}$) reported for $\alpha$-helices which are fully substituted with hydrogen (Rothschild & Clark, 1979*b*). The authors speculated that the reason for this unusually high frequency may be a distortion of the regular $\alpha$-helix. Normal mode calculations seemed to support the idea that the $\alpha$-helices in BR might be $\alpha_{II}$-helices, i.e. right-handed $\alpha$-helices with somewhat different $\phi$ and $\psi$ angles resulting in 0·14 Å longer H-bonds compared to the standard $\alpha_I$-helices (Krimm & Dwivedi, 1982). However, Grigorieff *et al.* (1996) found no evidence for $\alpha_{II}$-helices in their refined structure of BR and $3_{10}$ helices were only spuriously present at the ends of some $\alpha$-helices. *What then are the reasons for the increased amide I frequency in BR?* Shifts in amide I frequencies are frequently attributed to changes in the hydrogen bond strength (or length) with weaker H-bonds producing an upshift and stronger H-bonds producing a downshift of the amide I band. This general conclusion is supported by studies of polypeptides in different solvents. Changing the solvent usually changes several parameters including the dielectric constant, the hydrogen bonding capacity of the solvent, and the conformation of the polypeptide which are not easy to separate. A systematic investigation of the amide I frequency of the antibiotic valinomycin in different solvents yields some useful insight into this problem (Jackson & Mantsch, 1991*a*). Dispersed in micelles or bilayers valinomycin H-bonds to water molecules producing an amide I frequency of 1656–1658 $cm^{-1}$ which shifts to 1652 $cm^{-1}$ upon H/D exchange. A similar frequency (1659 $cm^{-1}$) is observed for valinomycin in chloroform in which case valinomycin forms intramolecular H-bonds. DMSO is a solvent of high polarity (dielectric constant $\sim$ 40), but unlike water does not offer any protons for H-bonding to the amide carbonyl groups. It has been shown by NMR spectroscopy that interaction with DMSO disrupts most intramolecular H-bonds of valinomycin (Bystrov *et al.* 1977). Therefore, the amide I frequency of $\gtrsim$ 1666 $cm^{-1}$ measured for valinomycin in DMSO is characteristic for amide carbonyls that are free or participate in only very weak intramolecular H-bonds. In agreement with these results obtained with valinomycin are experiments conducted with various model proteins which are predominantly $\alpha$-helical, $\beta$-sheet, or unordered in water, but whose amide I frequencies all shift to 1662–1663 $cm^{-1}$ in DMSO which disrupts stable secondary structures (Jackson & Mantsch, 1991*b*). However, glycerol and methanol, i.e. two solvents that also denature proteins and that have dielectric constants similar to that of DMSO, but which are good H-bond donors, do not produce these large frequency shifts. Collectively, these studies provide quite strong evidence that amide I frequencies around 1665 $cm^{-1}$ are representative of structures with free or weak H-bonds and that changes of the dielectric constant of the solvent may be of secondary importance. Therefore, *the increased amide I frequencies in helical membrane proteins may be the hallmark of more flexible and/or more stretched $\alpha$-helices*. This

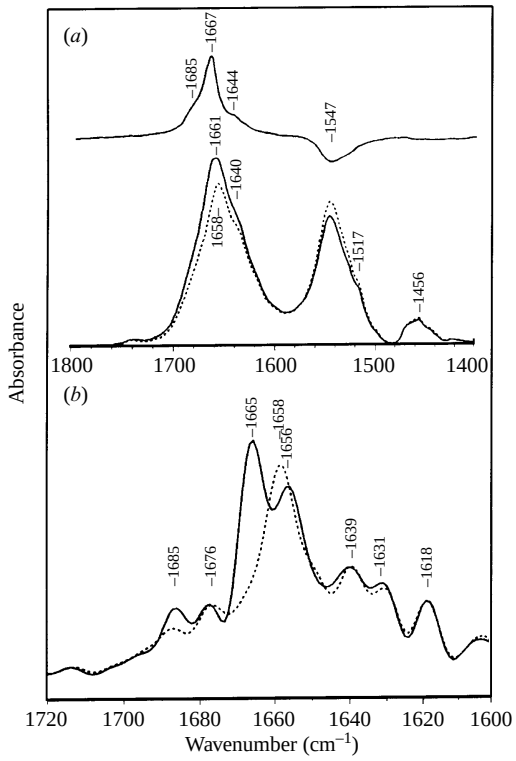


Fig. 8. Polarized transmission FTIR spectra in the amide I and II region of bacteriorhodopsin in hydrated oriented purple membranes. (*a*) Spectra recorded with a parallel (solid line) and perpendicular (dashed line) polarized IR beam. The spectrum on the top is the linear dichroism spectrum, $A_{\parallel}-A_{\perp}$. (*b*) Expanded amide I region of spectra recorded with a parallel (solid line) and perpendicular (dashed line) polarized IR beam at 80 K after Fourier self-deconvolution. The main amide I peak is split into two components ($\sim$ 1665 and $\sim$ 1656 $cm^{-1}$) of which the higher frequency component exhibits stronger dichroism. (Adapted from Earnest *et al.* 1990, with permission).

interpretation is consistent with the previously mentioned frequency increases in hydrophobic model peptides that were stretched when reconstituted into 'mismatched' thick lipid bilayers (Zhang *et al.* 1995*b*) and with a more readily amide hydrogen-exchanging class of $\alpha$-helices that was recently found in membrane-bound phospholipase $A_2$ (Tatulian *et al.* 1997; and see Section 10·2). A recent study of the temperature-dependence of the amide I′ band of helix-forming model peptides is also consistent with more flexible helices at higher temperatures exhibiting higher frequencies than more rigid helices at low temperatures (Graff *et al.* 1997).

The average orientation of the $\alpha$-helices of BR in purple membranes that were oriented on the IR windows by simple drying or by the isopotential spin dry method has been measured to be 24–27° from the membrane normal (Rothschild & Clark, 1979*a*; Nabedryk *et al.* 1985; Earnest *et al.* 1990), i.e. in reasonable agreement with the electron diffraction data. Greater than 80–90 % of the residues

in these helices do not H/D exchange even after 48 hours of exposure to $D_2O$ (Earnest *et al.* 1990), presumably because interhelical contacts and the lipid bilayer limit the access of water to most residues. Representative polarized IR spectra of bacteriorhodopsin are shown in Fig. 8.

Very similar studies have been carried out with the G-protein coupled photoreceptor rhodopsin in oriented or unoriented rod outer segment or reconstituted membranes (Michel-Villaz *et al.* 1979; Rothschild *et al.* 1980; Downer *et al.* 1986; Haris *et al.* 1989). Rhodopsin has a normal helical amide I frequency and does not exhibit the upshift that was observed with BR. Its helices are oriented predominantly perpendicular to the plane of the membrane. In contrast to BR, only about 50% of all amide protons are resistant to H/D exchange.

*Porins*. Another class of integral membrane proteins with a relatively simple structural motif are the porins which form 16- to 18-stranded $\beta$-barrels in the outer membranes of gram-negative bacteria (Weiss *et al.* 1991; Cowan *et al.* 1992). Several years before the X-ray structure of the first porin was solved, FTIR studies established that the porins consisted predominantly of antiparallel $\beta$-sheets, with very few or possibly no residues in an $\alpha$-helical conformation (Kleffel *et al.* 1985; Nabedryk *et al.* 1988). About 30% of the amide protons exchanged with deuterons after 3 hours. Linear dichroism measurements indicated that the transition dipole moments of the amide I and amide II vibrations were tilted on average at $47 \pm 3°$ from the membrane normal, i.e. not too far from the value that was later confirmed from the crystal structure. Polarized IR spectra of OmpF porin are shown in Fig. 9. Outer membrane protein A (OmpA) whose crystal structure is not known has also been investigated by ATR–FTIR spectroscopy (Rodionova *et al.* 1995). It also forms predominantly $\beta$-sheets in membranes and the average strand angle in the proposed 8-stranded $\beta$-barrel was found to be $\sim 36°$ with respect to the membrane normal. Interest in OmpA arises because it can be refolded into membranes from solution (Kleinschmidt & Tamm 1996). A proposed folding intermediate has a large part of the $\beta$-structure already formed at the membrane surface (Rodionova *et al.* 1995).

*Acetylcholine receptor*. The nicotinic acetylcholine receptor (AChR) is a much more complex multimeric membrane protein with large extra-membranous domains. Based on electron diffraction studies, the trans-membrane portion has been suggested to consist of $\alpha$- and $\beta$-structures (Unwin, 1993). AChR has been reconstituted in a functional form in thin membrane films on ATR plates and small conformational changes have been measured as a function of agonist (carbamylcholine) binding (Baenziger *et al.* 1992). Transmission FTIR studies showed that the trans-membrane domain of the receptor after proteinase K digestion of the aqueous domains consisted of 50% helix, 40% $\beta$-structure and turns, and 10% unordered structure (Görne-Tschelnokow *et al.* 1994). These findings are in qualitative agreement with the electron diffraction results, but contradict previous secondary structure models based on hydropathy plots alone. Fernandez-Ballester *et al.* (1994) observed that the secondary structure of AChR depends on the presence of cholesterol in the reconstituted liposomes, with

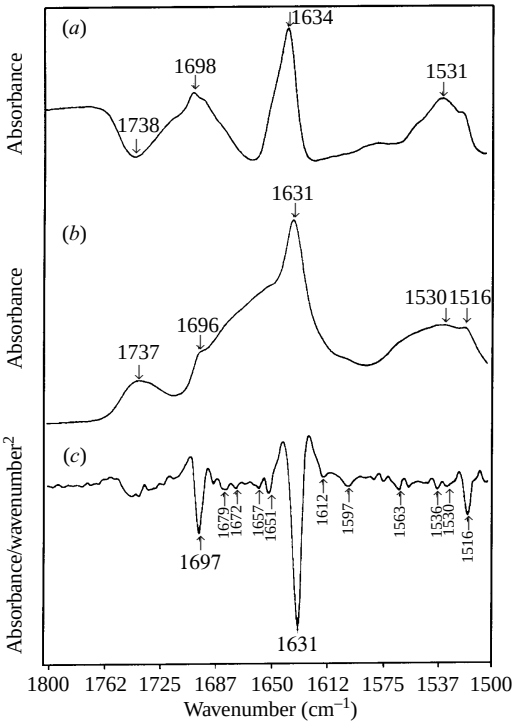


Fig. 9. Polarized transmission FTIR spectra in the amide I and II region of OmpF porin in air-dried oriented stacks of bilayers. (*a*) Linear dichroism spectrum, $A_{\parallel}-A_{\perp}$. (*b*) Absorbance spectrum. (*c*) Second derivative spectrum. The major amide I (and II) band components that are typical for antiparallel $\beta$-pleated sheet are clearly visible in all spectra. (Adapted from Nabedryk *et al*. 1988, with permission).

cholesterol increasing the fractions of $\alpha$-helix and $\beta$-sheet. This increase in ordered secondary structures correlated with an increase in cation channel activity of the receptor as a function of cholesterol.

*ATP-driven ion pumps*. The secondary structure of the $Ca^{2+}$-ATPase from sarcoplasmic reticulum was investigated by FTIR spectroscopy and no major conformational changes were found between the $E_1$ and $E_2$ state of the enzyme (Villalaín *et al*. 1989; Buchet *et al*. 1991). However, very small differences in secondary structure could be detected by difference spectroscopy when the $E_2$ state was generated in the same sample by photolysis of caged ATP (Barth *et al*. 1991). ATR–FTIR spectra of the plasma membrane $Na^+/K^+$-ATPase have been measured in hydrated single membrane films (Fringeli *et al*. 1989). Small conformational/orientational changes could be detected in several absorbance bands depending on whether the enzyme was exposed to buffers containing $Na^+$, $K^+$ or no alkali ions. 24 % of the amide protons were resistant to H/D exchange. Vigneron *et al*. (1995) investigated the structure of the P-type $H^+$-ATPase from the plasma membrane of *Neurospora crassa* by ATR–FTIR spectroscopy. The intact enzyme was found to contain 38 % helix and 26 % $\beta$-sheet. When the water-exposed domain was digested with proteinase K, the transmembrane domain

contained 59% helices in a membrane-spanning orientation and 25% $\beta$-sheet. About 50% and 40% of all amide protons were H/D exchanged after 24 hours of exposure to $D_2O$ vapour in intact and proteinase K-treated ATPase, respectively. The $\sim$ 230 $\alpha$-helical residues in the TM domain are consistent with 10 TM helices that were predicted by hydropathy analysis for this enzyme, but an additional $\sim$ 100 residues of membrane-embedded $\beta$-structures are postulated based on the IR data.

*Other enzymes and transporters*. The average orientation of the helices in the photosynthetic reaction centre from *Rh. spaeroides* has been estimated to be less than 35° from the membrane normal (Nabedryk *et al*. 1982*b*), i.e. in good agreement with the later determined crystal structure of this protein (Allen *et al*. 1987). In beef heart cytochrome *c* oxidase the helices were found to be oriented on average 20–36° from the membrane normal (Bazzi & Woody, 1985), again as later confirmed by X-ray crystallography (Iwata *et al*. 1995). The glucose transporter from erythrocytes has been predicted to span the membrane 12 times in the form of $\alpha$-helices. FTIR results support a model of the glucose transporter with a majority of TM oriented $\alpha$-helices, but the presence of some $\beta$-structure was also detected in this protein (Chin *et al*. 1986; Alvarez *et al*. 1987). In contrast to most other integral membrane proteins, a large fraction (80–90%) of all amide protons exchange rapidly, a result which has been taken as evidence for an aqueous pore in the protein. EmrE, a small ($\sim$ 100 residues) bacterial multi-drug transporter, was about 80% helical in lipid bilayers (Arkin *et al*. 1996*a*). The helices were oriented approximately perpendicular to the plane of the membrane and their amide protons could not H/D exchange, leading to a membrane-inserted 4-helix bundle model for this protein. Diacylglycerol kinase from *E. coli* is an helical integral membrane protein with three predicted TM helices. FTIR studies established that about 90% of all residues were in $\alpha$-helices and that the protein consisted of 3 membrane-spanning hydrophobic and 2 peripheral, surface-oriented amphipathic $\alpha$-helices (Sanders *et al*. 1996).

*Single-pass receptors*. There are very few FTIR studies of receptors that span the membrane with a single $\alpha$-helix. Polarized FTIR studies of this class of membrane proteins have been limited mainly by problems with sample preparation and the preservation of the native structure of these proteins in oriented samples. However, the opportunity to study such proteins in fully hydrated single supported bilayers offers new possibilities for polarized ATR–FTIR spectroscopy under more physiological conditions. Some first success in this direction was achieved with the hemagglutinin (HA) of influenza virus whose molecular axis was shown to tilt upon exposure to target lipid bilayers at pH 5·0, i.e. conditions that support HA-mediated membrane fusion (Tatulian *et al*., 1995*a*; Tatulian & Tamm, 1996). Conformational changes of HA as a function of pH and/or presentation of target membranes have been investigated by difference spectroscopy on the same samples which eliminates the need for curve fitting and resolution enhancement techniques that can be cumbersome with proteins of complex structures (Gray & Tamm, 1997). The difference spectra in Fig. 10 indicate that upon acidification helical and turn structures are induced and $\beta$-

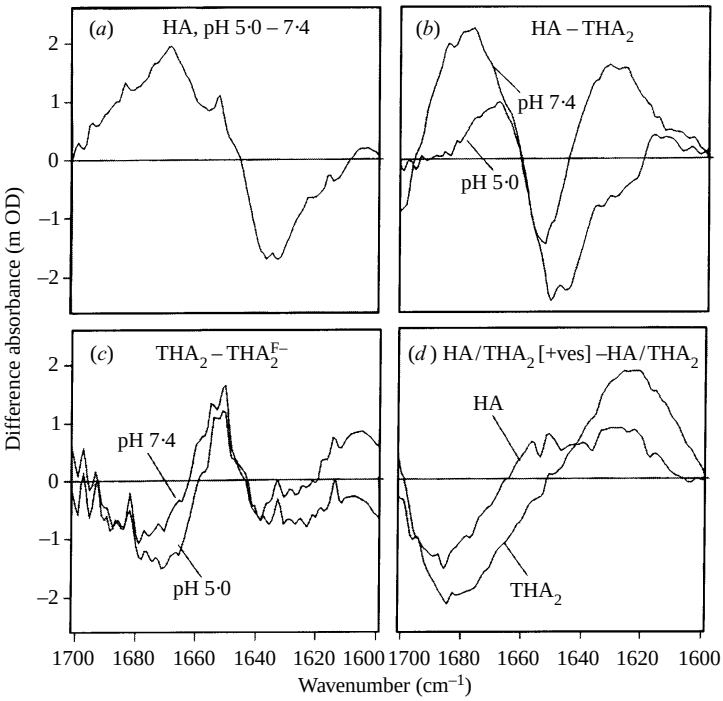


Fig. 10. Difference ATR–FTIR spectra in the amide I′ region of reconstituted influenza virus hemagglutinin and its fragments in fully hydrated single supported lipid bilayers at pH 7·4 and 5 and with and without bound target vesicles. The molecular species and buffer conditions are indicated in each panel. HA, hemagglutinin; $THA_2$, HA treated with trypsin under limiting conditions which liberates the $HA_1$ chain from the membrane bound $HA_2$ chain; $THA_2^{F-}$, $THA_2$ with the fusion peptide removed; ves, target vesicles composed of POPC:POPG (4:1). (Adapted from Gray & Tamm, 1997.)

structures appear to be reduced (panel *a*). They also indicate that complete HA probably contains more $\beta$-structure than a proteolytic product comprising the fusogenic $HA_2$ chain only (panel *b*), that the first 40 residues of $HA_2$ which include the fusion peptide are probably largely helical (panel *c*), and that the presentation of target vesicles induces the largest changes in regions of the spectrum that are best attributed to $\beta$-structures (panel *d*). In addition to conformational changes, dynamic changes were detected in this study between HA molecules in the different conformational states by conducting amide H/D exchange experiments at pH 7 and pH 5 in the absence and presence of bound target lipid bilayers.

## 10. PERIPHERAL MEMBRANE PROTEINS

### 10.1 *Binding of peripheral membrane proteins to lipid bilayers*

The binding of peripheral membrane proteins to supported lipid bilayers can be measured by ATR–FTIR spectroscopy. Typically, increasing protein concentrations are injected to a preformed supported bilayer in a liquid ATR cell

and absorbance spectra are recorded as a function of concentration. Surface concentrations $\Gamma$ are then calculated from the peak or integrated absorbance of the amide I or another protein band by using the relation (Fringeli, 1993)

$$\Gamma = \frac{Ad}{nm\epsilon d_e} \tag{18}$$

where $d$ is the membrane thickness, $n$ the number of peptide bonds per molecule, $m$ the number of active internal reflections, $\epsilon$ the per-residue molar extinction coefficient of the corresponding absorbance band, and $d_e$ the effective thickness. Depending on the choice of peak or integrated absorbance, the corresponding values of $\epsilon$ should be used. $A_\parallel$ or $A_\perp$ in combination with corresponding values of $d_{e\parallel}$ or $d_{e\perp}$ may also be used to measure membrane-binding of proteins from polarized ATR experiments. Eqn (18) with appropriate coefficients also applies to the determination of lipid surface concentrations from measurements of lipid (e.g. the methylene stretching) absorbance bands. By rationing protein and lipid surface concentrations, the parameters $d$, $d_e$, and $m$ can be eliminated. Therefore, the protein-to-lipid molar ratio is given by

$$\mathrm{P/L} = \frac{\Gamma_P}{\Gamma_L} = \frac{A_P n_L \epsilon_L}{A_L n_P \epsilon_P}, \tag{19}$$

where the subscripts P and L refer to protein and lipid, respectively, $n_L$ is the number of functional groups of the lipid, and $\epsilon_L$ is the corresponding extinction coefficient. Since the lipid cross-sectional areas, $a$, are known (e.g. $\sim 70$ Å$^2$ per molecule of POPC), the protein surface concentration may be calculated from the protein-to-lipid ratios, i.e. $\Gamma_P = (2/a)(\mathrm{P/L})$. In oriented samples a correction for anisotropic absorption should be introduced to calculate surface concentrations (Fringeli, 1993). This is accomplished by using the expression (Tamm & Tatulian, 1993)

$$\mathrm{P/L} = \frac{A_{\perp P} \sigma_L \epsilon_L n_L}{A_{\perp L} \sigma_P \epsilon_P n_P}, \tag{20}$$

where $\sigma_i = (S_i \sin^2 \alpha_i)/2 + (1 - S_i)/3$ and $S_i$ is the corresponding order parameter which is determined as outlined in Section 5.2. Finally, since the extinction coefficients of polypeptide chains depend on their secondary structure and since some amino acid side chains absorb in the amide I region (Chirgadze *et al.* 1975; Venyaminov & Kalnin, 1990*a*, *b*), special attention should be given to chose the appropriate value of $\epsilon_P$.

An example of using ATR–FTIR spectroscopy to determine membrane binding are recent studies on the interfacial activation of phospholipase $A_2$ ($PLA_2$) from the snake venom of *A. p. piscivorus* (Tatulian *et al.* 1997). ATR spectra were recorded as a function of injected enzyme concentration. Protein-to-lipid molar ratios were determined from the amide I band areas integrated between 1700 and 1600 cm$^{-1}$ and the lipid $\nu(CH_2)$ band areas integrated between 2990 and 2820 cm$^{-1}$. The isotherms of $PLA_2$ binding to supported bilayers composed of

DPPC and DPPG (3:2) at ionic strengths varying from 8·5 mM to 1 M indicate that binding at low ionic strength is strong and appears to be cooperative whereas binding at high ionic strength is weaker and non-cooperative (S. A. Tatulian, unpublished results).

### 10.2 *Conformation of and lipid perturbation by peripheral membrane proteins*

*Cytochrome c*. The conformation of horse heart cytochrome *c* has been studied in aqueous buffer and bound to bilayers containing acidic lipids by FTIR spectroscopy (Dousseau & Pézolet, 1990; Muga *et al*. 1991*a*; Heimburg & Marsh, 1993). Binding to DMPG, DPPG, or DOPG bilayers in the gel or liquid-crystalline phase resulted in only very small secondary structure changes, but led to a destabilization of the tertiary structure as evidenced by a decreased melting temperature and an increased rate of amide H/D exchange of the protein (Muga *et al*. 1991*a*). These effects correlate with the amount of acidic lipid in the bilayer. In contrast to DOPG, cardiolipin decreased the fraction of $\alpha$-helix and increased the fraction of random coil in membrane-bound cytochrome *c* (Choi & Swanson, 1995). A detailed analysis of amide hydrogen exchange experiments of membrane-bound cytochrome *c* revealed a fast and a slowly exchanging class of hydrogens (Heimburg and Marsh, 1993). The kinetics of the slower component are highly temperature-dependent and show a break in Arrhenius plots between 22 and 29° C, which is far below the temperature of denaturation (49 to 55° C for membrane-bound cytochrome *c*). Therefore, it appears that cytochrome *c* binds to bilayers in two different conformations which are characterized by similar secondary structures, but different amide hydrogen exchange rates. The structure above 30° C may be more open and more flexible than the more compact and more rigid structure observed below 20° C.

Interaction of apocytochrome *c* with DMPG bilayers decreased the methylene stretching frequencies of the lipid fatty acyl chains and dramatically decreased the cooperativity of the lipid phase transition, but had a much smaller effect on the DMPG component in binary mixtures of DMPG and DMPC-$d_{54}$ (Muga *et al*. 1991*b*). This result was interpreted as evidence against a protein-induced lateral phase separation of the lipid components in this system. Apocytochrome *c* also strongly perturbed the ester carbonyl band in pure DMPG, but not in mixed DMPG/DMPC bilayers. Binding of cytochrome *c* to cardiolipin bilayers decreased the lower frequency component of the ester carbonyl band at 1728 $cm^{-1}$ but did not affect the higher frequency component at 1743 $cm^{-1}$, indicating dehydration of the bilayer interface (Choi & Swanson, 1995).

*Myelin basic protein*. Myelin basic protein (MBP) does not exhibit much regular secondary structure in aqueous buffer. However, when bound to DMPG bilayers, it assumes 15% $\alpha$-helix and 53% $\beta$-sheet (Surewicz *et al*. 1987*b*). In contrast, binding to eggPA and DMPA bilayers led to the formation of 40% $\alpha$-helix and 35% $\beta$-sheet (Nabet *et al*. 1994). The perturbation of acidic lipids upon MBP binding was also studied by these authors. Similar to cytochrome *c*, binding of MBP to acidic lipid bilayers decreased the cooperativity of the lipid phase

transition, decreased the lipid acyl chain conformational order in the gel phase, and decreased the lipid phase transition temperature, as judged from the temperature-dependence of the methylene stretching frequency (Surewicz *et al.* 1987*b*; Nabet *et al.* 1994). Analysis of the lipid ester carbonyl bands showed that interaction with the protein resulted in a stronger hydration of the bilayer interface in the gel phase and a dehydration in the liquid-crystalline phase. Nabet *et al.* (1994) also demonstrated by ATR spectroscopy that the orientational order of eggPA was increased after binding of MBP.

*Phospholipases.* The conformations of various secreted phospholipases $A_2$ ($PLA_2$) were studied by FTIR spectroscopy in their free and lipid-bound forms. Soluble bovine and porcine pancreatic $PLA_2$ contained $\sim 54\,\%$ $\alpha$-helix, $\sim 15\,\%$ $\beta$-sheet and $\sim 23\,\%$ $\beta$-turns (Kennedy *et al.* 1990). A slightly higher content of $\beta$-sheet was found in the rattle snake venom $PLA_2$ from *C. d. terrificus* (Arêas *et al.* 1989). Another snake venom $PLA_2$ (from *A. p. piscivorus* with an aspartate in position 49; APPD49) exhibited a total helix content of $\sim 45\,\%$ in solution (Tatulian *et al.* 1997). Binding of neither $Ca^{2+}$ nor the monomeric non-hydrolyzable substrate analog *n*-alkylphosphocholine induced noticeable conformational changes in the pancreatic enzymes. However, binding of the same inhibitory pseudosubstrate in micellar form increased the content of $\alpha$-helix and decreased the contents of $\beta$-sheet and $\beta$-turn in these enzymes (Kennedy *et al.* 1990).

In a recent study, we compared the conformation of APPD49 $PLA_2$ free in solution and bound to lipid bilayers of various compositions using transmission and ATR FTIR spectroscopy (Tatulian *et al.* 1997). In solution, $PLA_2$ exhibited a single $\alpha$-helical component at $\sim 1651\ cm^{-1}$. Interestingly, when $PLA_2$ was bound to bilayers composed of POPC and POPG (4:1, supported bilayers or vesicles) an additional component appeared at $\sim 1658\ cm^{-1}$, indicating structural changes in this enzyme induced by membrane binding. It was concluded that upon membrane binding some of the standard helices were transformed to more flexible helices, for the following reasons. First, quantitative amide hydrogen exchange experiments showed that the membrane-bound enzyme undergoes more extensive H/D exchange than $PLA_2$ in solution. Second, the intensity of the component at $\sim 1658\ cm^{-1}$ decreases progressively, whereas the component at $\sim 1650\ cm^{-1}$ remains unchanged during H/D exchange (Fig. 11). Third, increased amide I frequencies generally correspond to more weakly H-bonded secondary structures as has been discussed in more detail in Section 9. Essentially identical results were obtained when APPD49 $PLA_2$ was bound to bilayers of non-hydrolyzable lipids or when the enzyme bound to hydrolyzable lipid bilayers was inhibited by EGTA. Taken together, these data suggest that interfacial adsorption and binding of the substrate (or its analog) to the active centre of the enzyme are two distinct events, which both contribute to the 'interfacial activation' of $PLA_2$ (Tatulian *et al.* 1997).

*Colicins and cardiotoxins.* Colicins and several protein toxins not only bind, but also penetrate the lipid bilayer. In many cases, electrostatic and hydrophobic interactions are involved and changes in secondary and/or tertiary structure are

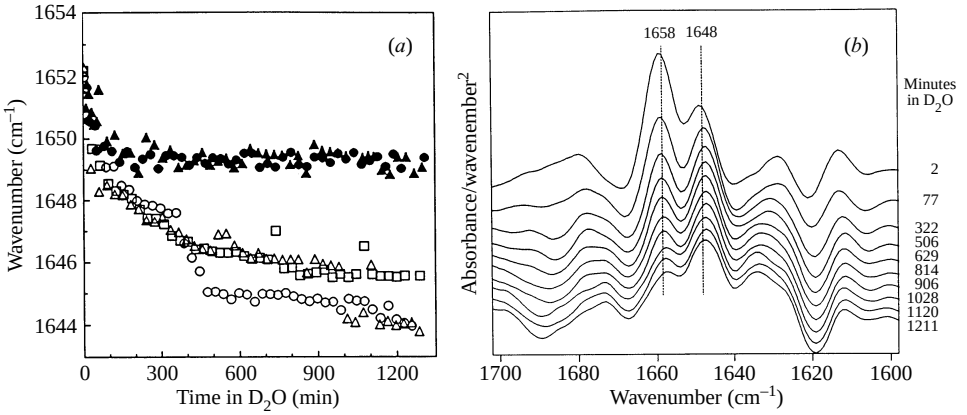


Fig. 11. Kinetic amide hydrogen/deuterium exchange experiments of free and membrane-bound ADPPD49 phospholipase $A_2$. (*a*) Shift of the amide I peak frequency of $PLA_2$ in solution (filled symbols) and bound to fully hydrated supported lipid bilayers (open symbols) as a function of time after exposure to $D_2O$ buffer. (*b*) Second derivative spectra in the amide I region of APPD49 $PLA_2$ bound to supported bilayers composed of non-hydrolyzable ether lipids as a function of time after exposure to $D_2O$ buffer. Note the decrease of the component at $\sim$ 1658 cm$^{-1}$ and the relatively constant shape of the component at $\sim$ 1648 cm$^{-1}$. (Adapted from Tatulian *et al.* 1997).

induced upon interaction with the lipid bilayer. The C-terminal pore-forming fragments of the bacterial colicins A and E1 have been investigated by FTIR spectroscopy (Rath *et al.* 1991; Goormaghtigh *et al.* 1991*b*). The secondary structures of these proteins remained largely helical upon membrane binding. A large fraction ($> 80\%$) of all amide hydrogens underwent rapid ($\sim$ 5 min) H/D exchange in the membrane-bound form, indicating that most helices were solvent-accessible, relatively dynamic, and not protected by the lipid bilayer. As judged from dichroic measurements, the helices appeared to be oriented more perpendicular than parallel to the plane of the lipid bilayer. However, the measured dichroism was not large, indicating that some of the helices may be oriented at different angles. Small changes in secondary structure and amide H/D exchangeability were also observed upon membrane binding of the two components of the anthrax lethal toxin which has a similar molecular architecture to diphtheria toxin (Wang *et al.* 1996).

Three different snake venom cardiotoxins were shown to contain large fractions of $\beta$-structure which increase upon binding to negatively charged lipid bilayers (Surewicz *et al.* 1988). A narrowing of the amide I band components of the membrane-bound form in comparison with the free form was taken as evidence for stabilized $\beta$-structure of membrane-bound cardiotoxin IIa (Désormeaux *et al.* 1992). Binding of this toxin to DMPA bilayers decreased the conformational and orientational order of the (gel phase) lipid acyl chains, as shown by an increase of the methylene stretching frequency and a decrease of the order parameter of that band. It was further concluded from an intensity increase of the lower frequency component of the lipid ester carbonyl band that water penetrated more deeply into

the interfacial region when the protein was bound. Binding of the basic protein also shifted the apparent p$K$ value of DMPA because at pH 6·5 the lipid phosphate groups became (partially) ionized to $DMPA^{2-}$ as judged from the disappearance of the antisymmetric phosphate stretching mode.

*Apolipoproteins*. The secondary structures of apolipoproteins in complex with lipids have been studied by FTIR spectroscopy. Apolipoprotein B-100 has been found to be rich in $\beta$-structure, but contained also elements of other secondary structures (Herzyk *et al*. 1987). The $\beta$-structure was particularly resistant to amide H/D exchange and to conformational changes caused by oxidation of the lipids. Several proteolytic and synthetic hydrophobic fragments of apo B-100 also adopted predominantly $\beta$-structure upon association with lipids (Goormaghtigh *et al*. 1993; Lins *et al*. 1994).

*Lung surfactant*. Dluhy *et al*. (1989) first recorded infrared spectra of intact pulmonary surfactant in monolayers spread at the air–water interface in a Langmuir trough by external reflection spectroscopy. Improvements in instrumentation and water vapour compensation later permitted determinations of secondary structures of peptides, including surfactant peptide SP-C, from the amide I region of external reflection spectra (Flach *et al*. 1994). SP-C was mainly $\alpha$-helical whereas SP-B consisted of a mixture of $\alpha$-helix and random structure when bound to DPPC monolayers (Pastrana-Rios *et al*. 1995). At very high surface pressures ($> 43$ mN m$^{-1}$), SP-B was squeezed out of the monolayer. The secondary structure of SP-C was also pressure-dependent with a small component of intermolecular $\beta$-sheet appearing at high surface pressures. Using DPPC-$d_{62}$ in mixed monolayers together with various phosphatidylglycerols lead to the conclusion that PGs with unsaturated fatty acyl chains were selectively squeezed out from the monolayer (Rana *et al*. 1993; Pastrana-Rios *et al*. 1994). The secondary structures of SP-C and SP-B were also studied by ATR–FTIR spectroscopy (Pastrana-Rios *et al*. 1991; Vandenbussche *et al*. 1992*a*, *b*). Both peptides were largely $\alpha$-helical with their helix axes oriented approximately parallel to the fatty acyl chains in dry or partially hydrated multibilayers of DPPC and DPPG. SP-B also contained other secondary structures, and a large fraction of the amide hydrogens were protected from H/D exchange. Recent polarized external reflection spectroscopy results indicated an orientation of the SP-C helix in DPPC monolayers at 28 mN m$^{-1}$ close to 70° to the monolayer normal, i.e. more parallel to the surface than in dry or partially rehydrated lipid bilayers (Gericke *et al*. 1997).

## 11. PROSPECTS AND LIMITATIONS OF MEMBRANE INFRARED SPECTROSCOPY

Modern FTIR spectroscopy offers excellent opportunities to study the low-resolution structure of proteins and lipids and particularly their mutual interactions in lipid bilayers under physiological conditions. The fact that all molecular groups in a given system vibrate at a particular frequency can be viewed either as an advantage or a disadvantage of vibrational spectroscopy. The

advantage is that vibrational spectra are extremely rich in information pertaining to all parts of all molecules in the sample, and the disadvantage is that the broad intrinsic linewidth of group vibrations in liquids means that overlapping vibrational bands are not always well resolved. However, the high sensitivity and stability of modern FTIR spectrometers make spectral subtractions feasible and highly reliable, especially in cases where the same samples can be compared before and after a certain perturbation. Therefore, conformational and orientational changes can be monitored by FTIR spectroscopy with high fidelity. Many lipid group vibrations are well isolated from interfering vibrational modes and are extremely well suited to study the conformation, packing, and state of hydrogen bonding of some of these groups, either in pure lipid bilayers or after perturbation by polypeptides. The conformational sensitivity of the amide vibrations has long been used to assess the secondary structure of proteins in general, and membrane proteins in particular. However, it has become increasingly clear that the correlations of amide vibrations with particular secondary structures are not absolute and that extreme care should be exercised when attempting to quantitate individual secondary structures in complex proteins (see Jackson & Mantsch, 1995, for a critical appraisal). An elegant solution to this problem is isotope-edited FTIR spectroscopy. For example, amide I frequencies are red-shifted by about 40 $cm^{-1}$ when the amide $^{12}C$ is replaced by a $^{13}C$ (Halverson *et al.* 1991; Tadesse *et al.* 1991; Ashburn *et al.* 1992). This shift allows the investigator specifically to assign the shifted peak of the labelled peptide groups. Although this technique has so far only been employed to probe the conformation of relatively small synthetic membrane-embedded peptides (Ludlam *et al.* 1996), site-directed labelling techniques should, at least in principle, allow one to study the local conformation of recombinant proteins (Sonar *et al.* 1994).

A relatively new analytical approach to better visualize correlated changes in infrared spectra in response to physical or chemical perturbations such as time, temperature, pressure, pH or ionic strength is to calculate two-dimensional correlated spectra (Noda, 1993; Gericke *et al.* 1996). This 2D method is different from acquiring 2D NMR spectra in the sense that conventional 1D IR spectra are recorded as a function of the perturbation and then spread into two frequency dimensions by cross-correlation. The cross-peaks in these 2D IR spectra contain new information that is not readily visible in the 1D spectra. Specifically, they indicate changes in different spectral regions that are correlated or uncorrelated as a function of the perturbation.

A particular advantage of ATR–FTIR spectroscopy of fully hydrated membrane samples is that ligands can be bound and, if desired, easily removed from solution. Therefore, difference spectroscopy on the same sample under different physiological conditions is particularly easy in this experimental configuration. Also, fully hydrated supported lipid bilayers have been shown to be realistic model membrane systems by several other techniques, including fluorescence recovery after photobleaching, atomic force microscopy, and neutron diffraction. For example, membrane lipids are laterally mobile in both leaflets of the bilayer and some membrane proteins also exhibit high lateral mobility after

reconstitution into supported bilayers. Despite many encouraging results that have been obtained by ATR–FTIR spectroscopy in these systems, further improvements are necessary. For example, membrane proteins with large hydrophilic domains on *both* sides of the lipid bilayer tend to interact with the substrate through at least one of their domains and this may adversely affect their structure. Reconstitution methods and new support systems need to be developed to minimize substrate-interactions of large membrane proteins. Other engineering problems that require further attention are precise assessments of the polarization properties of the incident beam, the flatness of the substrate, and the refractive indices of the different layers in the sample. Better, experimentally supported values of these parameters will permit a more reliable absolute quantitation of the observed order parameters and tilt angles. In the meantime, it is clear that *orientational changes* can already be reliably measured in these systems with the currently available approximations (see Gray & Tamm, 1997, for a recent example).

## 12. ACKNOWLEDGEMENTS

We thank Henry Mantsch and Richard Mendelsohn for critically reading the manuscript and Jose-Luis Arrondo and Derek Marsh for helpful discussions. We also thank Cameron Gray for preparing Fig. 10 and Jama Coartney for help with the preparation of Figs 2 and 6–9. Supported by grants AI30557 and GM51329 from the NIH (LKT) and 96-1364 from the American Heart Association (SAT).

## 13. REFERENCES

Aggeli, A., Boden, N., Cheng, Y.-L., Findlay, J. B. C., Knowles, P. F., Kovatchev, P., Turnbull, P. J. H., Horváth & Marsh, D. (1996). Peptides modeled on the transmembrane region of the slow voltage-gated IsK potassium channel: structural characterization of peptide assemblies in the $\beta$-strand conformation. *Biochemistry* **35**, 16213–16221.

Akutsu, H., Ikematsu, M. & Kyogoku, Y. (1981). Molecular structure and interaction of dipalmitoyl phosphatidylcholine in multilayers. Comparative study with phosphatidylethanolamine. *Chem. Phys. Lipids* **28**, 149–158.

Allen, J. P., Feher, G., Yeates, T. O., Komiya, H. & Rees, D. C. (1987). Structure of the reaction center from *Rhodabacter sphaeroides* R-26: the protein subunits. *Proc. Natl. Acad. Sci. USA* **84**, 6162–6166.

Altenbach, C., Froncisz, W., Hyde, J. S. & Hubbell, W. L. (1989). Conformation of spin-labeled melittin at membrane surfaces investigated by pulse saturation recovery and continuous wave power saturation electron paramagnetic resonance. *Biophys. J.* **56**, 1183–1191.

Alvarez, J., Lee, D. C., Baldwin, S. A. & Chapman, D. (1987). Fourier transform infrared spectroscopic study of the structure and conformational changes of the human erythrocyte glucose transporter. *J. Biol. Chem.* **262**, 3502–3509.

Arêas, E. P. G., Laure, C. J., Gabilan, N., Araugo, P. S. & Kawano, Y. (1989). Raman and infrared studies on the conformation of porcine pancreatic and *Crotalus durissus terrificus* phospholipase $A_2$. *Biochim. Biophys. Acta* **99**, 15–26.

Arkin, I. T., Rothman, M., Ludlam, C. F. C., Aimoto, S., Engelman, D. M., Rothschild, K. J. & Smith, S. O. (1995). Structural model of the phospholamban ion channel complex in phospholipid membranes. *J. Mol. Biol.* **248**, 824–834.

Arkin, I. T., Russ, W. P., Lebendiker, M. & Schuldiner, S. (1996*a*). Determining the secondary structure and orientation of EmrE, a multi-drug transporter, indicates a transmembrane four-helix bundle. *Biochemistry* **35**, 7233–7238.

Arkin, I. T., MacKenzie, K. R., Fisher, L., Aimoto, S., Engelman, D. M. & Smith, S. O. (1996*b*). Mapping the lipid-exposed surfaces of membrane proteins. *Nature Struct. Biol.* **3**, 240–243.

Arrondo, J. L. R., Muga, A., Castresana, J. & Goñi, F. M. (1993). Quantitative studies of the structure of proteins in solution by Fourier transform infrared spectroscopy. *Prog. Biophys. Mol. Biol.* **59**, 23–56.

Ashburn, T. T., Auger, M. & Lansbury, Jr., P. T. (1992). The structural basis of pancreatic amyloid formation: isotope-edited spectroscopy in the solid state. *J. Am. Chem. Soc.* **114**, 790–791.

Axelsen, P. H., Braddock, W. D., Brockman, H. L., Jones, C. M., Dluhy, R. A., Kaufman, B. K. & Puga II, F. J. (1995*a*). Use of internal reflectance infrared spectroscopy for the *in situ* study of supported lipid monolayers. *Appl. Spectroscopy* **49**, 526–531.

Axelsen, P. H. & Citra, M. J. (1996). Orientational order determination by internal reflection infrared spectroscopy. *Prog. Biophys. molec. Biol.* **66**, 227–253.

Axelsen, P. H., Kaufman, B. K., McElhaney, R. N. & Lewis, R. N. A. H. (1995*b*). The infrared dichroism of transmembrane helical polypeptides. *Biophys. J.* **69**, 2770–2781.

Azpiazu, I., Gomez-Fernandez, J. C. & Chapman, D. (1993). Biophysical studies of the Pf1 coat protein in the filamentous phage, in detergent micelles, and in a membrane environment. *Biochemistry* **32**, 10720–10726.

Babin, Y., D'Amour, J., Pigeon, M. & Pézolet, M. (1987). A study of the structure of polymyxin B-dipalmitoylphosphatidyglycerol complexes by vibrational spectroscopy. *Biochim. Biophys. Acta* **903**, 78–88.

Baenziger, J. E., Miller, K. W. & Rothschild, K. J. (1992). Incorporation of the nicotinic acetylcholine receptor into planar multilamellar films: characterization by fluorescence and Fourier transform infrared difference spectroscopy. *Biophys. J.* **61**, 983–992.

Bandekar, J. (1992). Amide modes and protein conformation. *Biochim. Biophys. Acta* **1120**, 123–143.

Barth, A., Mäntele, W. & Kreutz, W. (1991). Infrared spectroscopic signals arising from ligand binding and conformational changes in the catalytic cycle of sarcoplasmic reticulum calcium ATPase. *Biochim. Biophys. Acta* **1057**, 115–123.

Bauer, H. H., Müller, M., Goette, J., Merkle, H. P. & Fringeli, U. P. (1994). Interfacial adsorption and aggregation associated changes in secondary structure of human calcitonin monitored by ATR–FTIR spectroscopy. *Biochemistry* **33**, 12276–12282.

Bazzi, M. & Woody, R. W. (1985). Oriented secondary structure in integral membrane proteins. I. Circular dichroism and infrared spectroscopy of cytochrome oxidase in multilamellar films. *Biophys. J.* **48**, 957–966.

Bertie, J. E. & Ahmed, M. K. (1989). Infrared intensities of liquids. 5. Optical and dielectric constants, integrated intensities, and dipole moment derivatives of $H_2O$ and $D_2O$ at 22 °C. *J. Phys. Chem.* **93**, 2210–2218.

Blume, A., Hübner, W. & Messner, G. (1988). Fourier transform infrared spectroscopy of $^{13}C{=}O$-labeled phospholipids hydrogen bonding to carbonyl groups. *Biochemistry* **27**, 8239–8249.

Bouchard, M. & Auger, M. (1993). Solvent history dependence of gramicidin-lipid interactions: A Raman and infrared spectroscopic study. *Biophys. J.* **65**, 2484–2492.

Bradbury, E. M., Brown, L., Downie, A. R., Elliott, A., Fraser, R. D. B. & Hanby, W. E. (1962). The structure of the $\omega$-form of poly-$\beta$-benzyl-aspartate. *J. Mol. Biol.* **5**, 230–247.

Braiman, M. S. & Rothschild, K. J. (1988). Fourier transform infrared techniques for probing membrane protein structure. *Ann. Rev. Biophys. Biophys. Chem.* **17**, 541–570.

Brauner, J. W., Mendelsohn, R. & Prendergast, F. G. (1987). Attenuated total reflectance Fourier transform infrared studies of the interaction of melittin, two fragments of melittin, and $\delta$-hemolysin with phosphatidylcholines. *Biochemistry* **26**, 8151–8158.

Brian, A. & McConnell, H. M. (1984). Allogenic stimulation of cytotoxic T cells by supported planar membranes. *Proceedings of the National Academy of Sciences USA* **81**, 6159–6163.

Briggs, M. S., Cornell, D. G., Dluhy, R. A. & Gierasch, L. M. (1986). Conformations of signal peptides induced by lipids suggest initial steps in protein export. *Science* **233**, 206–208.

Brumm, T., Jorgensen, K., Mouritsen, D. G. & Bayerl, T. M. (1996). The effect of increasing membrane curvature on the phase transition and mixing behavior of a dimyristoyl-*sn*-glycero-3-phosphatidylcholine/distearoyl-*sn*-glycero-3-phosphatidylcholine lipid mixture, as studied by Fourier transform infrared spectroscopy and differential scanning calorimetry. *Biophys. J.* **70**, 1373–1379.

Buchet, R., Varga, S., Seidler, N. W., Molnar, E. & Martonosi, A. (1991). Polarized infrared attenuated total reflectance spectroscopy of the $Ca^{2+}$-ATPase of sarcoplasmic reticulum. *Biochim. Biophys. Acta* **1068**, 201–216.

Bush, S. F., Levin, H. & Levin, I. W. (1980). Cholesterol-lipid interactions: An infrared and Raman spectroscopic study of the carbonyl stretching mode region of 1,2-dipalmitoyl phosphatidylcholine bilayers. *Chem. Phys. Lipids* **27**, 101–111.

Byler, D. M. & Susi, H. (1986). Examination of the secondary structure of proteins by deconvolved FTIR spectra. *Biopolymers* **25**, 469–487.

Bystrov, V. F., Gavrilov, Y. D., Ivanov, V. T. & Ovchinnikov, Y. A. (1977). Refinement of the solution conformation of valinomycin with the aid of coupling constants from the $^{13}C$-nuclear-magnetic-resonance spectra. *Eur. J. Biochem.* **78**, 63–82.

Cameron, D. G., Casal, H. L. & Mantsch, H. H. (1980). Characterization of the pretransition in 1,2-dipalmitoyl-*sn*-glycero-3-phosphocholine by Fourier transform infrared spectroscopy. *Biochemistry* **19**, 3665–3672.

Casal, H. L. & Mantsch, H. H. (1984). Polymorphic phase behavior of phospholipid membranes studied by infrared spectroscopy. *Biochim. Biophys. Acta* **779**, 381–401.

Casal, H. L., Martin, A., Mantsch, H. H., Paltauf, F. & Hauser, H. (1987*a*). Infrared studies of fully hydrated unsaturated phosphatidylserine bilayers. Effects of $Li^+$ and $Ca^{2+}$. *Biochemistry* **26**, 7395–7401.

Casal, H. L., Mantsch, H. H. & Hauser, H. (1987*b*). Infrared studies of fully hydrated saturated phosphatidylserine bilayers. Effect of $Li^+$ and $Ca^{2+}$. *Biochemistry* **26**, 4408–4416.

Challou, N., Goormaghtigh, E., Cabiaux, V., Conrath, K. & Ruysschaert, J.-M.

(1994). Sequence and structure of the membrane-associated peptide of glycophorin A. *Biochemistry* **33**, 6902–6910.

Cheng, K. H. (1994). Infrared study of the bilayer stability behavior of binary and ternary phospholipid mixtures containing unsaturated phosphatidylethanolamine. *Chem. Phys. Lipids* **70**, 43–51.

Chia, N.-C. & Mendelsohn, R. (1992). $CH_2$ wagging modes of unsaturated acyl chains as IR probes of conformational order in methyl alkenoates and phospholipid bilayers. *J. Phys. Chem.* **96**, 10543–10547.

Chin, J. J., Jung, E. K. Y. & Jung, C. Y. (1986). Structural basis of human erythrocyte glucose transporter function in reconstituted vesicles. *J. Biol. Chem.* **261**, 7101–7104.

Chiou, J.-S., Krishna, P. R., Kamaya, H. & Ueda, I. (1992). Alcohols dehydrate lipid membranes: an infrared study on hydrogen bonding. *Biochim. Biophys. Acta* **1110**, 225–233.

Chirgadze, Yu. N., Fedorov, O. V. & Trushina, N. P. (1975). Estimation of amino acid residue side-chain absorption in the infrared spectra of protein solutions in heavy water. *Biopolymers* **14**, 679–694.

Chirgadze, Yu. N., Shestopalov, B. V. & Venyaminov, S. Yu. (1973). Intensities and other spectral parameters of infrared amide bands of polypeptides in the $\beta$- and random forms. *Biopolymers* **12**, 1337–1351.

Chirgadze, Yu. N. & Brazhnikov, E. V. (1974). Intensities and other spectral parameters of infrared amide bands of polypeptides in the $\alpha$-helical form. *Biopolymers* **13**, 1701–1712.

Choi, S. & Swanson, J. M. (1995). Interaction of cytochrome c with cardiolipin: an infrared spectroscopic study. *Biophys. Chem.* **54**, 271–278.

Choi, S., Ware, W., Jr., Lauterbach, S. R. & Phillips, W. M. (1991). Infrared spectroscopic studies on the phosphatidylserine bilayer interacting with calcium ions: Effect of cholesterol. *Biochemistry* **30**, 8563–8568.

Citra, M. J. & Axelsen, P. H. (1996). Determination of molecular order in supported lipid membranes by internal reflection Fourier transform infrared spectroscopy. *Biophys. J.* **71**, 1796–1805.

Clark, N. A., Rothschild, K. J., Luippold, D., & Simons, B. (1980). Surface induced lamellar orientation of multilayer membrane arrays: theoretical analysis and a new method with application to purple membrane fragments. *Biophys. J.* **31**, 65–95.

Contino, P. B., Hasselbacher, C. A., Ross, J. B. A. & Nemerson, Y. (1994). Use of an oriented transmembrane protein to probe the assembly of a supported phospholipid bilayer. *Biophys. J.* **67**, 1113–1116.

Cornell, D. G., Dluhy, R. A., Briggs, M. S., McKnight, C. J. & Gierasch, L. M. (1989). Conformations and orientations of a signal peptide interacting with phospholipid monolayers. *Biochemistry* **28**, 2789–2797.

Cortijo, M., Alonso, A., Gómez-Fernández, J. C. & Chapman, D. (1982). Intrinsic protein-lipid interactions. Infrared spectroscopic studies of gramicidin A, bacteriorhodopsin and $Ca^{2+}$-ATPase in biomembranes and reconstituted systems. *J. Mol. Biol.* **157**, 597–618.

Cowan, S. W., Schirmer, T., Rummel, G., Steiert, M., Ghosh, R., Pauptit, R. A., Jansonius, J. N. & Rosenbusch, J. P. (1992). Crystal structures explain functional properties of two *E. coli* porins. *Nature* **358**, 727–733.

Davis, J. H., Clare, D. M., Hodges, R. S. & Bloom, M. (1983). Interaction of a synthetic amphiphilic polypeptide and lipids in a bilayer structure. *Biochemistry* **22**, 5298–5305.

Désormeaux, A., Laroche, G., Bougis, P. E. & Pézolet, M. (1992). Characterization by infrared spectroscopy of the interaction of a cardiotoxin with phosphatidic acid and with binary mixtures of phosphatidic acid and phosphatidylcholine. *Biochemistry* **31**, 12173–12182.

Dibble, A. R. G., Hinderliter, A. K., Sando, J. J. & Biltonen, R. L. (1996). Lipid lateral heterogeneity in phosphatidylcholine/phosphatidylserine/diacylglycerol vesicles and its influence on protein kinase C activity. *Biophys. J.* **71**, 1877–1890.

Dluhy, R. A., Cameron, D. G., Mantsch, H. H. & Mendelsohn, R. (1983). Fourier transform infrared spectroscopic studies of the effect of calcium ions on phosphatidylserine. *Biochemistry* **22**, 6318–6325.

Dluhy, R. A., Moffatt, D., Cameron, D. G., Mendelsohn, R. & Mantsch, H. H. (1985). Characterization of cooperative conformational transitions by Fourier transform infrared spectroscopy : application to phospholipid binary mixtures. *Can. J. Chem.* **63**, 1925–1932.

Dluhy, R. A., Reilly, K. E., Hunt, R. D., Mitchell, M. L., Mautone, A. J. & Mendelsohn, R. (1989). Infrared spectroscopic investigations of pulmonary surfactant. Surface film transitions at the air–water interface and bulk phase thermotropism. *Biophys. J.* **56**, 1173–1181.

Dluhy, R. A., Stephens, S. A., Widayati, S. & Williams, A. D. (1995). Vibrational spectroscopy of biophysical monolayers. Applications of IR and Raman spectroscopy to biomembrane model systems at interfaces. *Spectrochim. Acta* Part A **51**, 1413–1447.

Dousseau, F. & Pézolet, M. (1990). Determination of the secondary structure content of proteins in aqueous solutions from their amide I and amide II infrared bands. Comparison between classical and partial least-squares methods. *Biochemistry* **29**, 8771–8779.

Downer, N. W., Bruchman, T. J. & Hazzard, J. H. (1986). Infrared spectroscopic study of photoreceptor membrane and purple membrane. *J. Biol. Chem.* **261**, 3640–3647.

Downing, H. D. & Williams, D. (1975). Optical constants of water in the infrared. *J. Geophys. Res.* **80**, 1656–1661.

Durrer, P., Galli, C., Hoenke, S., Corti, C., Glück, Vorrherr T. & Brunner, J. (1996). $H^+$-induced membrane insertion of influenza virus hemagglutinin involves the HA2 amino-terminal fusion peptide but not the coiled coil region. *J. Biol. Chem.* **271**, 13417–13421.

Earnest, T. N., Herzfeld, J. & Rothschild, K. J. (1990). Polarized Fourier transform infrared spectroscopy of bacteriorhodopsin. Transmembrane alpha helices are resistant to hydrogen/deuterium exchange. *Biophys. J.* **58**, 1539–1546.

Erb, E.-M., Tangemann, K., Bohrmann, B., Müller, B. & Engel, J. (1997). Integrin $\alpha$IIb$\beta$3 reconstituted into lipid bilayers is nonclustered in its activated state but clusters after fibrinogen binding. *Biochemistry* **36**, 7395–7402.

Erne, D. & Schwyzer, R. (1987). Membrane structure of bombesin studied by infrared spectroscopy. Prediction of membrane interactions of gastrin-releasing peptide, neuromedinB, and neuromedin C. *Biochemistry* **26**, 6316–6319.

Erne, D., Sargent, D. F., & Schwyzer, R. (1985). Preferred conformation, orientation, and accumulation of dynorphin A-(1-13)-tridecapeptide on the surface of neutral lipid membranes. *Biochemistry* **24**, 4261–4263.

Flach, C. R. & Mendelsohn, R. (1993). A new infrared spectroscopic marker for cochleate phases in phosphatidylserine-containing model membranes. *Biophys. J.* **64**, 1113–1121.

Flach, C. R., Brauner, J. W. & Mendelsohn, R. (1993). Calcium ion interactions with insoluble phospholipid monolayer films at the A/W interface. External reflection-absorption IR studies. *Biophys. J.* **65**, 1994–2001.

Flach, C. R., Brauner, J. W., Taylor, J. W., Baldwin, R. C. & Mendelsohn, R. (1994). External reflection FTIR of peptide monolayer films *in situ* at the air/water interface: Experimental design, spectra-structure correlations, and effects of hydrogen-deuterium exchange. *Biophys. J.* **67**, 402–410.

Fox, Jr., R. O. & Richards, F. M. (1982). A voltage-gated ion channel model inferred from the crystal structure of alamethicin at 1·5-Å resolution. *Nature* **330**, 325–330.

Fraser, R. D. B. & Suzuki, E. (1970). A quantitative study of the Amide I vibrations in the infra-red spectrum of $\beta$-keratin. *Spectrochim. Acta* **26A**, 426–428.

Fraser, R. D. B. & MacRae, T. P. (1973). *Conformation in Fibrous Proteins & Related Synthetic Polypeptides*. Academic Press, New York, Chapter 5, pp. 95–125.

Frey, S. & Tamm, L. K. (1991). Orientation of melittin in phospholipid bilayers. A polarized attenuated total reflection infrared study. *Biophys. J.* **60**, 922–930.

Fringeli, U. P. (1993). *In situ* infrared attenuated total reflection membrane spectroscopy. In *Internal Reflection Spectroscopy, Theory and Applications*. F. M. Mirabella, Jr. (Ed.) Marcel Dekker, Inc.: New York, pp. 255–324.

Fringeli, U. P. & Fringeli, M. (1979). Pore formation in lipid membranes by alamethicin. *Proc. Natl. Acad. Sci. USA* **76**, 3852–3856.

Fringeli, U. P. & Günthard, H. H. (1981). Infrared membrane spectroscopy. In *Membrane Spectroscopy* (ed. E. Grell), pp. 270–332. Berlin: Springer-Verlag.

Fringeli, U. P., Apell, H.-J., Fringeli, M. & Läuger, P. (1989). Polarized infrared absorption of $Na^+/K^+$-ATPase studied by attenuated total reflection spectroscopy. *Biochim. Biophys. Acta* **984**, 301–312.

Gazit, E., Miller, I. R., Biggin, P. C., Sansom, M. S. P. & Shai, Y. (1996). Structure and orientation of the mammalian antibacterial peptide cecropin P1 within phospholipid membranes. *J. Mol. Biol.* **258**, 860–870.

Gericke, A., Gadaleta, S. J., Brauner, J. W. & Mendelsohn, R. (1996). Characterization of biological samples by two-dimensional infrared spectroscopy: simulation of frequency, bandwidth, and intensity changes. *Biospectroscopy* **2**, 341–351.

Gericke, A., Flach, C. R. & Mendelsohn, R. (1997). Structure and orientation of lung surfactant SP-C and L-$\alpha$-dipalmitoylphosphatidylcholine in aqueous monolayers. *Biophys. J.* **73**, 492–499.

Gierasch, L. M. (1989). Signal sequences. *Biochemistry* **28**, 923–930.

Goormaghtigh, E. & Ruysschaert, J.-M. (1990). Polarized attenuated total reflection infrared spectroscopy as a tool to investigate the conformation and orientation of membrane components. In *Molecular Description of Biological Membranes by Computer-Aided Conformational Analysis* (ed. R. Brasseur), pp. 285–329 (Chapter 1.B.3). Boca Raton, FL: CRC Press.

Goormaghtigh, E., De Meutter, J., Szoka, F., Cabiaux, V., Parente, R. A. & Ruysschaert, J.-M. (1991*a*). Secondary structure and orientation of the amphipathic peptide GALA in lipid structures. An infrared-spectroscopic approach. *Eur. J. Biochem.* **195**, 421–429.

Goormaghtigh, E., Vigneron, L., Knibiehler, M., Lazdunski, C. & Ruysschaert, J.-M. (1991*b*). Secondary structure of the membrane-bound form of the pore-forming domain of colicin A. An attenuated total-reflection polarized Fourier-transform infrared spectroscopy study. *Eur. J. Biochem.* **202**, 1299–1305.

Goormaghtigh, E., Cabiaux, V., De Meutter, J., Rosseneu, M. & Ruysschaert, J.-M. (1993). Secondary structure of the particle associating domain of apolipoprotein B-100 in low-density lipoprotein by attenuated total reflection infrared spectroscopy. *Biochemistry* **32**, 6104–6110.

Goormaghtigh, E., Cabiaux, V. & Ruysschaert, J.-M. (1994). Determination of soluble and membrane protein structure by Fourier transform infrared spectroscopy. I. Assignments and model compounds. II. Experimental aspects, side chain structure, and H/D exchange. III. Secondary structures. In *Subcellular Biochemistry*, *Volume 23 : Physicochemical Methods in the Study of Biomembranes* (ed. H. J. Hilderson and G. B. Ralston), pp. 329–450 (Chapters 8–10). New York: Plenum Press.

Görne-Tschelnokow, U., Strecker, A., Kaduk, C., Naumann, D. & Hucho, F. (1994). The transmembrane domains of the nicotinic acetylcholine receptor contain $\alpha$-helical and $\beta$ structures. *EMBO J.* **13**, 338–341.

Graff, D. F., Pastrana-Rios, B., Venyaminov, S. Yu. & Prendergast, F. G. (1997). The effects of chainlength and thermal denaturation on helix-forming peptides: a mode-specific analysis using 2D FT-IR. *J. Am. Chem. Soc.* **119**, 11282–11294.

Gray, C. & Tamm, L. K. (1997). Structural studies on membrane-embedded influenza hemagglutinin and its fragments. *Protein Science* **6**, 1993–2006.

Gray, C., Tatulian, S. A., Wharton, S. A. & Tamm, L. K. (1996). Effect of the N-terminal glycine on the secondary structure, orientation and interaction of the influenza hemagglutinin fusion peptide with lipid bilayers. *Biophys. J.* **70**, 2275–2286.

Grdadolnik, J., Kidric, J. & Hadzi, D. (1991). Hydration of phosphatidylcholine reverse micelles and multilayers – an infrared spectroscopic study. *Chem. Phys. Lipids* **59**, 67–68.

Gremlich, H.-U., Fringeli, U.-P. & Schwyzer, R. (1983). Conformational changes of adrenocorticotropin peptides upon interaction with lipid membranes revealed by infrared attenuated total reflection spectroscopy. *Biochemistry* **22**, 4257–4264.

Gremlich, H.-U., Fringeli, U.-P. & Schwyzer, R. (1984). Interaction of adrenocorticotrophin-(11–24)-tetradecapeptide with neutral lipid membranes revealed by infrared attenuated total reflection spectroscopy. *Biochemistry* **23**, 1808–1810.

Grigorieff, N., Ceska, T. A., Downing, K. H., Baldwin, J. M. & Henderson, R. (1996). Electron-crystallographic refinement of the structure of bacteriorhodopsin. *J. Mol. Biol.* **259**, 393–421.

Halverson, K. J., Sucholeiki, I., Ashburn, T. T. & Lansbury, Jr., P. T. (1991). Location of $\beta$-sheet-forming sequences in amyloid proteins by FTIR. *J. Am. Chem. Soc.* **113**, 6701–6703.

Haris, P. I. & Chapman, D. (1988). Fourier transform infrared spectra of the polypeptide alamethicin and a possible structural similarity with bacteriorhodopsin. *Biochim. Biophys. Acta* **943**, 375–380.

Haris, P. I. & Chapman, D. (1995). The conformational analysis of peptides using Fourier transform IR spectroscopy. *Biopolymers* (*Peptide Science*) **37**, 251–263.

Haris, P. I., Coke, M. & Chapman, D. (1989). Fourier transform infrared spectroscopic investigation of rhodopsin structure and its comparison with bacteriorhodopsin. *Biochim. Biophys. Acta* **995**, 160–167.

Haris, P. I., Ramesh, B., Sansom, M. S. P., Kerr, I. D., Srai, K. S. & Chapman, D. (1994). Studies of the pore forming domain of a voltage-gated potassium channel protein. *Prot. Eng.* **7**, 255–262.

Harrick, N. J. (1967). *Internal Reflection Spectroscopy*. Ossining, N.Y: Harrick Scientific Corporation.

HEIMBURG, T. & MARSH, D. (1993). Investigation of secondary and tertiary structural changes of cytochrome c in complexes with anionic lipids using amide hydrogen exchange measurements: an FTIR study. *Biophys. J.* **65**, 2408–2417.

HEIMBURG, T., SCHUENEMANN, J., WEBER, K. & GEISLER, N. (1996). Specific recognition of coiled coils by infrared spectroscopy: analysis of the three structural domains of Type III intermediate filament proteins. *Biochemistry* **35**, 1375–1382.

HERZYK, E., LEE, D. C., DUNN, R. C., BRUCKDORFER, K. R. & CHAPMAN, D. (1987). Changes in the secondary structure of apolipoprotein B-100 after $Cu^{2+}$-catalyzed oxidation of human low-density lipoproteins monitored by Fourier transform infrared spectroscopy. *Biochim. Biophys. Acta* **992**, 145–154.

HINTERDORFER, P., BABER, G. & TAMM, L. K. (1994). Reconstitution of membrane fusion sites: a total internal reflection fluorescence microscopy study of influenza hemagglutinin-mediated membrane fusion. *J. Biol. Chem.* **269**, 20360–20368.

HÜBNER, W. & MANTSCH, H. H. (1991). Orientation of specifically $^{13}C{=}O$ labeled phosphatidylcholine multilayers from polarized attenuated total reflection FT-IR spectroscopy. *Biophys. J.* **59**, 1261–1272.

HÜBNER, W., MANTSCH, H. H., PALTAUF, F. & HAUSER, H. (1994). Conformation of phosphatidylserine in bilayers as studied by Fourier transform infrared spectroscopy. *Biochemistry* **33**, 320–326.

HUSCHILT, J. C., MILLMAN, B. M. & DAVIS, J. H. (1989). Orientation of $\alpha$-helical peptides in a lipid bilayer. *Biochim. Biophys. Acta* **979**, 139–141.

IKURA, T., NOBUHIRO, G. & INAGAKI, F. (1991). Refined structure of melittin bound to perdeuterated dodecylphosphocholine micelles as studied by 2D-NMR and distance geometry calculation. *Proteins* **9**, 81–89.

ISHIGURO, R., KIMURA, N. & TAKAHASHI, S. (1993). Orientation of fusion-active synthetic peptides in phospholipid bilayers: determination by Fourier transform infrared spectroscopy. *Biochemistry* **32**, 9792–9797.

ISHIGURO, R., MATSUMOTO, M. & TAKAHASHI, S. (1996). Interaction of fusogenic synthetic peptide with phospholipid bilayers: orientation of the peptide $\alpha$-helix and binding isotherm. *Biochemistry* **35**, 4976–4983.

IWATA, S., OSTERMEIER, C., LUDWIG, B. & MICHEL, H. (1995). Structure at 2·8 Å resolution of cytochrome *c* oxidase from *Paracoccus denitrificans*. *Nature* **376**, 660–668.

JACKSON, M. & MANTSCH, H. H. (1991*a*). Valinomycin and its interaction with ions in organic solvents, detergents, and lipids studied by Fourier transform IR spectroscopy. *Biopolymers* **31**, 1205–1212.

JACKSON, M. & MANTSCH, H. H. (1991*b*). Beware of proteins in DMSO. *Biochim. Biophys. Acta* **1078**, 231–235.

JACKSON, M. & MANTSCH, H. H. (1993). Biomembrane structure from FT–IR spectroscopy. *Spectrochim. Acta Rev.* **15**, 53–69.

JACKSON, M. & MANTSCH, H. H. (1995). The use and misuse of FTIR spectroscopy in the determination of protein structure. *Crit. Rev. Biochem. Mol. Biol.* **30**, 95–120.

JACKSON, M., MANTSCH, H. H. & SPENCER, J. H. (1992). Membrane environments probed by Fourier transform infrared spectroscopy. *Biochemistry* **31**, 7289–7293.

KALB, E., FREY, S. & TAMM, L. K. (1992). Formation of supported planar bilayers by fusion of vesicles to supported phospholipid monolayers. *Biochim. Biophys. Acta* **1103**, 307–316.

KENNEDY, D. F., SLOTBOOM, A. J., DE HAAS, G. H. & CHAPMAN, D. (1990). A Fourier transform infrared spectroscopic (FTIR) study of porcine and bovine pancreatic

phospholipase $A_2$ and their interaction with substrate analogues and a transition-state inhibitor. *Biochim. Biophys. Acta* **1040**, 317–326.

Kennedy, D. F., Crisma, M., Toniolo, C. & Chapman, D. (1991). Studies of peptides forming $3_{10}$- and $\alpha$-helices and $\beta$-bend ribbon structures in organic solution and in model biomembranes by Fourier transform infrared spectroscopy. *Biochemistry* **30**, 6541–6548.

Kleinschmidt, J. H. & Tamm, L. K. (1996). Folding intermediates of a $\beta$-barrel membrane protein. Kinetic evidence for a multi-step membrane insertion mechanism. *Biochemistry* **35**, 12993–13000.

Kleinschmidt, J. H., Mahaney, J. E., Thomas, D. D. & Marsh, D. (1997). Interaction of bee venom melittin with zwitterionic and negatively charged phospholipid bilayers: a spin-label electron spin resonance study. *Biophys. J.* **72**, 767–778.

Kleffel, B., Garavito, R. M., Baumeister, W. & Rosenbusch, J. P. (1985). Secondary structure of a channel-forming protein: porin from *E. coli* outer membranes. *EMBO J.* **4**, 1589–1592.

Krimm, S. & Abe, Y. (1972). Intermolecular interaction effects in the Amide I vibrations of $\beta$ polypeptides. *Proc. Natl. Acad. Sci. USA* **69**, 2788–2792.

Krimm, S. & Bandekar, J. (1986). Vibrational spectroscopy and conformation of peptides, polypeptides, and proteins. *Adv. Prot Chem.* **38**, 181–364.

Krimm, S. & Dwivedi, A. M. (1982). Infrared spectrum of the purple membrane: Clue to a proton conduction mechanism? *Science* **216**, 407–408.

Kuhn, H. (1983). Functionalized monolayer assembly manipulation. *Thin Solid Films* **99**, 1–16.

Levin, I. W., Mushayakarara, E. & Bittman, R. (1982). Vibrational assignment of the sn1 and sn2 carbonyl stretching modes of membrane phospholipids. *J. Raman Spectrosc.* **13**, 231–234.

Lewis, R. N. A. H. & McElhaney, R. N. (1993*a*). Studies of mixed-chain diacyl phosphatidylcholines with highly asymmetric acyl chains: A Fourier transform infrared spectroscopic study of interfacial hydration and hydrocarbon chain packing in the mixed interdigitated gel phase. *Biophys. J.* **65**, 1866–1877.

Lewis, R. N. A. H. & McElhaney, R. N. (1993*b*). Calorimetric and spectroscopic studies of the polymorphic phase behavior of a homologous series of n-saturated 1,2-diacyl phosphatidylethanolamines. *Biophys. J.* **64**, 1081–1096.

Lewis, R. N. A. H. & McElhaney, R. N. (1996). Fourier transform infrared spectroscopy in the study of hydrated lipids and lipid bilayer membranes. In *Infrared Spectroscopy of Biomolecules* (ed. H. H. Mantsch and D. Chapman), pp. 159–202. Wiley-Liss, Inc.

Lewis, R. N. A. H., McElhaney, R. N., Monck, M. A. & Cullis, P. R. (1994*a*). Studies of highly asymmetric mixed-chain diacyl phosphatidylcholines that form mixed-interdigitated gel phases: Fourier transform infrared and $^2$H NMR spectroscopic studies of hydrocarbon chain conformation and orientational order in the lipid-crystalline state. *Biophys. J.* **67**, 197–207.

Lewis, R. N. A. H., McElhaney, R. N., Pohle, W. & Mantsch, H. H. (1994*b*). Components of the carbonyl stretching band in the infrared spectra of hydrated 1,2-diacylglycerolipid bilayers: a reevaluation. *Biophys. J.* **67**, 2367–2375.

Lewis, R. N. A. H., Pohle, W. & McElhaney, R. N. (1996). The interfacial structure of phospholipid bilayers: differential scanning calorimetry and Fourier transform infrared spectroscopic studies of 1,2-dipalmitoyl-*sn*-glycero-3-phosphorylcholine and its dialkyl and acyl-alkyl analogs. *Biophys. J.* **70**, 2736–2746.

Lieckfeld, R., Villalaín, J., Gómez-Fernández, J. C. & Lee, G. (1995). Apparent pKa of the fatty acids within ordered mixtures of model human stratum corneum lipids. *Pharm. Res.* **12**, 1614–1617.

Lins, L., Brasseur, R., Rosseneu, M., Yang, C.-Y., Sparrow, D. A., Sparrow, J. T., Gotto Jr., A. M. & Ruysschaert, J.-M. (1994). Structure and orientation of Apo B-100 peptides into a lipid bilayer. *J. Protein Chem.* **13**, 77–88.

López-García, F., Villalaín, J. & Gómez-Fernández, J. C. (1995). Effect of sphingosine and stearylamine on the interaction of phosphatidylserine with calcium. A study using DSC, FT–IR and $^{45}Ca^{2+}$-binding. *Biochim. Biophys. Acta* **1236**, 279–288.

López-García, F., Villalaín, J., Gómez-Fernández, J. C. & Quinn, P. J. (1994). The phase behavior of mixed aqueous dispersions of dipalmitoyl derivatives of phosphatidylcholine and diacylglycerol. *Biophys. J.* **66**, 1991–2004.

Ludlam, C. F. C., Arkin, I. T., Liu, X.-M., Rothman, M. S., Rath, P., Aimoto, S., Smith, S. O., Engelman, D. M. & Rothschild, K. J. (1996). Fourier transform infrared spectroscopy and site-directed isotope labeling as a probe of local secondary structure in the transmembrane domain of phospholamban. *Biophys. J.* **70**, 1728–1736.

Lüneberg, J., Martin, I., Nüßler, Ruysschaert, J.-M. & Herrmann, A. (1995). Structure and topology of the influenza virus fusion peptide in lipid bilayers. *J. Biol. Chem.* **270**, 27606–27614.

Mäntele, W. (1993). Infrared spectroscopy of the photosynthetic reaction center. *The Photosynthetic Reaction Center, Vol. II* (ed. H. Deisenhofer and J. R. Norris), pp. 239–283. San Diego: Academic Press.

Mantsch, H. H. & McElhaney, R. N. (1991). Phospholipid phase transitions in model and biological membranes as studied by infrared spectroscopy. *Chem. Phys. Lipids* **57**, 213–226.

Mantsch, H. H., Martin, A. & Cameron, D. G. (1981). Characterization by infrared spectroscopy of the bilayer to nonbilayer phase transition of phosphatidylethanolamines. *Biochemistry* **20**, 3138–3145.

Marsh, D. (1997). Dichroic ratios in polarized Fourier transform infrared for nonaxial symmetry of $\beta$-sheet structures. *Biophys. J.* **72**, 2710–2718.

Martin, I., Defrise-Quertain, F., Decroly, E., Vandenbranden, M., Brasseur, R. & Ruysschaert, J.-M. (1993). Orientation and structure of the $NH_2$-terminal HIV-1 gp41 peptide in fused and aggregated liposomes. *Biochim. Biophys. Acta* **1145**, 124–133.

Martin, I., Schaal, H., Scheid, A. & Ruysschaert, J.-M. (1996). Lipid membrane fusion induced by the human immunodeficiency virus type 1 gp41 N-terminal extremity is determined by its orientation in the lipid bilayer. *J. Virol.* **70**, 298–304.

Martinez, G. & Millhauser, G. (1995). FTIR spectroscopy of alanine-based peptides: Assignment of the amide I′ modes for random coil and helix. *J. Struct. Biol.* **114**, 23–27.

Matsuzaki, K., Shioyama, T., Okamura, E., Umemura, J., Takenaka, T., Takaishi, Y., Fujita, T. & Miyajima, K. (1991). A comparative study on interactions of $\alpha$-aminoisobutyric acid containing antibiotic peptides, trichopolyn I and hypelcin A with phosphatidylcholine bilayers. *Biochim. Biophys. Acta* **1070**, 419–428.

Matsuzaki, K., Nakayama, M., Fukui, M., Otaka, A., Funakoshi, S., Fujii, N., Bessho, K. & Miyajima, K. (1993). Role of disulfide linkages in tachyplesin-lipid interactions. *Biochemistry* **32**, 11704–11710.

Mendelsohn, R. & Mantsch, H. H. (1986). Fourier transform infrared studies of lipid-protein interaction. In *Progress in Protein-Lipid Interactions 2* (ed. A. Watts and J. J. H. H. M. DePont), pp. 103–146. Amsterdam: Elsevier Science Publishers.

Mendelsohn, R. & Snyder, R. G. (1996). Infrared spectroscopic determination of conformational disorder and microphase separation in phospholipid acyl chains. In *Biological Membranes : A Molecular Perspective from Computation and Experiment* (ed. K. M. Merz and B. Roux), pp. 145–174. Boston: Birkhäuser.

Mendelsohn, R., Dluhy, R., Taraschi, T., Cameron, D. G. & Mantsch, H. H. (1981). Raman and Fourier transform infrared spectroscopic studies of the interaction between glycophorin and dimyristoylphosphatidylcholine. *Biochemistry* **20**, 6699–6706.

Mendelsohn, R., Brauner, J. W., Faines, L., Mantsch, H. H. & Dluhy, R. A. (1984*a*). Calorimetric and Fourier transform infrared spectroscopic studies on the interaction of glycophorin with phosphatidyl-serine/dipalmitoylphosphatidylcholine-$d_{62}$ mixtures. *Biochim. Biophys. Acta* **774**, 237–246.

Mendelsohn, R., Dluhy, R. A., Crawford, T. & Mantsch, H. H. (1984*b*). Interaction of glycophorin with phosphatidylserine: A Fourier transform infrared investigation. *Biochemistry* **23**, 1498–1504.

Mendelsohn, R., Davies, M. A., Brauner, J. W., Schuster, H. F. & Dluhy, R. A. (1989). Quantitative determination of conformational disorder in the acyl chains of phospholipid bilayers by infrared spectroscopy. *Biochemistry* **28**, 8934–8939.

Mendelsohn, R., Brauner, J. W. & Gericke, A. (1995*a*). External infrared reflection absorption spectrometry of monolayer films at the air–water interface. *Annu. Rev. Phys. Chem.* **46**, 305–334.

Mendelsohn, R., Liang, G. L., Strauss, H. L. & Snyder, R. G. (1995*b*). IR spectroscopic determination of gel state miscibility in long-chain phosphatidylcholine mixtures. *Biophys. J.* **69**, 1987–1998.

Michel-Villaz, M., Saibil, H. R. & Chabre, M. (1979). Orientation of rhodopsin $\alpha$-helices in retinal rod outer segment membranes studied by infrared linear dichroism. *Proc. Natl. Acad. Sci. USA* **76**, 4405–4408.

Miick, S. M., Martinez, G. V., Fiori, W. R., Todd, A. P. & Millhauser, G. L. (1992). Short alanine-based peptides may form $3_{10}$ helices and not $\alpha$-helices in aqueous solution. *Nature* **359**, 653–655.

Miyazawa, T. (1960). Perturbation treatment of the characteristic vibrations of polypeptide chains in various configurations. *J. Chem. Phys.* **32**, 1647–1652.

Miyazawa, T. & Blout, E. R. (1961). The infrared spectra of polypeptides in various conformations: Amide I and II bands. *J. Am. Chem. Soc.* **83**, 712–719.

Moore, D. J., Sills, R. H., Patel, N. & Mendelsohn, R. (1996). Conformational order of phospholipids incorporated into human erythrocytes: an FTIR spectroscopy study. *Biochemistry* **35**, 229–235.

Moore, D. J., Sills, R. H. & Mendelsohn, R. (1997). Conformational order of specific phospholipids in human erythrocytes: correlations with changes in cell shape. *Biochemistry* **36**, 660–664.

Moore, W. H. & Krimm, S. (1976). Vibrational analysis of peptides, polypeptides, and proteins. II. $\beta$-poly(L-alanine) and $\beta$-poly(L-alanylglycine). *Biopolymers* **15**, 2465–2483.

Muga, A., Mantsch, H. H. & Surewicz, W. K. (1991*a*). Membrane binding induces destabilization of cytochrome *c* structure. *Biochemistry* **30**, 7219–7224.

Muga, A., Mantsch, H. H. & Surewicz, W. K. (1991*b*). Apocytochrome *c* interaction with phospholipid membranes studied by Fourier-transform infrared spectroscopy. *Biochemistry* **30**, 2629–2635.

Muga, A., Neugebauer, W., Hirama, T. & Surewicz, W. K. (1994). Membrane interaction and conformational properties of the putative fusion peptide of PH-30, a protein active in sperm-egg fusion. *Biochemistry* **33**, 4444–4448.

Müller, E. & Blume, A. (1993). FTIR spectroscopic analysis of the amide and acid bands of ganglioside $G_{M1}$, in pure form and in mixtures with DMPC. *Biochim. Biophys. Acta* **1146**, 45–51.

Müller, E., Giehl, A., Schwarzmann, G., Sandhoff, K. & Blume, A. (1996). Oriented 1,2-dimyristoyl-sn-glycero-3-phosphorylcholine/ganglioside membranes: a Fourier transform infrared attenuated total reflection spectroscopic study. Band assignments; orientational, hydrational and phase behavior; and effects of $Ca^{2+}$ binding. *Biophys. J.* **71**, 1400–1421.

Mushayakarara, E. C., Wong, P. T. T. & Mantsch, H. H. (1986). Detection by high pressure infrared spectrometry of hydrogen-bonding between water and triacetyl glycerol. *Biochem. Biophys. Res. Comm.* **134**, 140–145.

Nabedryk, E. (1996). Light-induced Fourier transform infrared difference spectroscopy of the primary electron donor in photosynthetic reactions centers. In *Infrared Spectroscopy of Biomolecules* (ed. H. H. Mantsch & D. Chapman). pp. 39–81. Wiley-Liss, Inc.

Nabedryk, E., Gingold, M. P. & Breton, J. (1982*a*). Orientation of gramidicin A transmembrane channel. *Biophys. J.* **38**, 243–249.

Nabedryk, E., Tiede, D. M., Dutton, P. L. & Breton, J. (1982*b*). Conformation and orientation of the protein in the bacterial photosynthetic reaction center. *Biochim. Biophys. Acta* **682**, 273–280.

Nabedryk, E., Bardin, A. M. & Breton, J. (1985). Further characterization of the protein secondary structure in purple membrane by circular dichroism and polarized infrared spectroscopies. *Biophys. J.* **48**, 873–876.

Nabedryk, E., Garavito, R. M. & Breton, J. (1988). The orientation of $\beta$-sheets in porin. A polarized Fourier transform infrared spectroscopic investigation. *Biophys. J.* **53**, 671–676.

Nabet, A., Boggs, J. M. & Pézolet, M. (1994). Study by infrared spectroscopy of the interaction of bovine myelin basic protein with phosphatidic acid. *Biochemistry* **33**, 14792–14799.

Nieva, J. L., Nir, S., Muga, A., Goñi, F. M. & Wilschut, J. (1994). Interaction of the HIV-1 fusion peptide with phospholipid vesicles: different structural requirements for fusion and leakage. *Biochemistry* **33**, 3201–3209.

Noda, I. (1993). Generalized two-dimensional correlation method applicable to infrared, Raman, and other types of spectroscopy. *Applied Spectroscopy* **47**, 1329–1336.

Okamura, E., Umemura, J. & Takenaka, T. (1986). Orientation of gramicidin D incorporated into phospholipid multibilayers: a Fourier transform infrared-attenuated total reflection spectroscopic study. *Biochim. Biophys. Acta* **856**, 68–75.

Okamura, E., Umemura, J. & Takenaka, T. (1990). Orientation studies of hydrated dipalmitoylphosphatidylcholine multibilayers by polarized FTIR–ATR spectroscopy. *Biochim. Biophys. Acta* **1025**, 94–98.

Pastrana-Rios, B., Mautone, A. J. & Mendelsohn, R. (1991). Fourier transform infrared studies of secondary structure and orientation of pulmonary surfactant SP-

C and its effect on the dynamic surface properties of phospholipids. *Biochemistry* **30**, 10058–10064.

Pastrana-Rios, B., Flach, C. R., Brauner, J. W., Mautone, A. J. & Mendelsohn, R. (1994). A direct test of the 'squeeze-out' hypothesis of lung surfactant function. External reflection FT–IR at the air/water interface. *Biochemistry* **33**, 5121–5127.

Pastrana-Rios, B., Taneva, S., Keough, K. M. W., Mautone, A. J. & Mendelsohn, R. (1995). External reflection absorption infrared spectroscopy study of lung surfactant proteins SP-B and SP-C in phospholipid monolayers at the air/water interface. *Biophys. J.* **69**, 2531–2540.

Pebay-Peyroula, E., Rummel, G., Rosenbusch, J. P. & Landau, E. M. (1997). X-ray structure of bacteriorhodopsin at 2·5 angstroms from microcrystals grown in lipidic cubic phases. *Science* **277**, 1676–1681.

Peled-Zehavi, H., Arkin, I. T., Engelman, D. M. & Shai, Y. (1996). Coassembly of synthetic segments of Shaker $K^+$ channel within phospholipid membranes. *Biochemistry* **35**, 6828–6838.

Peng, J. B., Prakash, M., Macdonald, R., Dutta, P. & Ketterson, J. B. (1987). Formation of multilayers of dipalmitoylphosphatidylcholine using the Langmuir-Blodgett technique. *Langmuir* **3**, 1096–1097.

Rafalski, M., Lear, J. D. & DeGrado, W. F. (1990). Phospholipid interactions of synthetic peptides representing the N-terminus of HIV gp41. *Biochemistry* **29**, 7917–7922.

Rana, F. R., Mautone, A. J. & Dluhy, R. A. (1993). Surface chemistry of binary mixtures of phospholipids in monolayers. Infrared studies of surface composition at varying surface pressures in a pulmonary surfactant model system. *Biochemistry* **32**, 3169–3177.

Rath, P., Bousché, Merrill, A. R., Cramer, W. A. & Rothschild, K. J. (1991). Fourier transform infrared evidence for a predominantly alpha-helical structure of the membrane bound channel forming COOH-terminal peptide of colicin E1. *Biophys. J.* **59**, 516–522.

Reinl, H. M. & Bayerl, T. M. (1994). Lipid transfer between small unilamellar vesicles and single bilayers on a solid support: self-assembly of supported bilayers with asymmetric lipid distribution. *Biochemistry* **33**, 14091–14099.

Reis, O., Winter, R. & Zerda, T. W. (1996). The effect of high external pressure on DPPC-cholesterol multilamellar vesicles: a pressive tuning Fourier transform infrared spectroscopy study. *Biochim. Biophys. Acta* **1279**, 5–16.

Reisdorf, Jr., W. C. & Krimm, S. (1995). Infrared dichroism of amide I and amide II modes of $\alpha_I$- and $\alpha_{II}$-helix segments in membrane proteins. *Biophys. J.* **69**, 271–273.

Reisdorf, Jr., W. C. & Krimm, S. (1996). Infrared amide I′ band of the coiled coil. *Biochemistry* **35**, 1383–1386.

Rodionova, N. A., Tatulian, S. A., Surrey, T., Jähnig, F. & Tamm, L. K. (1995). Characterization of two membrane-bound forms of OmpA. *Biochemistry* **34**, 1921–1929.

Rothschild, K. J. & Clark, N. A. (1979*a*). Polarized infrared spectroscopy of oriented purple membrane. *Biophys. J.* **25**, 473–488.

Rothschild, K. J. & Clark, N. A. (1979*b*). Anomalous amide I infrared absorption of purple membrane. *Science* **204**, 311–312.

Rothschild, K. J., Sanches, R., Hsiao, T. L. & Clark, N. A. (1980). A spectroscopic study of rhodopsin alpha-helix orientation. *Biophys. J.* **31**, 53–64.

Salgado, J., Villalaín, J. & Gómez-Fernández, J. C. (1995). Metastability of

dimyristoylphosphatidylethanolamine as studied by FT–IR and the effect of α-tocopherol. *Biochim. Biophys. Acta* **1239**, 213–225.

Sanders II, C. R., Czerski, L., Vinogradova, O., Badola, P., Song, D. & Smith, S. O. (1996). *Escherichia coli* diacylglycerol kinase is an α-helical polytopic membrane protein and can spontaneously insert into preformed lipid vesicles. *Biochemistry* **35**, 8610–8618.

Seelig, J. & Seelig, A. (1980). Lipid conformation in model membranes and biological membranes. *Quart. Rev. Biophys.* **13**, 19–61.

Senak, L., Moore, D. & Mendelsohn, R. (1992). $CH_2$ wagging progressions as IR probes of slightly disordered phospholipid acyl chain states. *J. Phys. Chem.* **96**, 2749–2754.

Simmerman, H. K. B., Kobayashi, Y. M., Autry, J. M. & Jones, L. R. (1996). A leucine zipper stabilizes the pentameric membrane domain of phospholamban and forms a coiled-coil pore structure. *J. Biol. Chem.* **271**, 5941–5946.

Sipos, D., Andersson, M. & Ehrenberg, A. (1992). The structure of the mammalian antibacterial peptide cecropin P1 in solution, determined by proton-NMR. *Eur. J. Biochem.* **209**, 163–169.

Smith, S. O., Jonas, R., Braiman, M. & Bormann, B. J. (1994). Structure and orientation of the transmembrane domain of glycophorin A in lipid bilayers. *Biochemistry* **33**, 6334–6341.

Snyder, R. G., Strauss, H. L. & Cates, D. A. (1995). Detection and measurement of microaggregation in binary mixtures of esters and of phospholipid dispersions. *J. Phys. Chem.* **99**, 8432–8439.

Snyder, R. G., Liang, G. L., Strauss, H. L. & Mendelsohn, R. (1996). IR spectroscopic study of the structure and phase behavior of long-chain diacylphosphatidylcholines in the gel state. *Biophys. J.* **71**, 3186–3198.

Sonar, S., Lee, C.-P., Coleman, M., Patel, Nilam, Liu, X., Marti, T., Khorana, H. G., RajBhandary, U. L. & Rothschild, K. R. (1994). Site-directed isotope labeling and FTIR spectroscopy of bacteriorhodopsin. *Struct. Biol.* **1**, 512–517.

Surewicz, W. K. & Mantsch, H. H. (1988). Conformational properties of angiotensin II in aqueous solution and in a lipid environment: a Fourier transform infrared spectroscopic investigation. *J. Am. Chem. Soc.* **110**, 4412–4414.

Surewicz, W. K., Mantsch, H. H., Stahl., G. L. & Epand, R. M. (1987*a*). Infrared spectroscopic evidence of conformational transitions of an atrial natriuretic peptide. *Proc. Natl. Acad. Sci. USA* **84**, 7028–7030.

Surewicz, W. K., Moscarello, M. A. & Mantsch, H. H. (1987*b*). Fourier transform infrared spectroscopic investigation of the interaction between myelin basic protein and dimyristoylphosphatidylglycerol bilayers. *Biochemistry* **26**, 3881–3886.

Surewicz, W. K., Stepanik, T. M., Szabo, A. G. & Mantsch, H. H. (1988). Lipid-induced changes in the secondary structure of snake venom cardiotoxins. *J. Biol. Chem.* **263**, 786–790.

Surewicz, W. K., Mantsch, H. H. & Chapman, D. (1993). Determination of protein secondary structure by Fourier transform infrared spectroscopy: A critical assessment. *Biochemistry* **32**, 389–394.

Suzuki, E. (1967). A quantitative study of the amide vibrations in the infra-red spectrum of silk fibroin. *Spetrochim. Acta* **23A**, 2303–2308.

Tadesse, L., Nazarbaghi, R. & Walters, L. (1991). Isotopically enhanced infrared spectroscopy: a novel method for examining secondary structure at specific sites in conformationally heterogeneous peptides. *J. Am. Chem. Soc.* **113**, 7036–7037.

Tamm, L. K. (1988). Lateral diffusion and fluorescence microscope studies on a monoclonal antibody specifically bound to supported phospholipid bilayers. *Biochemistry* **27**, 1450–1457.

Tamm, L. K. (1991). Membrane insertion and lateral mobility of synthetic amphiphilic signal peptides in lipid model membranes. *Biochim. Biophys. Acta* **1071**, 123–148.

Tamm, L. K. & Kalb, E. (1993). Microspectrofluorometry on supported planar membranes. In *Molecular Luminescence Spectroscopy*, *Part 3* (ed. Stephen G. Schulman), pp. 253–305. Chemical Analysis Series, Vol. 77. John Wiley & Sons, Inc.

Tamm, L. K. & McConnell, H. M. (1985). Supported Phospholipid Bilayers. *Biophys. J.* **47**, 105–113.

Tamm, L. K. & Tatulian, S. A. (1993). Orientation of functional and non-functional PTS permease signal sequences in lipid bilayers. A polarized FTIR study. *Biochemistry* **32**, 7720–7726.

Tatulian, S. A. & Tamm, L. K. (1996). Reversible pH-dependent conformational change of reconstituted influenza hemagglutinin. *J. Mol. Biol.* **260**, 312–316.

Tatulian, S. A., Hinterdorfer, P., Baber, G. & Tamm, L. K. (1995*a*). Influenza hemagglutinin assumes a tilted conformation during membrane fusion as determined by attenuated total reflection FTIR spectroscopy. *EMBO J.* **14**, 5514–5523.

Tatulian, S. A., Jones, L. R., Reddy, L. G., Stokes, D. L. & Tamm, L. K. (1995*b*). Secondary structure and orientation of phospholamban reconstituted in supported bilayers from polarized attenuated total reflection FTIR spectroscopy. *Biochemistry* **34**, 4448–4456.

Tatulian, S. A., Biltonen, R. & Tamm, L. K. (1997). Structural changes in a secretory phospholipase $A_2$ induced by membrane binding: A clue to interfacial activation? *J. Mol. Biol.* **268**, 809–815.

Terwilliger, T. C., Weissman, L. & Eisenberg, D. (1982). The structure of melittin in the form I crystals and its implication for melittin's lytic and surface activities. *Biophys. J.* **37**, 353–361.

Thiaudière, E., Soekarjo, M., Kuchinka, E., Kuhn, A. & Vogel, H. (1993). Structural characterization of membrane insertion of M13 procoat, M13 coat, and Pf3 coat proteins. *Biochemistry* **32**, 12186–12196.

Thompson, T. E., Sankaram, M. B., Biltonen, R. L., Marsh, D. & Vaz, W. L. (1995). Effects of domain structure on in-plane reactions and interactions. *Mol. Membr. Biol.* **12**, 157–162.

Tsuboi, M. (1962). Infrared dichroism and molecular conformation of $\alpha$-form poly-$\gamma$-benzyl-L-glutamate. *J. Polymer Sci.* **59**, 139–153.

Tuchtenhagen, J., Ziegler, W. & Blume, A. (1994). Acyl chain conformational ordering in liquid-crystalline bilayers: comparative FT–IR and $^2$H-NMR studies of phospholipids differing in headgroup structure and chain length. *Eur. Biophys. J.* **23**, 323–335.

Tupper, S., Wong, P. T. T. & Tanphaichitr, N. (1992). Binding of $Ca^{2+}$ to sulfogalactosylglyceramide and the sequential effect on the lipid dynamics. *Biochemistry* **31**, 11902–11907.

Tupper, S., Wong, P. T. T., Kates, M. & Tanphaichitr, N. (1994). Interaction of divalent cations with germ cell specific sulfogalactosylglycerolipid and the effect on lipid chain dynamics. *Biochemistry* **33**, 13250–13258.

Ueda, I., Chiou, J.-S., Krishna, P. R. & Kamaya, H. (1994). Local anesthetics destabilize lipid membranes by breaking hydration and shell: infrared and calorimetric studies. *Biochim. Biophys. Acta* **1190**, 421–429.

Unwin, N. (1993). Nicotinic acetylcholine receptor at 9 Å resolution. *J. Mol. Biol.* **229**, 1101–1124.

Vandenbussche, G., Clercx, A., Clercx, M., Curstedt, T., Johansson, J., Jörnvall, H. & Ruysschaert, J.-M. (1992*a*). Secondary structure and orientation of the surfactant protein SP-B in a lipid environment. A Fourier transform infrared spectroscopic study. *Biochemistry* **31**, 9169–9176.

Vandenbussche, G., Clercx, A., Curstedt, T., Johansson, J., Jörnvall, H. & Ruysschaert, J.-M. (1992*b*). Structure and orientation of the surfactant-associated protein C in a lipid bilayer. *Eur. J. Biochem.* **203**, 201–209.

Venyaminov, S. Yu. & Kalnin, N. N. (1990*a*). Quantitative IR spectrophotometry of peptide compounds in water ($H_2O$) solutions. I. Spectral parameters of amino acid residue absorption bands. *Biopolymers* **30**, 1243–1257.

Venyaminov, S. Yu. & Kalnin, N. N. (1990*b*). Quantitative IR spectrophotometry of peptide compounds in water ($H_2O$) solutions. II. Amide absorption bands of polypeptides and fibrous proteins in $\alpha$-, $\beta$-, and random coil conformations. *Biopolymers* **30**, 1259–1271.

Vigneron, L., Ruysschaert, J.-M. & Goormaghtigh, E. (1995). Fourier transform infrared spectroscopy study of the secondary structure of the reconstituted *Neurospora crassa* plasma membrane $H^+$-ATPase and of its membrane-associated proteolytic peptides. *J. Biol. Chem.* **270**, 17685–17696.

Villalaín, J., Gómez-Fernández, J. C., Jackson, M. & Chapman, D. (1989). Fourier transform infrared spectroscopic studies on the secondary structure of the $Ca^{2+}$-ATPase of sarcoplasmic reticulum. *Biochim. Biophys. Acta* **978**, 305–312.

Villalaín, J. & Gómez-Fernández, J. C. (1992). Fourier transform infrared spectroscopic study of mixtures of palmitic acid with dipalmitoylphosphatidylcholine using isotopic substitution. *Chem. Phys. Lipids* **62**, 19–29.

Vogel, H. (1987). Comparison of the conformation and orientation of alamethicin and melittin in lipid membranes. *Biochemistry* **26**, 4562–4572.

Vogel, H. & Jähnig, F. (1986). The structure of melittin in membranes. *Biophys. J.* **50**, 573–582.

Vogel, H., Jähnig, F., Hoffmann, V. & Stümpel, J. (1983). The orientation of melittin in lipid membranes. A polarized infrared spectroscopic study. *Biochim. Biophys. Acta* **733**, 201–209.

Wang, X.-M., Mock, M., Ruysschaert, J.-M. & Cabiaux, V. (1996). Secondary structure of anthrax lethal toxin proteins and their interaction with large unilamellar vesicles: a Fourier-transform infrared spectroscopy approach. *Biochemistry* **35**, 14939–14946.

Weaver, A. J., Kemple, M. D., Brauner, J. W., Mendelsohn, R. & Prendergast, F. G. (1992). Fluorescence, CD, attenuated total reflectance (ATR) FTIR, and $^{13}C$ NMR characterization of the structure and dynamics of synthetic melittin and melittin analogues in lipid environments. *Biochemistry* **31**, 1301–1313.

Weiss, M. S., Abele, U., Weckesser, J., Welte, W., Schiltz, E. & Schulz, G. E. (1991). Molecular architecture and electrostatic properties of a bacterial porin. *Science* **254**, 1627–1630.

Wenzl, P., Fringeli, M., Goette, J. & Fringeli, U. P. (1994). Supported phospholipid bilayers prepared by the 'LB/vesicle method': A Fourier transform infrared attenuated total reflection spectroscopic study on structure and stability. *Langmuir* **10**, 4253–4264.

Wong, P. T. T. & Mantsch, H. H. (1988). High pressure infrared spectroscopic evidence of water binding sites in 1,2-diacyl phospholipids. *Chem. Phys. Lipids* **46**, 213–224.

Zhang, Y.-P., Lewis, R. N. A. H., Hodges, R. S. & McElhaney, R. N. (1992*a*). FTIR spectroscopic studies of the conformation and amide hydrogen exchange of a peptide model of the hydrophobic transmembrane $\alpha$-helices of membrane proteins. *Biochemistry* **31**, 11572–11578.

Zhang, Y.-P., Lewis, R. N. A. H., Hodges, R. S. & McElhaney, R. N. (1992*b*). Interaction of a peptide model of a hydrophobic transmembrane $\alpha$-helical segment of a membrane protein with phosphatidylcholine bilayers: Differential scanning calorimetric and FTIR spectroscopic studies. *Biochemistry* **31**, 11579–11588.

Zhang, Y.-P., Lewis, R. N. A. H., Henry, G. D., Sykes, B. D., Hodges, R. S. & McElhaney, R. N. (1995*a*). Peptide models of helical hydrophobic transmembrane segments of membrane proteins. 1. Studies of the conformation, intrabilayer orientation, and amide hydrogen exchangeability of Ac-$K_2$-$(LA)_{12}$-$K_2$-amide. *Biochemistry* **34**, 2348–2361.

Zhang, Y.-P., Lewis, R. N. A. H., Hodges, R. S. & McElhaney, R. N. (1995*b*). Peptide models of helical hydrophobic transmembrane segments of membrane proteins. 2. Differential scanning calorimetric and FTIR spectroscopic studies of the interaction of Ac-$K_2$-$(LA)_{12}$-$K_2$-amide with phosphatidylcholine bilayers. *Biochemistry* **34**, 2362–2371.